BIOLOGICAL RESPONSES TO ULTRAVIOLET RADIATION AND THE EFFECT OF INTRA-S CHECKPOINT INHIBITION ON ULTRAVIOLET RADIATION-INDUCED MUTAGENESIS

Christopher D. Sproul

A dissertation submitted to the faculty of the University of North Carolina at Chapel Hill in partial fulfillment of the requirements for the degree of Doctor of Philosophy in the Curriculum of Toxicology

Chapel Hill
2013

Approved by:
Marila Cordeiro-Stone, PhD
William Kaufmann, PhD
James Samet, PhD
Nancy Thomas, MD, PhD
Cyrus Vaziri, PhD

ABSTRACT

CHRISTOPHER D. SPROUL: Biological Responses to Ultraviolet Radiation and the Effect of Intra-S Checkpoint Inhibition on Ultraviolet Radiation-Induced Mutagenesis
(Under Direction of Marila Cordeiro-Stone, PhD)

Sunlight emits a spectrum of electromagnetic radiation that includes ultraviolet, visible, and infrared wavelengths. It is widely accepted that the ultraviolet radiation (UVR) component is responsible for the mutagenic and carcinogenic effects of sunlight. UVR is further sub-divided into three wavelength ranges: UVC (100-280 nm), UVB (280-315 nm) and UVA (315-400 nm) and each of these induce differing types and proportions of DNA damage. Despite much research, there is debate about the relative contributions from different wavelengths in initiating and promoting mutagenesis and carcinogenesis. DNA damage responses have been widely characterized using UVC, which is effectively filtered out by the Earth's atmosphere, while comparatively fewer studies have been conducted utilizing UVA and UVB. The research reported here assessed the biological outcomes of irradiating human dermal fibroblasts with UVR of different wavelengths, using DNA damage dosimetry to allow comparison between different irradiation sources. Cylobutane pyrimidine dimer (CPD) and 6-4 pyrimidine-pyrimidone photoproduct (6-4PP) densities were quantified and used as biomarkers following irradiation with lamps emitting UVA, UVB, or UVC. Comparing fluences that produced equal CPD densities, cytotoxicity, intra-S phase checkpoint response, and mutagenesis were assessed. Regardless of the source of UVR, results showed a striking similarity in the biological outcomes measured when exposures

were compared on the basis of CPD dosimetry, suggesting that this UV-induced photolesion significantly contributed to the measured effect.

The S-phase checkpoint response to UVR is a signaling cascade that recognizes damaged DNA or abnormal DNA structures and halts or slows new/ongoing DNA replication, potentially reducing the chance that damaged DNA will be replicated prior to its repair. Experiments reported here tested the hypothesis that this checkpoint is a protective system that reduces UVR-induced mutagenesis. Essential S-phase checkpoint components ATR or CHK1 were depleted using siRNA, or the CHK1 kinase pharmacologically inhibited using TCS2312, thereby inhibiting the S-phase checkpoint response to UVR. Subsequently, the UVR-induced mutation frequency at the *HPRT* locus was measured. Results showed that despite reversing the S-phase checkpoint response to UVR, the mutation frequency in the irradiated population was not increased, challenging the broadly accepted role of this signaling cascade in minimizing mutation burden.

ACKNOWLEDGEMENTS

I would like to give profound thanks to Dr. Marila Cordeiro-Stone. I have met very few people with her combination of sincere devotion to research and education, unwavering integrity, and uncompromising focus on student development. A testament to her patience, I have never witnessed her express anger, frustration, or loss of faith. Instead, she has used every hurdle and setback as an opportunity to help her students grow into independent, critically-thinking scientists. When presented with challenges, Marila's attitude has always been to help formulate and implement plans to overcome such obstacles, and to do so in a manner that upholds her outstanding commitment to research excellence and integrity. It is my hope that I will be able to emulate much of her scientific inquisitiveness, dedication to quality, and results-minded approach to problem solving. I count myself fortunate to have had her as an advisor.

I would also like to thank my family for their support throughout my academic career. I know that I would not have made it to this point without all that comes with the support and dedication that my immediate family has provided throughout my lifetime. I would particularly like to thank my wife, Pamela Sproul, who has been devoted and constantly encouraging. She too has taught me the powerful role of love, faith, patience, and self-sacrifice in helping others to achieve; traits that I strive to incorporate into my personal life and my professional career.

There have been many other people who have contributed to portions of this research, including committee members, collaborators, fellow students, and other colleagues. I have tried to acknowledge such contributions in the Preface and within the chapters themselves.

PREFACE

Research presented in Chapter 2 compared biological responses of normal human fibroblasts (NHF1) to three sources of ultraviolet radiation (UVR), each emitting primarily UVA, UVB, or UVC wavelengths. The endpoints measured were cytotoxicity, intra-S checkpoint activation, inhibition of DNA replication, and mutagenicity. The overall goals of this project were to examine mechanisms of UV-induced intra-S checkpoint activation and the influence of the intra-S checkpoint on mutagenesis. Little is known about how different wavelengths of UVR contribute to intra-S checkpoint activation or how different wavelengths of UVR contribute to UV-induced mutagenesis. These studies used DNA damage dosimetry to allow comparisons between three different wavelength ranges of UVR and to characterize activation of the intra-S checkpoint by different wavelengths. In addition, mutagenesis induced by different wavelengths was assessed on the basis of DNA damage dosimetry.

DNA damage dosimetry was performed to quantify levels of CPD (both by immunoblot and RIA), 6-4PP, and 8-oxo-dG. Assay of CPD and 6-4PP by RIA were performed in the laboratory of Dr. David Mitchell using DNA purified from irradiated cells by Chris Sproul. The purification of DNA for the assay of 8-oxo-dG and the assay itself were performed by the UNC-CEHS using irradiated cells provided by Chris Sproul. The immunoblot showing DNA damage responses in NHM (see **Figure S2.1**) was provided by Dr. William Kaufmann and Dr. Dennis Simpson. The CPD and 6-4PP repair kinetic curves in NHM and NHF (see **Figure S2.2**) were also provided by Dr. William Kaufmann, with the experiment being performed in his laboratory and the dosimetry performed in the laboratory of Dr. David Mitchell. Statistical analysis was performed by Shangbang Rao and Dr. Joseph

Ibrahim. All other work presented in this chapter, including CPD dosimetry, cytotoxicity experiments, intra-S checkpoint experiments, and mutagenesis experiments were performed by Chris Sproul. The contents of this chapter are being prepared as a manuscript to be submitted to *Photochemistry and Photobiology*.

The research presented in Chapter 3 examines the effect of intra-S checkpoint inhibition on UV-induced mutation frequency. The overall goals of this project were to examine mechanisms of UV-induced intra-S checkpoint activation and the influence of the intra-S checkpoint on mutagenesis. These experiments tested the hypothesis that intra-S checkpoint inhibition would increase UV-induced mutagenesis. The hypothesis was tested by depleting or inhibiting key components of the intra-S checkpoint signaling pathway and examining UV-induced mutation frequencies at the *HPRT* locus.

All experiments presented in this chapter were performed by Chris Sproul, including all siRNA depletions, velocity sedimentation experiments, immunoblots, CHK1 inhibitor characterization experiments, and mutagenesis experiments. Dr. William Kaufmann provided valuable suggestions and regular input throughout the development of this study. Statistical analysis was performed by Shangbang Rao and Dr. Joseph Ibrahim. The contents of this chapter are being prepared as a manuscript to be submitted to *Carcinogenesis*.

TABLE OF CONTENTS

ACKNOWLEDGEMENTS iv

PREFACE vi

LIST OF TABLES xi

LIST OF FIGURES xii

LIST OF ABBREVIATIONS xiv

CHAPTER

1. INTRODUCTION 1

Cancer 1

Skin cancers and UVR 3

UVR-induced DNA damage and mutations 6

Direct absorption of UVR by DNA 6

The UV signature mutation 9

UVA-induced DNA damage 11

UVA-induced mutation spectrum 12

UVA and melanoma 14

Cell cycle checkpoints 16

Overview: The intra-S phase checkpoint 16

The ATR/CHK1 dependent intra-S phase checkpoint response to UVR 18

Summary of work in this dissertation 24

2. CYCLOBUTANE PYRIMIDINE DIMER DENSITY AS A PREDICTIVE BIOMARKER OF THE BIOLOGICAL EFFECTS OF ULTRAVIOLET RADIATION IN NORMAL HUMAN FIBROBLASTS 26

Introduction 26

Results 29
Dosimetry curves 29
Cytotoxicity 33
Activation of the intra-S phase checkpoint....33
Mutagenesis 38
Discussion 41
Support....46
Materials and methods....47
Cell culture....47
Irradiation....47
Cytoxicity 48
Immuno-slot blot quantification of CPD 49
Radioimmunoassay....49
Western blotting and antibodies 50
Velocity sedimentation 50
HAT selection....51
Mutagenesis 51
Statistical methods....52
Supplemental material 54
3. IS ACTIVATION OF THE INTRA-S CHECKPOINT IN HUMAN FIBROBLASTS AN IMPORTANT FACTOR IN PROTECTION AGAINST UV-INDUCED MUTAGENESIS?....57
Introduction....57
Results 60
Depletion of ATR or CHK1 abrogated the intra-S phase checkpoint triggered by UV....60
Depletion of ATR or CHK1 did not increase the UV-induced mutation frequency at the *HPRT* locus 63

Pharmacological inhibition of CHK1 with TCS2312 abrogated the UV-induced intra-S phase checkpoint 65

CHK1 inhibition did not increase the UV-induced mutation frequency at the HPRT locus 65

Colony forming efficiency and UV-induced cytotoxicity following ATR/CHK1 depletion or CHK1 inhibition 68

Discussion 70

Materials and methods 75

Cell culture and UV treatment 75

Protein depletion 75

CHK1 inhibitor TCS2312 75

Western blotting and antibodies 76

Velocity sedimentation 76

HAT selection 77

Mutagenesis 78

Cytotoxicity experiments 78

Statistical methods 79

Supplemental material 80

4. CONCLUSIONS AND FUTURE DIRECTIONS 84

5. REFERENCES 95

LIST OF TABLES

Table 2.1 Quantification of 8-oxo-dG in NHF1 cells exposed to UVA or UVC.....32

LIST OF FIGURES

Figure 1.1 The solar spectrum of electromagnetic radiation 5

Figure 1.2 Cyclobutane pyrimidine dimer (CPD) 7

Figure 1.3 The 6-4 pyrimidine-pyrimidone photoproduct (6-4PP) 8

Figure 1.4 The UVR signature mutation 10

Figure 1.5 The mispairing of 8-oxo-dG with adenine 13

Figure 1.6 The intra-S checkpoint 17

Figure 2.1 CPD dosimetry curves 30

Figure 2.2 6-4PP dosimetry curves 31

Figure 2.3 Cytotoxicity as a function of CPD burden for NHF1 exposed to UVA, UVB, or UVC 34

Figure 2.4 CHK1 phosphorylation in NHF1 exposed to UVA or UVC 35

Figure 2.5 Inhibition of replicon initiation by UVC or UVA 37

Figure 2.6 Inhibition of DNA strand growth by UVC or UVA 39

Figure 2.7 UVA or UVC-induced mutation frequency at the HPRT locus 40

Figure S2.1 Activation of the intra-S checkpoint by UV-induced DNA damage in normal human melanocytes 54

Figure S2.2 Repair of CPD or 6-4PP in NHF1 and NHM4 55

Figure S2.3 Relative spectral output for UVA, UVB, and UVC sources used in these experiments 56

Figure 3.1 Depletion of ATR abrogates the intra-S checkpoint response 61

Figure 3.2 Depletion of CHK1 abrogates the intra-S checkpoint response 62

Figure 3.3 Depletion of ATR or CHK1 does not increase UV-induced mutation frequency at the HPRT locus 64

Figure 3.4 CHK1 inhibitor TCS2312 abrogates the intra-S checkpoint response 66

Figure 3.5 CHK1 inhibitor TCS2312 does not increase UV-induced mutation frequency at the HPRT locus 67

Figure 3.6 Influence of ATR or CHK1 depletion, or CHK1 inhibition, on colony forming efficiency or UV-induced cytotoxicity 69

Figure S3.1 Depletion of DNA polymerase η increases UV-induced mutagenesis 80

Figure S3.2 Inhibition of DNA synthesis by TCS2312 81

Figure S3.3 Inhibition of CHK1 kinase activity enhances CHK1 phosphorylation 82

Figure S3.4 Velocity sedimentation analysis of nascent DNA from NHF1 cells treated with the CHK1 inhibitor TCS2312 83

LIST OF ABBREVIATIONS

$^1O_2$	singlet oxygen
6-4PP	6-4 pyrimidine-pyrimidone photoproduct
8-oxo-dG	8-oxo-7,8-dihydro-2'-deoxyguanosine
9-1-1	Rad9-Rad1-Hus1
AIMP3	aminoacyl tRNA synthetase interacting multifunctional protein 3
AT	ataxia telangiectasia
ATM	ataxia telangiectasia mutated
ATR	ataxia telangiectasia and Rad3-related
ATRIP	ATR interacting protein
ave	average
BCC	basal cell carcinoma
BER	base excision repair
BPDE	benzo[a]pyrene diolepoxide
C	cytosine
CEHS	Center for Environmental Health and Susceptibility (UNC-CH)
CHK1	checkpoint kinase 1
CHK2	checkpoint kinase 2
CPD	cyclobutane pyrimidine dimer
D_0	increase in fluences required to decrease the surviving fraction from 100% to 37%
DDK	DBF4-dependent kinase
DDR	DNA damage response
dsb	double stranded breaks
ECL	enhanced chemical luminescence

h	hour
HBSS	Hank’s balanced saline solution
HPRT	hypoxanthine phosphoribosyltransferase
HRP	horseradish peroxidase
IR	ionizing radiation
MCM	minichromosome maintenance
min	minute
MSI	microsatellite instability
MW	molecular weight
NER	nucleotide excision repair
NHDF	normal human dermal fibroblasts
NHF	normal human fibroblasts
NMSC	non-melanoma skin cancer
NTC	non-targeted control
ORC	origin recognition complex
PAH	polycyclic aromatic hydrocarbon
PBS	phosphate buffered saline
PI3K	phosphatidylinositol-3' kinase
pol η	DNA polymerase eta
pre-RC	pre-replication complex
PTC	PATCHED
PUVA	psoralen + UVA
RFPC	replication fork protection complex
RIA	radio-immuno assay
ROS	reactive oxygen species
SCC	squamous cell carcinoma

SEM	standard error of the mean
siRNA	small interfering RNA
SSC	saline sodium citrate
stdev	standard deviation
T	thymidine
TCA	trichloroacetic acid
TIM	TIMELESS
TIPIN	TIMELESS interacting protein
TLS	trans-lesion synthesis
TopBP1	DNA topoisomerase binding protein 1
U	uracil
UV	ultraviolet
UVR	ultraviolet radiation
XP	xeroderma pigmentosum
XPV	xeroderma pigmentosum variant

CHAPTER 1

INTRODUCTION

Cancer

Cancer is often thought of as a disease of mis-regulated cellular proliferation and differentiation. Damage to the cellular genetic material, DNA, by endogenous or exogenous sources is widely accepted to result in permanent mutations that alter the abundance or function of protein-coding genes. Cancers acquire mutations in genes that regulate growth signaling and growth potential, control programmed cell death, and regulate differentiation, allowing cancer cells to grow unrestrained and to invade neighboring tissue or metastasize (Hanahan and Weinberg, 2000; Hanahan and Weinberg, 2011). Mutations in cancer cells also allow tumors to facilitate the growth of their own blood supply (angiogenesis), and to evade host immune responses. Cancers were originally thought to result from the mutation of one or only a few genes. It is now widely accepted that cells acquire mutations to perhaps a dozen or more genes in progressive steps toward malignancy. Furthermore, cancer cells appear to acquire mutations at abnormally high rates, further selecting for cells with mutations in each of these key hallmark pathways (Beckman and Loeb, 2005; Loeb, 1991). This mutator phenotype can occur when primary mutations disrupt the cell's genome surveillance and maintenance systems that would normally detect and resolve aberrant genomic material. These DNA-maintenance pathways usually ensure that spontaneous mutation rates remain low, and disruptions to these protective pathways can promote the genomic instability that results in the mutator phenotype.

Genome maintaining pathways detect damaged DNA or aberrant DNA structures and activate subsequent systems designed to repair or tolerate the damage and/or prevent

the damaged DNA from being replicated. Cells have evolved multiple pathways to repair specific forms of damaged DNA. Homologous recombination, mismatch repair, non-homologous end joining, base excision repair (BER), and nucleotide excision repair (NER) are among the pathways that cells use to repair damaged DNA (Sancar *et al.*, 2004). Germ-line mutations have fostered much of our understanding of how disruptions to these repair pathway genes promote enhanced mutagenesis. For example, individuals with the genetic disorder xeroderma pigmentosum most often harbor an inherited mutation in genes regulating NER, diminishing their capacity to repair NER substrates, such as those induced by ultraviolet radiation (UVR). These individuals exhibit extreme sensitivity to UVR and acquire UVR-induced skin cancers at rates 2000-10000 higher than normal (Lehmann *et al.*, 2011). Similarly, individuals with Bloom's syndrome present with elevated cancer incidence and have been shown to have defects in homologous recombination.

Tightly linked with repair pathways, cell cycle checkpoints monitor the transition between the phases of the cell cycle and inhibit cell cycle progression when damaged DNA or aberrant genomic structures are detected. The somatic cell cycle ensures that the genome is completely and accurately replicated once and only once during S-phase, and that the duplicated genome is segregated to identical daughter cells during mitosis. Progression through the cell cycle with damaged DNA, abnormal DNA structures, or insufficient resources to carry out cellular duplication faithfully can lead to genetic instability. Cell cycle checkpoints survey cell cycle phases and their transitions to inhibit progression in the presence of such damage, and are thought to allow cells time to repair genomic damage before it is replicated (Kastan and Bartek, 2004; Kaufmann and Paules, 1996; Shackelford *et al.*, 1999). Inherited or somatic mutations to checkpoint genes are also thought to potentially contribute to the mutator phenotype. For example, individuals with the genetic instability syndrome ataxia telangiectasia inherit mutations to the *ATM* (ataxia telangiectasia

mutated) gene and display a predisposition to cancer. *ATM* is a protein kinase involved in sensing chromatin structures associated with DNA double strand breaks and facilitates the activation of multiple cell cycle checkpoints and DNA repair pathways. Because such genetic disorders have provided some mechanistic insight into cancer initiation and progression, researchers continue to examine these and other pathways that contribute to DNA damage repair and tolerance in hopes of elucidating molecular mechanisms of carcinogenesis and perhaps improving cancer prevention or therapeutics.

Skin cancers and UVR

Skin cancers are the most common form of human malignancy, with more than three million new cases of non-melanoma skin cancer (NMSC) and more than 70,000 new cases of malignant melanoma projected for the USA in 2012 (www.cancer.org; ACS cancer facts and figures 2012). Skin cancers predominantly occur as melanoma or NMSC, which is largely divided into basal and squamous cell carcinomas (BCC and SCC, respectively). While BCC is the most common malignancy in Caucasians and the most common NMSC, accounting for ~80% of all NMSC, it rarely metastasizes and thus displays relatively low mortality rates. SCC accounts for ~20% of all NMSC, but is more likely than BCC to invade and metastasize and thus results in higher mortality than does BCC. Although melanoma is much less common than NMSC, accounting for ~3% of all skin cancers in the USA, it accounts for more than 75% of all skin cancer deaths. Exposure to solar ultraviolet radiation (UVR) is the primary environmental risk factor for all forms of skin cancer.

Cellular DNA is damaged through direct absorption of UVR wavelengths and also potentially through indirect energy transfer via endogenous photosensitizers. In addition to direct genotoxic effects, acute dermal exposure to UVR can cause inflammatory erythema (i.e. sunburn), tanning (increased melanogenesis), epidermal hyperplasia (skin thickening), and local immune suppression. Increased skin cancer rates in immunosuppressed

individuals suggests immune involvement in skin cancer protection (Hill, 1976; Hoxtell *et al.*, 1977), and also provides a plausible reason to suspect local UVR-induced immunosuppresion as a risk factor for disease progression. In addition to photoaging, chronic dermal exposure to UVR causes accumulation of DNA damage that can lead to mutations, which combined with further immune suppression are thought to lead to skin carcinogenesis (Ichihashi *et al.*, 2003; Matsumura and Ananthaswamy, 2004).

Because UVR is a direct mutagen and also causes cellular proliferation and immune suppression, it is considered a prototypical complete carcinogen that contributes to each stage of the initiation, promotion, and progression model. As with other carcinogens, UVR can cause mutations that lead to the activation of oncogenes and the inactivation of tumor suppressor genes. Common UVR mutations in NMSC are found in the tumor suppressor genes *p53* and PATCHED (*PTC*), the *CDKN2A* locus encoding both $p16^{INK4a}$ and $p19^{ARF}$, and members of the *RAS* family of oncogenes (Matsumura and Ananthaswamy, 2004). Common mutations identified in melanomas include activation of the oncogenes *BRAF* or *NRAS*, loss of *PTEN*, or other mutations that activate the PI3K pathway, and *TGF-β* (Matsumura and Ananthaswamy, 2004).

Sunlight is a continuous spectrum of electromagnetic radiation that includes ultraviolet, visible, and infrared wavelengths (**Figure 1.1**). The UVR spectrum can be further sub-divided into three wavelength ranges: UVC (100-280 nm), UVB (280-315 nm) and UVA (315-400 nm). In contrast to UVA and UVB, the wavelengths in the UVC range are absorbed by the Earth's stratospheric ozone layer and do not reach the surface of the planet. UVR that does reach the surface of the planet consists of approximately 5-10% UVB and 90-95% UVA. Much research has been devoted to deciphering the biological effects elicited by different wavelengths of UVR and to determine how different wavelengths contribute to

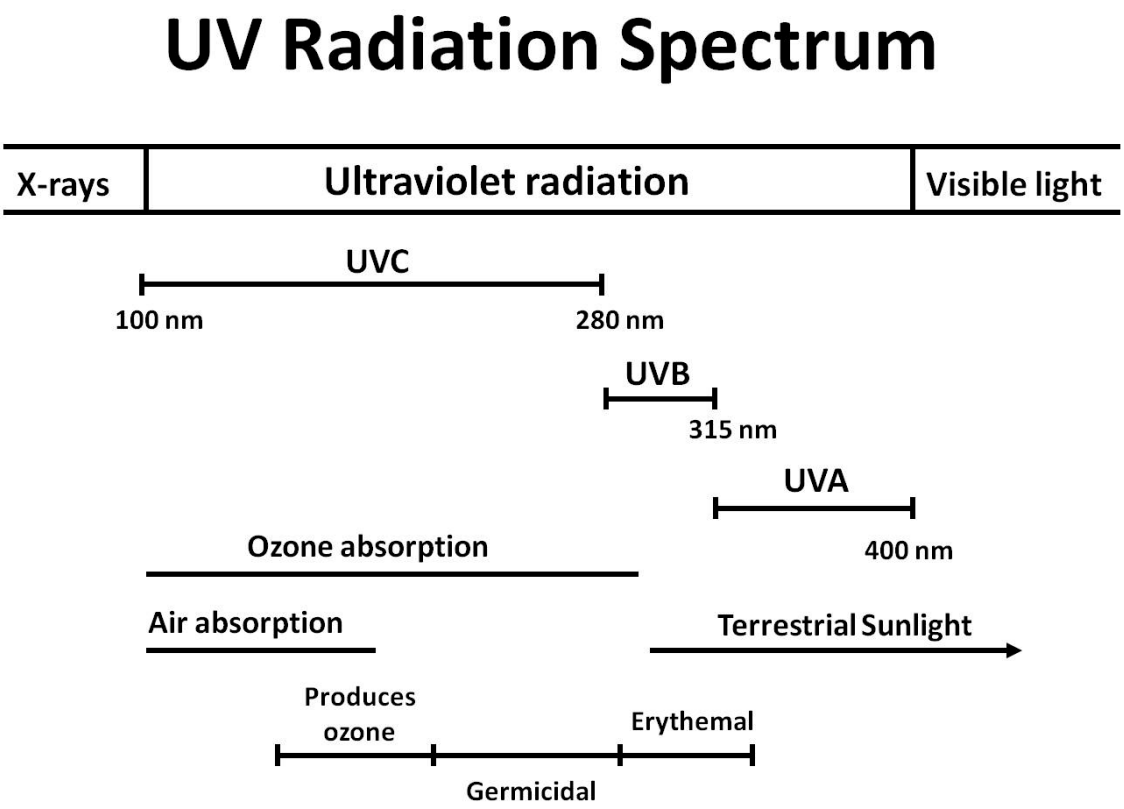

Figure 1.1 The solar spectrum of electromagnetic radiation. Sunlight is a continuous spectrum of electromagnetic radiation that includes ultraviolet, visible, and infrared wavelengths.The UVR spectrum is further sub-divided into three wavelength ranges: UVC (100-280 nm), UVB (280-315 nm) and UVA (315-400 nm). UVC is absorbed in the stratospheric ozone layer, while UVB and UVA reach the Earth's surface. [Adapted from Matsumura and Ananthaswamy, *Appl Parmacol* 2004 Mar 15;195(3):298-308]

mutagenesis and carcinogenesis. Despite the volume of research devoted to this topic, there is still much controversy surrounding the significance of the various UVR wavelengths.

UVR-induced DNA damage and mutations

Direct absorption of UVR by DNA

The absorption spectrum for DNA ranges from approximately 200 nm to 310 nm, with the lowest absorption at 232 nm, and the maximum absorption at 260 nm. The direct absorption of UVR energy by DNA bases is known to cause photochemical reactions resulting in alterations to native DNA structure (reviewed in (Cadet *et al.*, 2005; Ichihashi *et al.*, 2003). These photochemical reactions induce multiple forms of base alterations, most commonly the formation of photodimers or photoadducts between adjacent pyrimidines. The most common form of UVR-induced DNA damage is the cyclobutane pyrimidine dimer (CPD, **Figure 1.2**), which is the formation of a cyclobutane ring between the C4 and C5 carbon atoms of adjacent cytosine (C) or thymidine (T) residues. The 6-4 pyrimidine-pyrimidone photoproduct (6-4PP, **Figure 1.3**) is also formed by direct absorption of UVR, causing a cross-link between the C6 carbon of the 5' base with the C4 carbon of the 3' base. The formation of a secondary photoproduct, the Dewer isomer, can also result from the photoisomerization of the 6-4PP after subsequent exposure to UVA wavelengths (Cadet *et al.*, 2005; Matsunaga *et al.*, 1991). The wavelength action spectrum for the formation of the CPD and 6-4PP strongly overlaps with the UV-absorption spectrum of DNA, with efficient formation occurring between 220 nm and 300 nm (Matsunaga *et al.*, 1991; Mitchell *et al.*, 1991), although the formation of CPD has been reported at longer wavelengths (Courdavault *et al.*, 2004; Mouret *et al.*, 2006). The CPD to 6-4PP density ratio is generally reported as anywhere from 3 to 10 for UVR wavelengths that correspond to the DNA UV-absorption spectrum, and even higher when examining UVR that mimics the solar spectrum (Besaratinia *et al.*, 2011; Cadet *et al.*, 2005; Mitchell *et al.*, 1991).

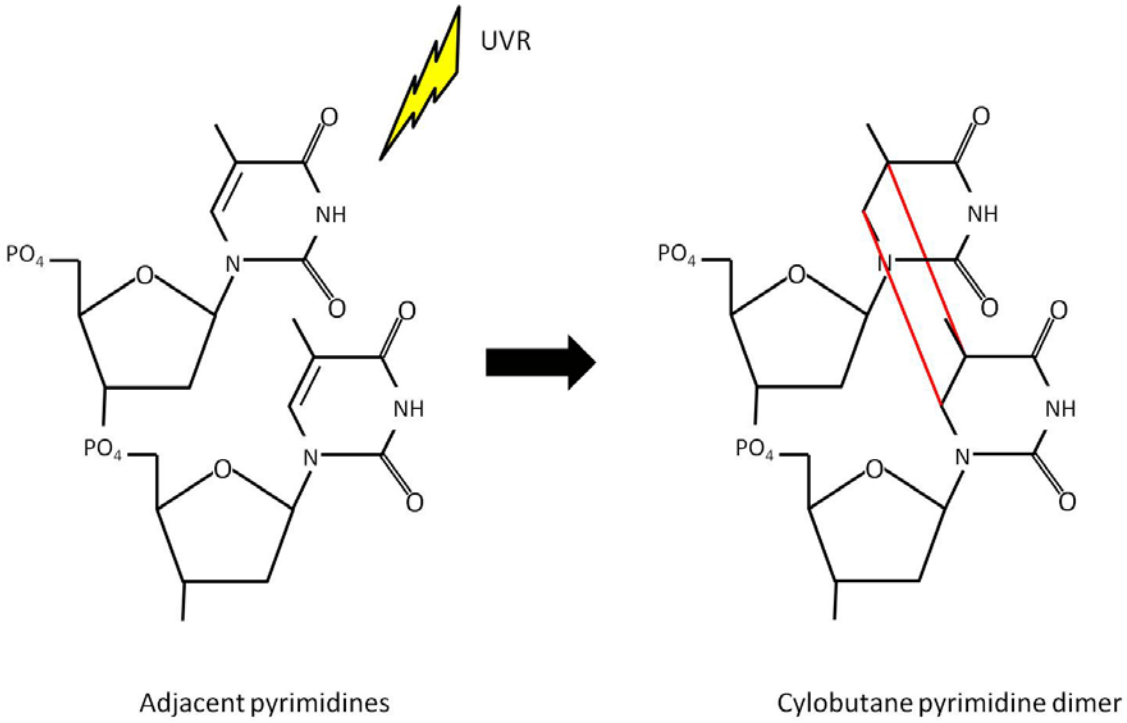

Figure 1.2 Cyclobutane pyrimidine dimer (CPD). The most abundant UV-induced DNA photolesion forms between the C4 and C5 carbon atoms of adjacent pyrimidines. The CPD forms after direct absorption of UVR or via indirect photosensitization reactions.

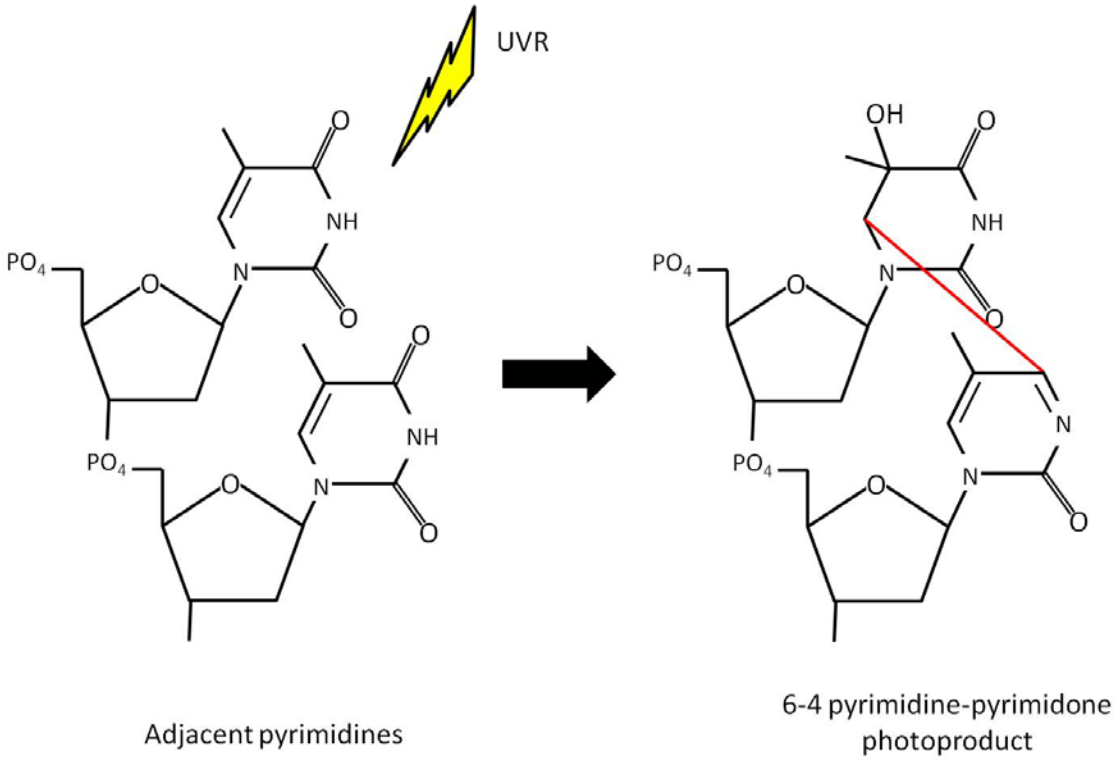

Figure 1.3 The 6-4 pyrimidine-pyrimidone photoproduct (6-4PP). The 6-4PP is formed by direct absorption of UVR, causing a cross-link between the C6 carbon of the 5' base with the C4 carbon of the 3' base.

The UV signature mutation

The C→T transition at dipyrimidine sites and the CC→TT tandem base substitutions have been termed UV-signature mutations, and have been observed in high frequencies in NMSC (Brash *et al.*, 1991; Brash *et al.*, 1996; Gailani *et al.*, 1996; Ziegler *et al.*, 1993). This signature mutation is thought to be primarily the result of accurate bypass of a CPD containing a deaminated cytosine (**Figure 1.4**) (reviewed in (Ikehata and Ono, 2011). Compared to an unaltered cytosine, the cytosine in a CPD is much more prone to deamination, resulting in the formation of uracil (U) at C-containing CPD. Upon encountering a CPD or 6-4PP on the template strand, the replicative polymerase is unable to replicate through this lesion. Specialized bypass polymerases are required to effectively replicate damaged DNA when the replicative polymerases are unable to do so. This trans-lesion synthesis (TLS) is performed by various Y-family polymerases; in the case of the CPD, TLS is carried out by DNA polymerase eta (pol η). Although more error prone than the replicative polymerases on undamaged DNA (Matsuda *et al.*, 2000), pol η is able to accommodate the CPD in its active site (Yoon *et al.*, 2009) and replicate past the lesion, thus preventing a prolonged arrest and potential collapse of the replication fork at the damage site, which would lead to the formation of a double stranded break. Accurate bypass of deaminated cytosines in CPD by pol η would therefore introduce an adenine opposite the uracil. Subsequent removal of the CPD or further replication of the A-containing strand would result in permanently altering the original G:C base pair to an A:T base pair (i.e., a C→T transition mutation). UV-signature mutations are still the most common UV-induced mutation in cells derived from individuals with xeroderma pigmentosum variant (XPV), which lack functional pol η (Choi and Pfeifer, 2005a; Stary *et al.*, 2003). Thus it has been argued that accurate bypass of deaminated cytosines by pol η cannot account for all UV-signature mutations. An argument has also been made for an error prone TLS-dependent model (Gueranger *et al.*, 2008) relying upon TLS polymerases that preferentially insert an adenine opposite damaged

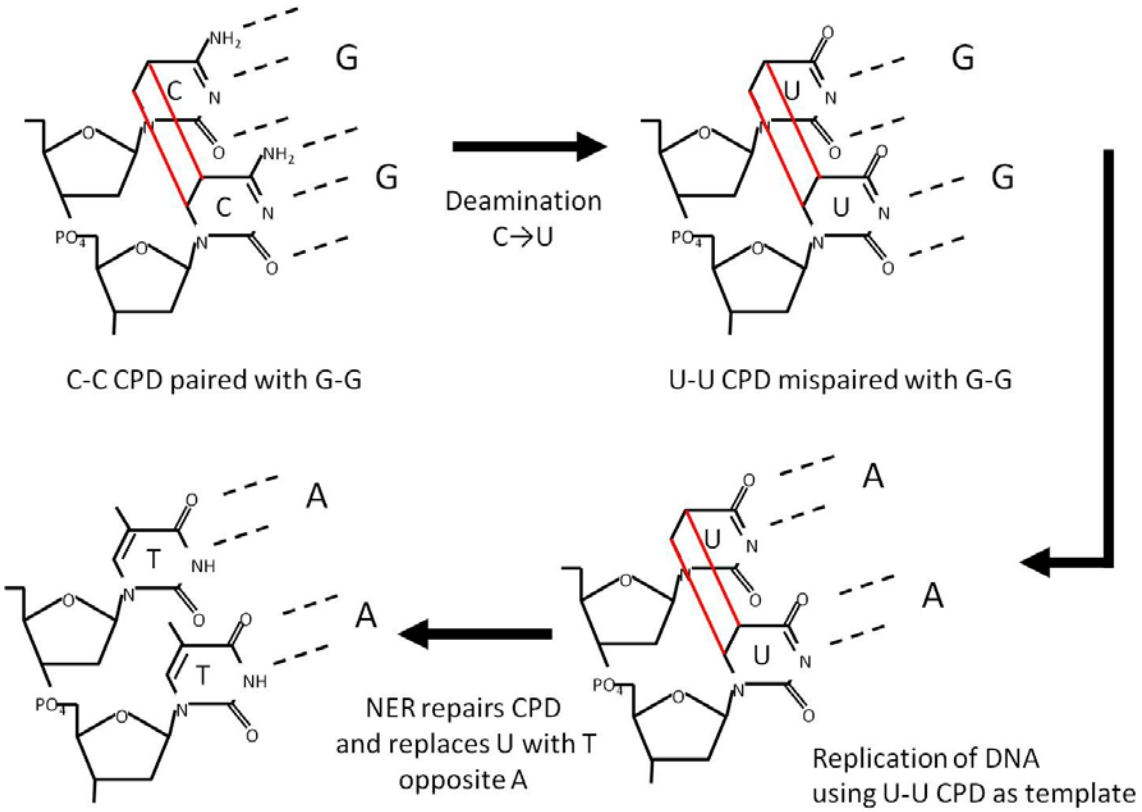

Figure 1.4 The UVR signature mutation. This signature mutation is thought to be primarily the result of accurate TLS bypass of a CPD containing deaminated cytosine(s). This mechanism leads to C→T or CC→TT transitions at dipyrimine sites.

template DNA and further rely upon polymerases that can extend past such mismatches. It should also be noted that UV-signature mutations following UVB or solar exposure (but not UVC) have been observed at higher frequencies in CPD containing 5-methyl-cytosine (Drouin and Therrien, 1997; Tommasi *et al.*, 1997), which are common in mammalian CpG sequences. Furthermore, the presence of 5-methyl cytosine increased the CPD yield in UVB irradiated DNA, but not in DNA irradiated with UVC (Rochette *et al.*, 2009). It has also been proposed that the 3' methyl-cytosine in a CPD deaminates even more rapidly than an unmethylated cytosine in the same sequence, enriching UV signature mutations at methyl-CpG sites (Lee and Pfeifer, 2003).

UVA-induced DNA damage

UVA is the most abundant and lowest energy component of solar UVR. Once thought relatively harmless, the UVA wavelengths have been the focus of intense research following evidence that exposure to sunbeds, primarily emitting UVA, increases the risk of NMSC and melanoma (reviewed in (Dore and Chignol, 2012). Despite the fact that energy from UVA is poorly absorbed by DNA, UVA has been shown to induce multiple forms of DNA damage. Following UVA exposure, CPD are detected in mammalian cells (Courdavault *et al.*, 2004; Douki *et al.*, 1999) and in human skin (Mouret *et al.*, 2006; Tewari *et al.*, 2012), while 6-4PP are generally not reported to be found (Besaratinia *et al.*, 2011; Perdiz *et al.*, 2000). Interestingly, the distribution of CPD in UVA irradiated cells is different than those observed following treatment with UVB, suggesting that they are formed by different mechanisms. While both UVA and UVB-induced CPD occur most frequently at TT sites, UVB exposure produces a higher proportion of C-containing CPD than does UVA, and UVA-induced CC-CPD are not observed (Douki *et al.*, 2003; Mouret *et al.*, 2006). Because DNA does not readily absorb UVA wavelengths, the predominant view is that the formation of UVA-induced CPD occurs via an indirect mechanism, relying on endogenous

photosensitizers that absorb UVA wavelengths and then deposit that energy on DNA (Cadet *et al.*, 2005). Despite the weak absorption of longer wavelengths by DNA, other researchers have proposed that UVA is still capable of directly damaging DNA without photosensitization reactions. CPD were reported following irradiation of purified plasmid DNA with filtered UVA that was thought to be absent of any photosensitizer (Kuluncsics *et al.*, 1999). Similarly, Jiang *et al* reported the production of CPD in purified plasmids following irradiation with narrow band UVA (Jiang *et al.*, 2009).

UVA-induced cytotoxicity and mutagenicity was shown to be at least partially oxygen dependent in bacteria and mammalian cells, providing evidence that molecular oxygen was involved in a UVA-photosensitization reaction (Danpure and Tyrrell, 1976; Webb and Malina, 1970). It was hypothesized that photosensitizers could undergo a direct one-electron reduction (type I photosensitization) and subsequent oxidation of DNA, or a transfer of energy to molecular oxygen (type II photosensitization) and the formation of highly reactive singlet oxygen ($^1O_2$) and that the formation of 8-oxo-7,8-dihydro-2'-deoxyguanosine (8-oxo-dG) would be the most likely form of oxidative DNA damage from either reaction. Although the mechanism is still in question, UVA-induced 8-oxo-dG has been reported in mammalian cells (Courdavault *et al.*, 2004; Douki *et al.*, 1999), in mouse skin (Ikehata *et al.*, 2008), and in human skin (Mouret *et al.*, 2006). It is still unclear, however, what contribution UVA-induced oxidative damage to DNA has on UV-induced carcinogenesis.

UVA-induced mutation spectrum

The mutation spectrum induced by UVA in mammalian cells has been examined in several studies. A UVA-fingerprint mutation was proposed when Drobetsky *et al* observed a high frequency of T→G transversions in the *APRT* gene of UVA-irradiated Chinese Hamster Ovary cells (Drobetsky *et al.*, 1995), and it was proposed that this mutation was the result of incorporation of 8-OH-dGTP opposite a template adenine (**Figure 1.5**). A similar result was

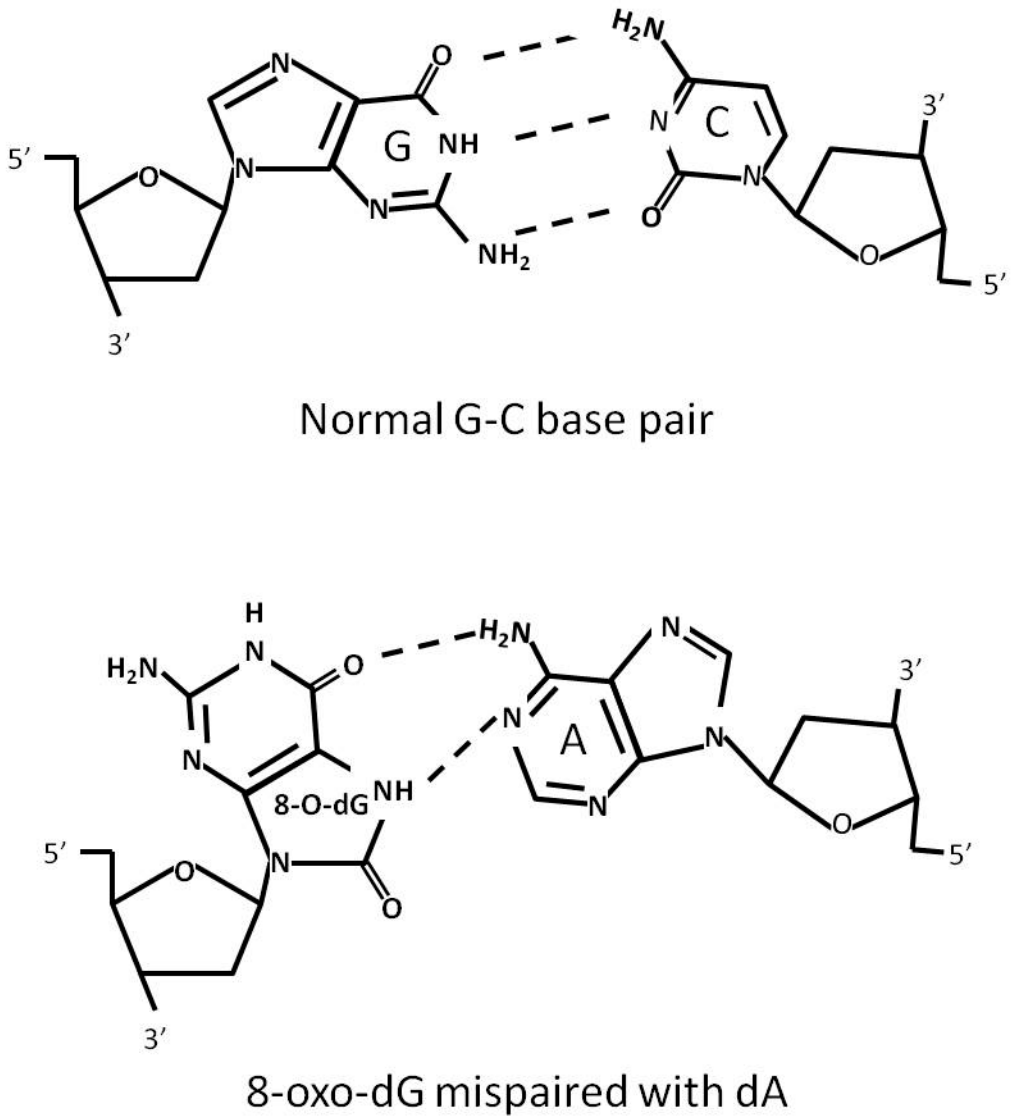

Figure 1.5 The mispairing of 8-oxo-dG with adenine. The most abundant damage to DNA induced by reactive oxygen species (ROS) is 8-oxo-dG, and long wavelength UVR has been reported to induce ROS-mediated 8-oxo-dG formation. Incorporation of 8-OH-dGTP opposite a template adenine results in T→G transversions, while mispairing of template 8-oxo-dG with dATP is reported to induce G→T transversions.

reported in the *p53* sequence of human squamous carcinoma (Agar *et al.*, 2004). The mispairing of template 8-oxo-dG with dATP (**Figure 1.5**) has also been proposed as a UVA signature mutation and the resultant G→T transversions were observed in the *CII* or *lacI* transgenes following UVA irradiation of Big Blue mouse embryonic fibroblasts (Besaratinia *et al.*, 2004; Besaratinia *et al.*, 2011; Kim *et al.*, 2007). (Besaratinia *et al.*, 2011)

The contribution of UV-induced oxidative damage to mutagenesis is not without controversy. Base excision repair deficient *ogg1*$^{-/-}$ mouse embryonic fibroblasts that are unable to repair 8-oxo-dG did not display enhanced UVA-induced mutagenesis (Kappes and Runger, 2005). Conversely, overexpression of human *OGG1* decreased the UVA-induced mutation frequency in the *hprt* (hypoxanthine phosphoribosyltransferase) gene of Chinese Hamster Ovary cells (referred to as gprt in (Dahle *et al.*, 2008). Furthermore, several other mutagenesis studies failed to find a significant contribution from UVA-induced signature mutations, and instead predominantly recovered C→T transitions at dipyrimidine sites in UVA-irradiated fibroblasts (Kappes and Runger, 2005; Kappes *et al.*, 2006), human embryonic kidney cells (Robert *et al.*, 1996a), or mouse skin (Ikehata *et al.*, 2003; Ikehata *et al.*, 2008).

UVA and melanoma

The role of UVA in initiating and promoting melanoma remains a controversial subject. Until recently, sunscreens have predominantly blocked UVB wavelengths to prevent erythema, allowing prolonged exposure to UVA without sunburn. It has been hypothesized that this increased exposure to UVA has led to increased melanoma incidence (Garland *et al.*, 1993). As previously mentioned, there is evidence that exposure to tanning sunbeds, primarily emitting UVA, increases the risk of melanoma (reviewed in (Dore and Chignol, 2012). Clinical/epidemiological data and animal models of UVA-induced melanoma have produced heterogeneous results. While early studies in the *Xiphophorus* fish model

suggested that UVA could induce melanoma (Setlow *et al.*, 1993), these data were later challenged (Mitchell *et al.*, 2010). Following 81 weeks of exposure, three times a week, UVA-induced melanocytic hyperplasias were reported in 22% of exposed opossum (*Monodelphis domestica*) (Ley, 1997). Mouse models of UV-induced carcinogenesis have largely found UVA capable of inducing NMSC, but have failed to produce melanomas (De Fabo *et al.*, 2004). Clinically, UVA (mostly combined with the photosensitizer psoralen, termed PUVA) is used to treat cutaneous diseases such as psoriasis, scleroderma, and dermatitis. Patients undergoing PUVA (psoralen + UVA) are prone to develop lentigines that are characterized by atypical, bi-nucleate, proliferating melanocytes, and may also be more prone to developing melanoma (Stern *et al.*, 1997). This result has also been challenged by other research (Hannuksela-Svahn *et al.*, 1999), and because psoralen itself may initiate carcinogenesis, the results are difficult to interpret.

The mutations found in melanomas themselves further confuse the contribution of UVA toward melanomagenesis. While melanomas frequently harbor UV signature C→T transitions in genes such as *TP53*, *PTEN,* and *CDKN2A*, mutations in *NRAS* and *BRAF* are commonly not UV signature mutations (Hocker and Tsao, 2007). The serine/threonine protein kinase BRAF is commonly mutated in cutaneous melanomas, and the majority of these mutations occur at or near codon 600 of exon 15, changing a valine to a glutamic acid (V600E). Melanoma mutations at V600 are not UV signature mutations, and cannot be attributed to a C→T transition at a dipyrimidine site, suggesting that these mutations may be the result of some other form of DNA damage, such as oxidative damage (Besaratinia and Pfeifer, 2008). Alternatively, it has been suggested that error-prone bypass of nearby UV-induced photoproducts by TLS polymerases could give rise to mutations at the *BRAF* V600 codon (Thomas *et al.*, 2006). It has even been suggested that the pigment melanin itself may contribute to UVA-induced carcinogenesis. It is well accepted that melanin absorbs UV

photons that can damage DNA, but it has also been proposed that melanin can act as a photosensitizer for UVA wavelengths, and that the production of reactive melanin radicals could contribute to oxidative damage to DNA (Mitchell and Fernandez, 2012; Runger, 2011).

Cell cycle checkpoints

As previously mentioned, cell cycle checkpoints monitor the phases of the cell cycle and their transitions and inhibit cell cycle progression when damaged DNA or aberrant genomic structures are detected. The prevailing dogma is that cell cycle checkpoints provide time for repair of damaged DNA, reducing the probability that damaged DNA will be replicated and segregated, thus reducing mutation frequencies and chromosomal aberrations. Indeed, checkpoint failures have been shown to result in chromosomal abnormalities, developmental defects, and predisposition to cancers (Kastan and Bartek, 2004; Kerzendorfer and O'Driscoll, 2009). Upon sensing damaged DNA, cell cycle checkpoints inhibit progression out of the G_1 and G_2 phases of the cell cycle, while the intra-S checkpoint slows progression through S-phase (Kastan and Bartek, 2004).

Overview: The intra-S phase checkpoint

The intra-S phase checkpoint can be divided into two main signaling cascades that respond to different forms of damaged DNA (**Figure 1.6**). The first recognizes chromatin structures associated with double strand breaks (dsb) in DNA, such as those induced by ionizing radiation (IR). The intra-S checkpoint response to IR requires the proteins ATM, MRE-11, RAD50 and NBS1 and involves activation of the checkpoint kinases CHK1 and CHK2, promoting proteolytic degradation of CDC25A. Loss of the CDC25A phosphatase prevents removal of the inhibiting phosphorylation at tyr15 of CDK2, thus maintaining CDK2 in its

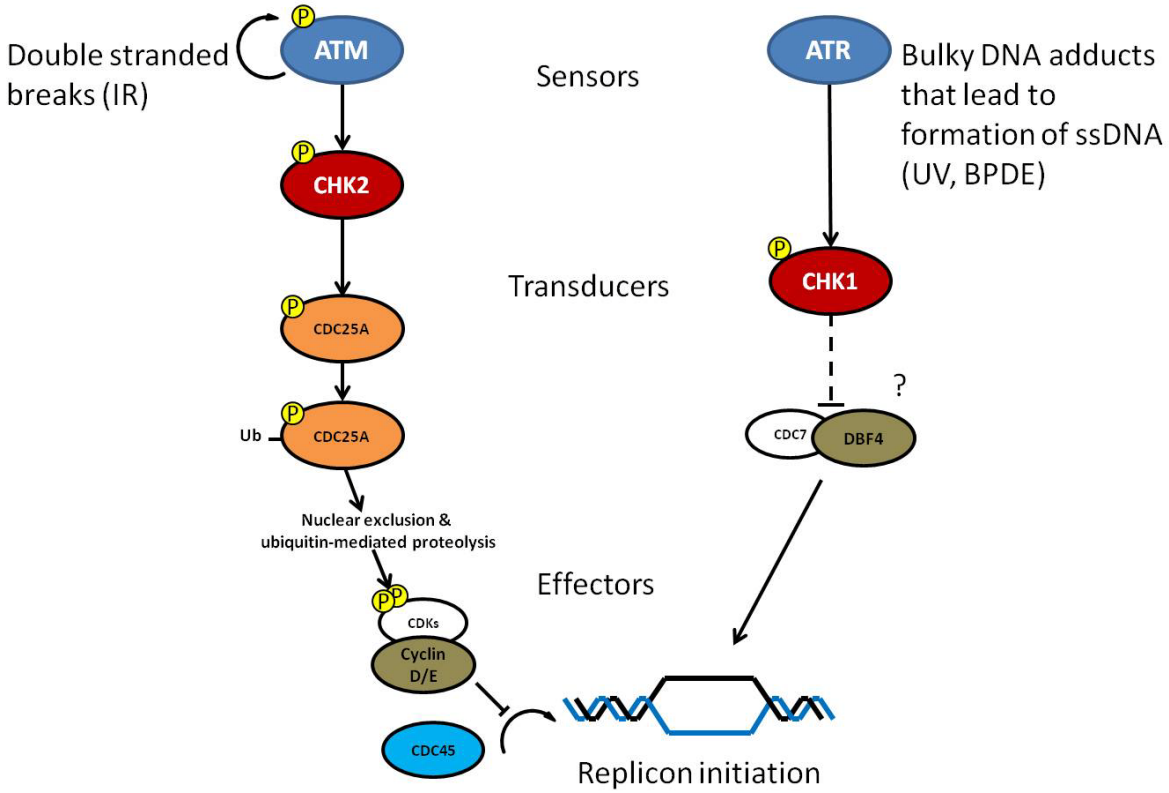

Figure 1.6 The intra-S checkpoint. Two pathways that activate the intra-S checkpoint. The first, employing the sensor protein ATM, responds to double stranded breaks in DNA, such as those caused by ionizing radiation. This pathway relies on the ubiquitin-mediated proteolysis of the CDC25A phosphatase to maintain CDK2 in its inhibited state, thereby preventing CDC45-dependent initiation at new replication origins. The second employs the sensor ATR and transducer kinase CHK1, and is thought to involve inhibition of DDK (CDC7 & DBF4) complex-dependent initiation at new replication origins. This diagram is a simplification as there is thought to be crosstalk between these two and other pathways, and many co-factors and accessory proteins have been omitted.

inhibited state, preventing CDC45-dependent initiation at new replication origins. ATM also maintains the intra-S checkpoint response by activation of p53 and subsequent induction of the CDK2 inhibitor $p21^{Waf1}$, and also by signaling through the cohesion subunits Smc1 and Smc3 (Kastan and Bartek, 2004).

The second main signaling cascade recognizes aberrant DNA structures produced during replication of bulky DNA adducts, such as those induced by UVR or benzo[a]pyrene diolepoxide (BPDE). This checkpoint response to UVR was found to require the activity of checkpoint proteins ataxia telangiectasia and Rad3-related (ATR) kinase, and its target CHK1, to act on downstream substrate(s) to inhibit the firing of new origins of replication (Chastain *et al.*, 2006; Heffernan *et al.*, 2002; Miao *et al.*, 2003) and to slow down rates of DNA chain elongation (Petermann *et al.*, 2006; Seiler *et al.*, 2007; Unsal-Kacmaz *et al.*, 2007). A 15 J/m^2 fluence of UVC resulted in the proteolysis of CDC25A, indicating that such a lethal dose activates a response that overlaps with the IR-induced activation of ATM (Mailand *et al.*, 2000). At sub-lethal fluences of UVR, however, the ATR/CHK1 pathway has been shown not to depend on degradation of CDC25A, but rather it has been proposed to act on the DBF4-dependent kinase (DDK) to prevent CDC45-dependent activation of the MCM helicase, thus inhibiting new replicon initiation (Heffernan *et al.*, 2007; Lee *et al.*, 2012).

The ATR/CHK1 dependent intra-S phase checkpoint response to UVR

Using velocity sedimentation in an alkaline sucrose gradient to analyze the abundance of different sizes of newly replicated DNA in HeLa and normal human dermal fibroblasts, it was observed that exposure to a sub-lethal fluence of UVR selectively inhibited the production of low molecular weight DNA intermediates that had initiated synthesis after irradiation (Kaufmann *et al.*, 1980b). This selective inhibition occurred for DNA intermediates that were roughly half the size of an average replicon leading to the interpretation that low

fluence UVR was inhibiting the firing of new origins of replication. It is now understood that when the replication fork encounters a template strand photoproduct, the replicative polymerase is stalled and uncoupled from the helicase, generating regions of single stranded DNA that initiate the intra-S checkpoint signaling (reviewed in (Kaufmann, 2009).

A similar phenomenon had also been observed in IR-exposed cells and it was determined that cells derived from patients with ataxia telangiectasia were resistant to IR-induced inhibition of DNA synthesis (Painter and Young, 1980). It has since been discovered that individuals afflicted with ataxia telangiectasia harbor inactivating mutations in *ATM*, which produces a protein product sharing homology with yeast and mammalian phosphatidylinositol-3' kinases (PI3K) (Savitsky *et al.*, 1995). ATM has since been shown to act as a serine/threonine kinase that responds to double stranded breaks in DNA and phosphorylates many targets to inhibit cell cycle progression. Because UVR and IR-irradiated cells shared a similar inhibition of DNA synthesis, and because cells lacking functional ATM displayed a radioresistant phenotype, it was initially hypothesized that ATM might also be involved in the UVR-induced inhibition of DNA synthesis (Painter, 1985). It was, however, eventually determined that $ATM^{-/-}$ cells retained an effective intra-S checkpoint response following treatment with UVC (Heffernan *et al.*, 2002), indicating that ATM was not required for UV-induced inhibition of replicon initiation.

ATR was identified as a human gene closely related to the yeast genes Rad3 (*S. pombe*) and Mec1 (*S. cerevisiae*), and the Drosophila gene mei-41, all of which were reported to produce PI3K proteins involved in DNA damage checkpoints. Furthermore, expression of the human *ATR* gene product in *S. cerevisiae* also complemented the IR-induced sensitivity in esr1-1 mutant yeast (inactivating mutation of Mec1) (Bentley *et al.*, 1996). Unlike *ATM*, *ATR* was found to be an essential gene whose deletion caused embryonic lethality in mice (Brown and Baltimore, 2000; de Klein *et al.*, 2000). The genetic

disorder Seckel syndrome is a consequence of an ATR hypomorphic splice mutant, and manifests as a developmental disease, with patients exhibiting dwarfism, microcephaly, and mental retardation. Cancer, however, is not typically associated with the disorder (Kerzendorfer and O'Driscoll, 2009). In addition to binding UV-damaged DNA (Unsal-Kacmaz *et al.*, 2002), ATR distributes into nuclear foci following treatment with aphidicolin (Tibbetts *et al.*, 2000). Further studies identified ATRIP (ATR interacting protein) co-localizing with ATR after treatment with UVR (Cortez *et al.*, 2001), and that this nuclear localization was inhibited following siRNA depletion of the single stranded DNA binding protein RPA (Zou and Elledge, 2003). Expression of kinase dead ATR was shown to act in a dominant–negative fashion and sensitize cells to IR, hydroxyurea, and UVR (Cliby *et al.*, 1998; Wright *et al.*, 1998) and ATR was subsequently shown to be required for the UV-induced inhibition of replicon initiation in both normal human dermal fibroblasts and in U2OS fibrosarcoma cells (Heffernan *et al.*, 2002). Taken together, these studies support a model by which ATR acts as the primary sensor in the UV-induced intra-S checkpoint response. In this model, the ATR-ATRIP complex binds RPA coated ss-DNA produced when UVR-induced photoproducts are encountered by the replicative polymerases while the helicase continues to unwind duplex DNA, and ATR kinase activity is essential for initiating the UV-induced intra-S phase checkpoint response. There is evidence that upon binding of ATRIP and RPA, ATR is fully activated after autophosphorylation at Thr1989, allowing it to act on downstream targets, including the effector kinase, CHK1 (Liu *et al.*, 2011; Nam *et al.*, 2011). The alternative clamp loading protein complex Rad17-RFC is also thought to be involved with the ATR-dependent sensing step as it loads the heterotrimeric ring-clamp, Rad9-Rad1-Hus1 (9-1-1) in response to UVR. Rad17 is itself a substrate for ATR kinase activity and seems to be required for downstream signaling of ATR (Zou *et al.*, 2002). Interactions between TopBP1 (DNA topoisomerase binding protein 1), the 9-1-1 complex, and ATR-ATRIP also seem to stimulate ATR kinase activity (Lee *et al.*, 2007; Mordes *et al.*, 2008).

The sensing functions of ATR and associated proteins are thought to propagate their signal via transducer kinases; primarily the checkpoint kinase protein CHK1, but also the structurally unrelated checkpoint kinase CHK2. The role of CHK1 in the S-phase checkpoint was examined in human lung cancer cell lines treated with the DNA damaging agent camptothecin after transient siRNA-mediated depletion of CHK1. It was found that CHK1 was required for the camptothecin-induced S-phase arrest and that CHK1 also mediated the proteolysis of CDC25A in response to camptothecin or doxorubicin (Xiao *et al.*, 2003). Furthermore, expression of a kinase-inactive CHK1 in U2OS cells or pharmacological inhibition of CHK1 in NHF1 attenuated the UVC-induced intra-S checkpoint response (Heffernan *et al.*, 2002; Miao *et al.*, 2003). Similarly, siRNA-mediated depletion of CHK1 in HeLa cells caused a reversal of the UVR-induced S-phase checkpoint when DNA fiber spreads were used to visualize active replication units (Chastain *et al.*, 2006). Unlike *CHK2*, *CHK1* is an essential gene whose deletion causes embryonic lethality (Takai *et al.*, 2000). It was shown that CHK1 was phosphorylated on S317 and S345 in Hela or U2OS cells in an ATR-dependent manner following treatment with hydroxyurea or UVR, and that these phosphorylations modulated the activity of CHK1 (Zhao and Piwnica-Worms, 2001). There is some suggestion that these ATR dependent phosphorylations may relieve inhibition by a C-terminal inhibitory domain. Truncations of the C-terminal domain of *Xenopus* CHK1 increases its kinase activity (Oe *et al.*, 2001), while a rat isoform of CHK1 containing only the C-terminus inhibited CHK1 kinase activity *in vitro* (Shann and Hsu, 2001). Although there is evidence for crosstalk between ATR/ATM and CHK1/CHK2, these studies provided strong evidence for CHK1 as the primary mediator of the ATR-dependent inhibition of DNA synthesis in response to UVR.

Initially, it was hypothesized that the ATR/CHK1 mediated S-phase checkpoint response was induced by the same mechanisms that are observed with the ATM-mediated

response to IR. Early studies did observe UV-induced degradation of CDC25A after irradiation with lethal dose of UVR (Goloudina *et al.*, 2003; Hassepass *et al.*, 2003; Mailand *et al.*, 2000). There was speculation that the UV-induced inhibition of replicon initiation might be regulated at the pre-replication complex (pre-RC) and/or the MCM (minichromosome maintenance) helicase complex (Jares *et al.*, 2000). The pre-RC forms at discrete origins of replication and requires the loading of the origin recognition complex (ORC), CTD6, CTD1, and the 6-subunit MCM. This pre-RC is "licensed" and subsequent firing of the origin is regulated by cyclin-dependent kinase phosphorylation of CDC6 and by DDK (DBF4-dependent kinase comprised of CDC7/DBF4) phosphorylation of MCM subunits. It is thought that the DDK-dependent phosphorylation of MCM induces its helicase activity and facilitates unwinding of the duplex DNA at the origins, allowing loading of the DNA polymerase α-DNA primase complex. The *S. pombe* homolog of human *CHK2*, *Cds1,* phosphorylates the spDbf4 protein after treatment with hydroxyurea (Takeda *et al.*, 2001). Similarly, in *Xenopus* extracts an etoposide-induced inhibition of replicon initiation was shown to be correlated with an abrogation of Dbf4 chromatin binding, thereby interfering with DDK activity (Costanzo *et al.*, 2000). The involvement of the DDK complex in the UV-induced inhibition of replicon initiation was further examined in NHF. Overexpression of Flag or Myc-tagged DBF4 attenuated the UVC-induced S-phase checkpoint response, but not that of IR (Heffernan *et al.*, 2007). In addition, the sub-lethal dose of UVC used in this experiment had no influence on CDC25A levels. Similarly, CDC45 binding to chromatin was reduced in human non-small lung carcinoma cells following treatment with BPDE and the inhibition of DNA synthesis also found to be independent of CDC25A degradation (Liu *et al.*, 2006). Although the targets of CHK1 remain unidentified, these data indicated that the UV-induced inhibition of replicon initiation does not depend on degradation of CDC25A as is seen with the IR-induced checkpoint response, but instead likely relies upon regulation of MCM loading to reduce origin firing.

Several other proteins have been identified as mediators of the ATR/CHK1 dependent S-phase checkpoint. The human analog of the TIM (TIMELESS) protein was implicated in the circadian clock of *Drosophila* (Sehgal *et al.*, 1994) and was proposed to have a similar function in mammals (Barnes *et al.*, 2003). This protein has been shown to have UV-induced interactions with CHK1 and ATR/ATRIP (Unsal-Kacmaz *et al.*, 2005) and to interact with MCM2 and DNA polymerase δ (Gotter *et al.*, 2007). TIM and its heterodimeric binding partner, TIPIN (Timeless-interacting protein), were also shown to mediate UV-induced activation of CHK1 (Unsal-Kacmaz *et al.*, 2007). Similarly, the protein CLASPIN was also implicated as an S-phase checkpoint mediator. CLASPIN was identified as a binding partner of CHK1 in *Xenopus* and extracts that were immuno-depleted of CLASPIN showed diminished CHK1 kinase activity (Kumagai and Dunphy, 2000). Analogs of TIM and TIPIN were termed the replication fork protection complex (RFPC) in yeast (Noguchi *et al.*, 2004) and this complex has been proposed to protect stalled replication forks from collapse (Kaufmann, 2009; Smith-Roe *et al.*, 2013).

As previously mentioned, many of the proteins involved in the S-phase checkpoint are essential proteins. In addition, loss of several RFPC proteins has been shown to affect chromosomal integrity (Brown and Baltimore, 2000; Focarelli *et al.*, 2009; Leman *et al.*, 2010; Smith-Roe *et al.*, 2013). It has been suggested that RFPC proteins contribute not only to DNA damage induced S-phase checkpoint signaling, but that stabilization of the replication fork and preservation of chromosomal stability are separate functions of these proteins (Smith-Roe *et al.*, 2013). DNA synthesis, chromosomal aberrations, and checkpoint signaling were examined in NHF cells depleted of RFPC proteins in the absence of exogenous DNA damaging agents. These experiments indicated a separation of checkpoint function from genome protection. For example, cells depleted of ATR showed a marked increase in chromosomal aberrations while cells depleted of CHK1 or TIPIN did not, despite

that depletion of TIPIN caused CHK1 activation. Furthermore, depletion of CHK1 inhibited DNA synthesis while depletion of ATR did not. In cells depleted of the various RFPC members, levels of CHK1 phosphorylation did not seem to correlate with the induction of chromosomal instability or survival in the absence of exogenous damage. These data show a complex interplay between RFPC members that participate in both checkpoint activation and in genome maintenance during normal replication.

Summary of work in this dissertation

The experimental work presented in this dissertation is divided between two chapters. The first details experiments designed to examine potential differences in biological outcomes in normal human dermal cells exposed to different wavelengths of UVR. This introduction has shown that different wavelengths of UVR induce differing types and proportions of DNA damage and that these aberrant DNA structures are induced by potentially different mechanisms. Furthermore, there is much debate about the relative contributions from different wavelengths in initiating and promoting mutagenesis and carcinogenesis. While much of the DNA damage responses have been characterized using UVC, comparatively fewer studies have been conducted utilizing wavelengths that model the more naturally occurring exposures to UVA and UVB. Furthermore, accurate dosimetry of specific types of DNA damage is not often included when reporting biological outcomes produced by exposure to UVR, making it difficult to accurately compare research from different laboratories. The research presented in Chapter 2 was designed to assess the biological outcomes of irradiating human dermal fibroblasts with UVR of different wavelengths and to do so using DNA damage dosimetry to provide a means by which to compare different irradiation sources. CPD and 6-4PP density were quantified and used as biomarkers of exposure following irradiation with UVA, UVB, or UVC. Comparing fluences of UVR that produced equal CPD densities, we assessed cytotoxicity induced by the three

wavelength ranges. Using the shortest (UVC) and the longest (UVA) wavelength range of UVR, we also characterized the activation of the intra-S phase checkpoint and compared the induced mutation frequencies. These experiments showed a striking similarity in the biological outcomes measured when exposure to various wavelengths were compared on the basis of CPD dosimetry. These results help to validate previous DNA damage response research that has utilized non-terrestrial UVC as a model for UVR exposure. In addition, this research highlights the importance of using DNA damage dosimetry or biomarkers to allow meaningful comparisons between UVR sources.

The S-phase checkpoint response to UVR is described as a signaling cascade designed to recognize damaged DNA or abnormal DNA structures and halt or slow new/ongoing DNA replication, thereby reducing the chance that damaged DNA will be replicated prior to its repair. It is overwhelmingly purported to be a protective system and hypothesized to protect against UV-induced mutagenesis. The research presented in Chapter 3 was designed to test this hypothesis. Essential S-phase checkpoint components ATR and CHK1 were each depleted using siRNA, and the UV-induced mutation frequency at the *HPRT* locus was measured. Similarly, mutation frequency was measured after the CHK1 inhibitor TCS2312 was used to block CHK1 kinase signaling and abrogate the S-phase checkpoint response to UVR. Results showed similar mutation frequencies in the irradiated populations with intact or with inactivated intra-S checkpoint responses. These findings challenge the belief that intra-S checkpoint activation helps prevent DNA damage-induced mutations.

CHAPTER 2

CYCLOBUTANE PYRIMIDINE DIMER DENSITY AS A PREDICTIVE BIOMARKER OF THE BIOLOGICAL EFFECTS OF ULTRAVIOLET RADIATION IN NORMAL HUMAN FIBROBLASTS[1]

Introduction

Ultraviolet radiation (UVR) is an established environmental carcinogen that induces DNA damage in basal keratinocytes and melanocytes, potentially leading to cancer development (Gilchrest *et al.*, 1999; Marrot and Meunier, 2008). The UVR spectrum is divided into three wavelength ranges: UVC (100-280 nm), UVB (280-315 nm) and UVA (315-400 nm). Wavelengths in the UVC range are absorbed by the Earth's atmosphere; hence UVR reaching the surface of the planet consists of approximately 5-10% UVB and 90-95% UVA. While the genotoxicity of UVB can be attributed to direct absorption of photons by DNA, the mechanism by which UVA causes genotoxicity is less clear. The predominant view has been that DNA does not readily absorb the energy from UVA and that endogenous photosensitizers are required to transfer the energy of UVA to DNA (Cadet *et al.*, 2005; Mouret *et al.*, 2006). However, experimental evidence that UVA can damage DNA directly has emerged (Jiang *et al.*, 2009; Kuluncsics *et al.*, 1999; Sage *et al.*, 2012). Although the mechanism is in question, it is widely accepted that wavelengths above 300 nm are capable of inducing the most common forms of DNA photodamage, including the

---

[1]Christopher D. Sproul, David L. Mitchell, Shangbang Rao, Joseph G. Ibrahim, William K. Kaufmann, Marila Cordeiro-Stone, manuscript in preparation for submission to *Photochemistry and Photobiology*

cyclobutane pyrimidine dimers (CPD) (Courdavault *et al.*, 2004; Perdiz *et al.*, 2000), and 6-4 pyrimidine-pyrimidone photoproducts (6-4PP) (Besaratinia *et al.*, 2011; Schuch *et al.*, 2009). In addition, there is evidence that long wavelengths of UVR induce oxidative damage to DNA, possibly through the formation of singlet oxygen or other reactive oxygen species, resulting in oxidized bases, such as 8-oxo-7,8-dihydroguanine (8-oxo-dG) (Cadet *et al.*, 2005; Mouret *et al.*, 2006).

Much of the research examining the biological effects of UVR have utilized UVC, while comparatively fewer studies have been conducted with wavelengths that model the more naturally occurring exposures to UVA and UVB. The common use of UVC lamps can be attributed to their availability and low cost, the convenience of using a highly energetic source that allows short irradiation times, and the belief that the most abundant DNA lesion triggering UVR-induced responses are produced by UVA, UVB, and UVC. Indeed, there is evidence that wavelengths in the entire UVR spectrum induce CPD in the nuclear DNA of cultured cells (Besaratinia *et al.*, 2011; Courdavault *et al.*, 2004; Mouret *et al.*, 2006; Snellman *et al.*, 2003), and are mutagenic (Besaratinia *et al.*, 2011; Enninga *et al.*, 1986). Although there is little doubt that the CPD is the primary mutagenic lesion following exposure to UVC or UVB, the role of the CPD in UVA-induced mutagenesis is less clear (reviewed in (Runger and Kappes, 2008)), but cannot be neglected (Jiang *et al.*, 2009; Kuluncsics *et al.*, 1999; Sage *et al.*, 2012).

UVR damage to DNA has been shown to trigger various DNA damage responses, including repair, apoptosis, translesion synthesis (TLS), and the activation of cell cycle checkpoints. In most of these studies, UVC was used to characterize the responses to UVR, including activation of the intra-S checkpoint (Kaufmann *et al.*, 1980b; Kaufmann and Cleaver, 1981). The intra-S checkpoint has been described as an active signaling system that recognizes UV-induced DNA damage and slows progression through S phase, thereby

reducing the probability that damaged DNA will be replicated, potentially lowering the risk for induced mutations (reviewed in (Kaufmann, 2009)). This checkpoint response to UVC was found to require the activity of checkpoint proteins ataxia telangiectasia and Rad3-related (ATR) kinase, and its substrate checkpoint kinase 1 (CHK1), to act on downstream targets to inhibit the firing of new origins of replication (Chastain *et al.*, 2006; Heffernan *et al.*, 2002; Miao *et al.*, 2003) and to slow rates of DNA chain elongation (Petermann *et al.*, 2006; Seiler *et al.*, 2007; Unsal-Kacmaz *et al.*, 2007). Comparatively less research has examined the intra-S checkpoint response to UVA and UVB, despite observations that the spectra of DNA damage induced by these wavelengths are not identical. At present, it is unclear which type of DNA damage is primarily responsible for UV activation of the intra-S checkpoint, although there is evidence that supports CPD, the most abundant, and 6-4PP as the UVC-induced lesions responsible for stalling of replication forks (Kaufmann, 2009).

The main objective of the experiments reported here was to assess the biological outcomes of irradiating human dermal fibroblasts with three sources of UVR, each emitting different spectra of wavelengths. CPD and 6-4PP densities were quantified and used as biomarkers of exposure following irradiation with the UVA, UVB, or UVC sources. Comparing fluences of UV that produced equal CPD densities, we then assessed UV-induced cytotoxicity for these three sources. Using the shortest (UVC) and the longest wavelength range of UVR (UVA), we also characterized the activation of the intra-S checkpoint and compared their mutagenic potential. Our results suggest that in our model system the CPD burden efficiently predicts the cytotoxicity, activation of the intra-S checkpoint, and mutagenicity induced by UVR.

Results

Dosimetry curves

Immunoblotting was first used to assess the induction of CPD in NHF1 cells exposed to UVA, UVB, or UVC (**Figure 2.1**). As expected, UVC was the most efficient UVR source, causing the formation of approximately 34 CPD per Mb of DNA for each 1 J/m^2 increase in incident fluence (slope of the fluence-response curve). UVB and UVA also produced CPD in a fluence dependent manner, although at much lower efficiencies (121 and 9.4 CPD/Mb per kJ/m^2, respectively). These dosimetry curves were used in all subsequent experiments to select exposures to different UVR sources in order to compare their biological effects on an equal CPD density basis.

Later experiments used DNA from independently irradiated NHF1 cultures and RIA to determine the UVR induction of both CPD and 6-4PP in the same DNA samples (**Figure 2.2).** The observed relative densities of 6-4PP per 100 CPD were 14, 11, and 7 for the UVC, UVB, and UVA sources, respectively. UVC was marginally more efficient at producing 6-4PP than UVB, but the difference did not reach statistical significance ($p=0.09$). UVC was significantly more efficient at producing 6-4PP than irradiation with the UVA source used in these experiments ($p=0.04$). DNA from irradiated cells was also analyzed for the presence of 8-oxo-dG, the most common oxidative DNA lesion; 8-oxo-dG was not formed in a fluence responsive manner and was not produced in levels appreciably higher than background (**Table 2.1**).

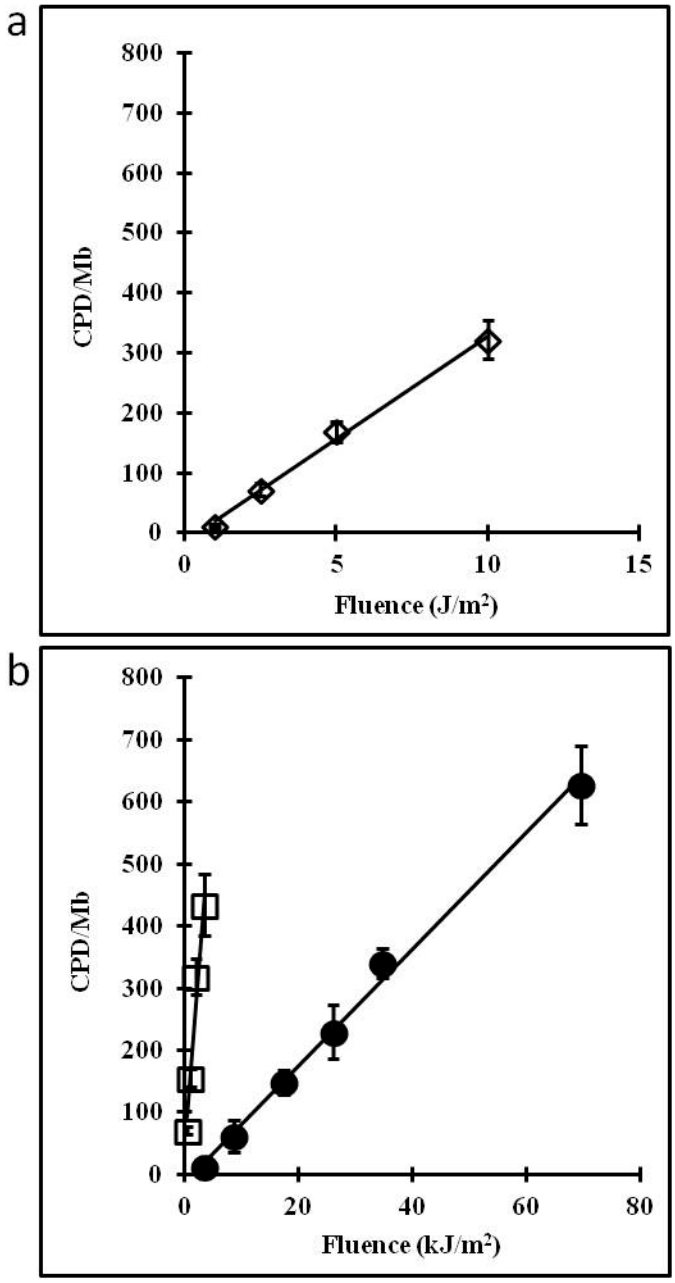

Figure 2.1 CPD dosimetry curves for NHF1 exposed to **a)** UVC (open diamonds) and **b)** UVB (open squares) or UVA (closed cicles). CPD densities determined by immunoblotting, using standard curves prepared with irradiated calf-thymus DNA with known CPD densities, which were independently determined by RIA (each point represents the mean of 2-4 measurements; error bars indicate SEM).

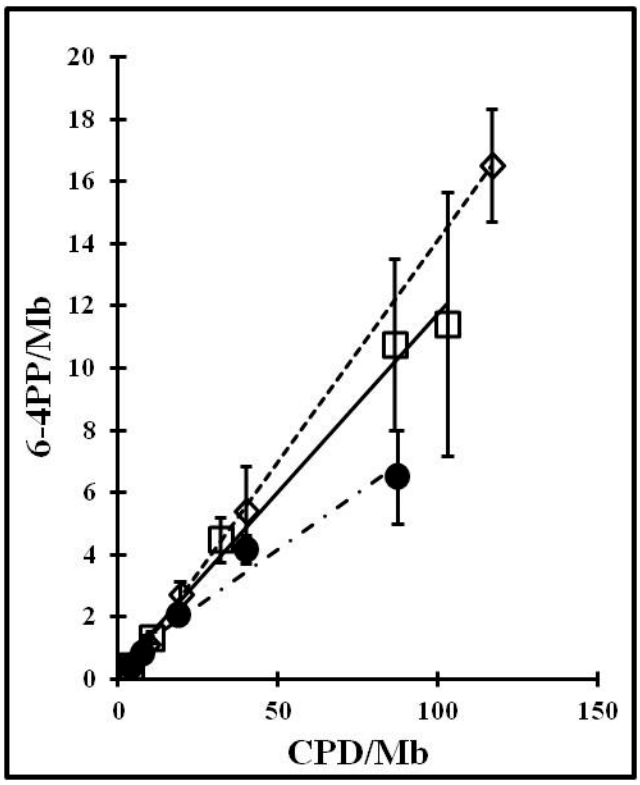

Figure 2.2 6-4PP dosimetry curves. Dose response curves for the formation of 6-4 pyrimidine-pyrimidone photoproduct in NHF1 exposed to UVA (closed circles), UVB (open squares) or UVC (open diamonds) as a function of CPD density. The 6-4PP density produced by UVC was statistically different than that produced by UVA ($p=0.04$ by linear regression analysis). Both lesions were quantified in each sample by RIA (n=3-4, mean ± SEM).

8-oxo-dG/10^6 dG	Experiment 1		Experiment 2		Experiment 3	
background calf thymus DNA1	0.85		0.85		0.68	
background calf thymus DNA2	None determined		2.15		0.82	
% recovery of 8-oxo-dG spiked calf thymus DNA	101%		106%		97%	
CPD/Mb	UVA	UVC	UVA	UVC	UVA	UVC
0.0	1.08		0.71	0.62	0.58	0.58
122.1	1.22		2.20	3.43	1.26	1.16
259.4	1.30		2.28	0.69	1.29	1.72
328.0		1.13				
396.6	1.64		1.53	0.64	0.85	2.58
396.6	1.86					

Table 2.1 Quantification of 8-oxo-dG in NHF1 cells exposed to UVA or UVC. LC/MS/MS was used to quantify 8-oxo-dG levels in NHF1 cells exposed to UVA (0, 14.7, 29.2, or 43.7 kJ/m^2) or UVC (0, 4, 8, 10, or 12 J/m^2). Fluences were chosen to produce equal CPD densities. Assay was performed by Biomarker Mass Spectrometry Core Facility, Center for Environmental Health and Susceptibility (CEHS), University of North Carolina, Chapel Hill as described in Boysen, G. *et al.* (2010). *J. Chromatogr. B. Analyt Technol. Biomed. Life. Sci.***878**, 375-380.

Cytotoxicity

Figure 2.3 shows the cytotoxicity curves for UVA, UVB and UVC, expressed as the percent survival relative to CPD burden. As expected, irradiation with each source of UVR produced a dose-dependent decrease in survival. The increase in fluences required to decrease the surviving fraction from 100% to 37% (D_0) were 16.8 kJ/m^2, 2.0 kJ/m^2, and 5.5 J/m^2, or 159, 236, and 190 CPD/Mb, for UVA, UVB and UVC, respectively. When expressed in terms of the CPD density, UVB and UVC caused similar toxicity profiles ($p=0.41$ for the comparison of D_0 values); while the UVA cytotoxicity curve did not overlap with those for UVB and UVC ($p<0.005$ for both UVA vs. UVB and UVA vs. UVC, linear regression analysis), the differences in the estimated D_0 did not reach statistical significance (UVA vs. UVB $p=0.17$, UVA vs. UVC $p=0.23$).

Activation of the intra-S phase checkpoint

The activation of the intra-S phase checkpoint was examined in NHF1 cells irradiated with either the UVA or the UVC lamps. Should there be significant differences in the biological responses to DNA damage induced by different wavelengths of UVR, they would most likely be observed between the two irradiation sources emitting at the opposite ends of the UV spectrum. Phosphorylation of CHK1 at serine 345 is commonly used as an index of DNA-damage-induced activation of the intra-S checkpoint. Based on the dosimetry curves illustrated in **Figure 2.1**, NHF1 cells were irradiated with fluences of UVA or UVC calculated to produce equal CPD densities. Cells were harvested 45 min post-irradiation and protein extracts were probed for P-CHK1 (S345), total CHK1, and ACTIN (**Figure 2.4a). Figure 2.4b** summarizes the quantification by densitometry of immunoblot signals from three independent experiments. The ratios of P-CHK1 to total CHK1 were normalized to the same

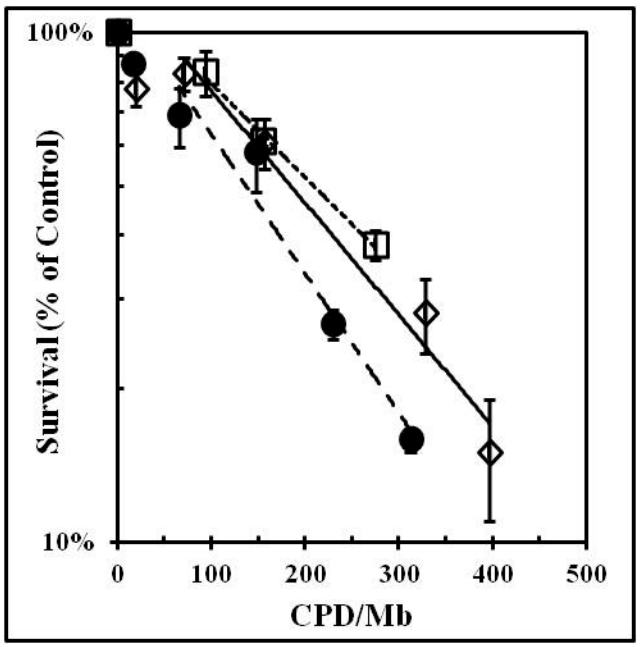

Figure 2.3 Cytotoxicity as a function of CPD burden for NHF1 exposed to UVA, UVB, or UVC. Cytotoxicity as a function of CPD burden for NHF1 exposed to UVA (closed circles), UVB (open squares), or UVC (open diamonds). Percent survival measured by [^{3}H]-thymidine incorporation 72 h post-irradiation as compared to the unirradiated sham (n=2-4, mean ± SEM). There was no statistical difference between the D_0 values expressed in terms of CPD density (Wald test p-values were 0.17 for UVA vs. UVB, 0.23 for UVA vs. UVC, and 0.41 for UVB vs. UVC).

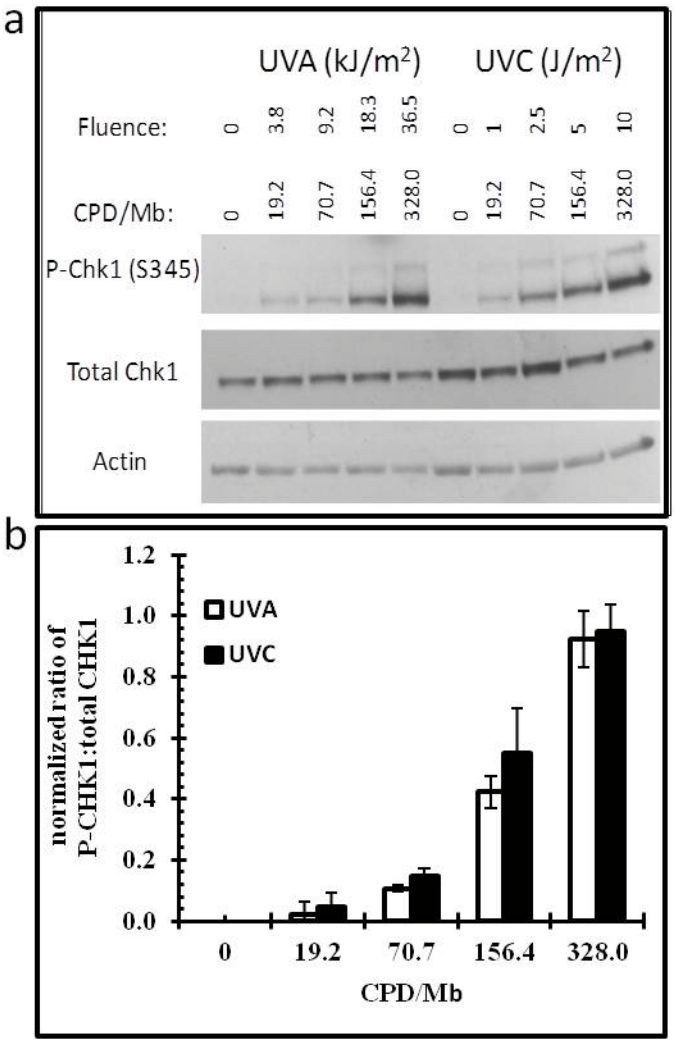

Figure 2.4 CHK1 phosphorylation in NHF1 exposed to UVA or UVC. Fluences of UVA or UVC were chosen so as to produce equivalent CPD burdens. **a)** Immunoblot showing P-CHK1 (S345), total CHK1, and ACTIN. **b)** Quantification of immunoblots (n=3) by densitometry ± SEM. Densitometry values were normalized to the highest ratio of P-CHK1:total CHK1 in each experiment. The normalized ratios of P-CHK1 to total CHK1 produced by the UVA source were not statistically different (Wilcoxon rank-sum test) from those produced by UVC at equal CPD densities.

ratio determined for the sample with the highest signal in each experiment and plotted against CPD/Mb. Both UVA and UVC induced CHK1 phosphorylation at S345 as the CPD burden increased and no statistically significant differences were observed in the magnitude of the responses induced by the two UVR sources.

Intra-S checkpoint activation was also functionally assessed by velocity sedimentation analyses of nascent DNA pulse-labeled with [^{3}H]-thymidine. This technique was used to determine the size distribution of newly replicated DNA and to examine how exposures to UVA or UVC affected that distribution. First, low fluences of UVR were used to examine the selective inhibition of synthesis of low molecular weight (MW), origin-proximal nascent DNA. NHF1 cells were exposed to 3.8 kJ/m^2 UVA or 1 J/m^2 UVC, fluences shown to result in similar CPD burdens (**Figure 2.1**) and cause minimal cytotoxicity (**Figure 2.3**, 86% and 78% survival, respectively). After irradiation, cells were incubated for 30 min, pulse-labeled with [^{3}H]-thymidine for 15 min, harvested and lysed on top of alkaline sucrose gradients (**Figure 2.5**). Low fluences of UVC have been previously shown to selectively inhibit the production of small MW DNA intermediates that initiated DNA synthesis during the 30 min incubation after irradiation or within the 15 min pulse-labeling with [^{3}H]-thymidine (Kaufmann *et al.*, 1980a; Kaufmann and Cleaver, 1981) and that this inhibition is dependent on signaling by the checkpoint kinases ATR and CHK1 (Heffernan *et al.*, 2002; Miao *et al.*, 2003). As a functional biomarker for the inhibition of replicon initiation, reduction in labeling of small MW nascent DNA was used to assess activation of the intra-S phase checkpoint. The observed inhibition was 34 ± 6% after a low fluence of UVA (3.8 kJ/m^2), by comparison to the matched sham control, and 40 ± 7% after 1 J/m^2 UVC.

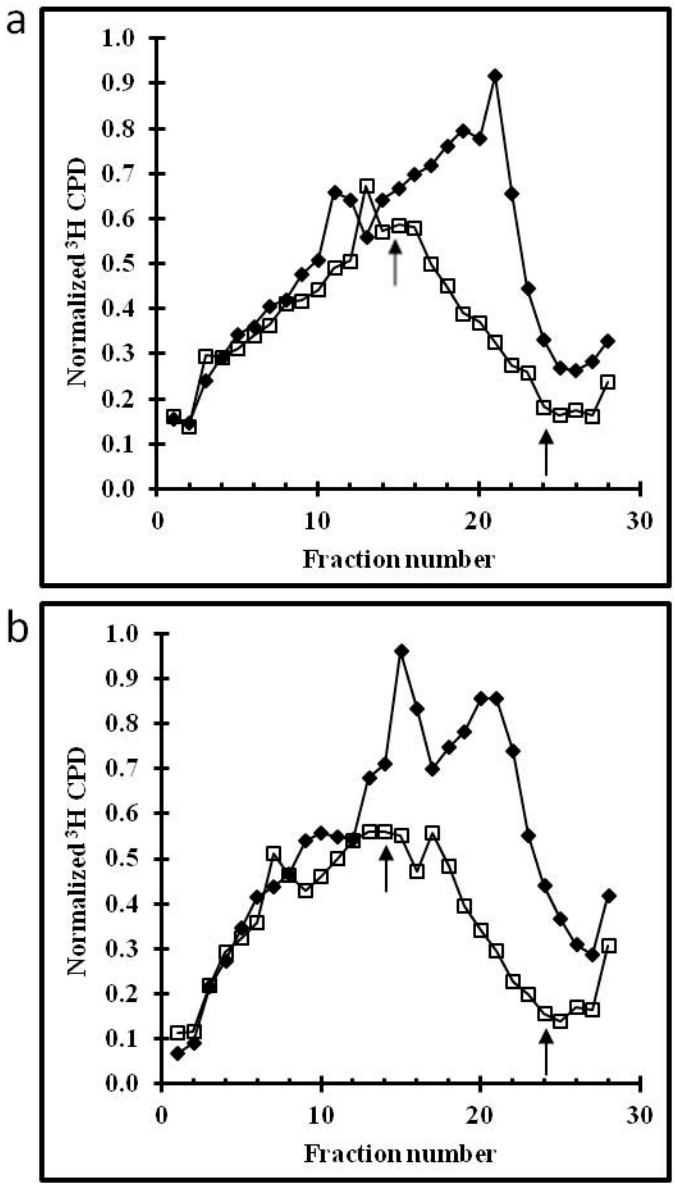

Figure 2.5 Inhibition of replicon initiation by UVC or UVA. Velocity sedimentation analysis of nascent DNA from NHF1 cells exposed to low fluences of **a)** UVC (sham-closed diamonds or 1 J/m^2-open squares) or **b)** UVA (sham-closed diamonds or 3.8 kJ/m^2-open squares). Fluences were chosen so as to induce equal CPD densities (~19 CPD/Mb). Inhibition of small MW DNA, measured from the area under the curve between the two arrows, was 34% ± 6% of sham (UVA) and 40% ± 7% (UVC) n=3 (mean ± SEM), and these values were not statistically different (p=0.4, Wilcoxon rank-sum test).

Velocity sedimentation can also be used to assess the effect of irradiation on DNA strand growth by examining the abundance of labeled DNA intermediates of high MW. Fluences of UVR higher than those used to document the inhibition of replicon initiation also inhibit the production of multi-replicon-sized DNA intermediates in a dose-dependent manner. Once again, fluences were chosen to cause similar CPD densities in cells irradiated with UVA (**Figure 2.6a**) or UVC (**Figure 2.6b**). **Figure 2.6c** summarizes the data from several experiments and shows that DNA strand growth was inhibited as the CPD burden increased, regardless of the source used to irradiate the fibroblasts.

Mutagenesis

UVR-induced mutation frequencies at the *HPRT* locus were measured in NHF1 cells exposed to either UVA or UVC fluences inducing similar densities of CPD. Colonies resistant to 6-thioguanine were counted as mutants lacking functional HPRT and the mutation frequency expressed per 10^6 surviving cells (**Figure 2.7**). Mutagenicity results from one experiment with XPV fibroblasts are included as a positive control, as these cells lack the translesion synthesis DNA polymerase eta and are known to be hypermutable in response to UVR (Bassett *et al.*, 2004). Both the lower fluence (4 J/m^2) and the higher fluence (7.5 J/m^2) of UVC induced mutation frequencies above the matched sham-irradiated controls (p=0.03 and 0.01 respectively). After normalizing for CPD burden, no significant difference was detected in the frequencies of induced mutations between NHF1 cells exposed to UVA or UVC.

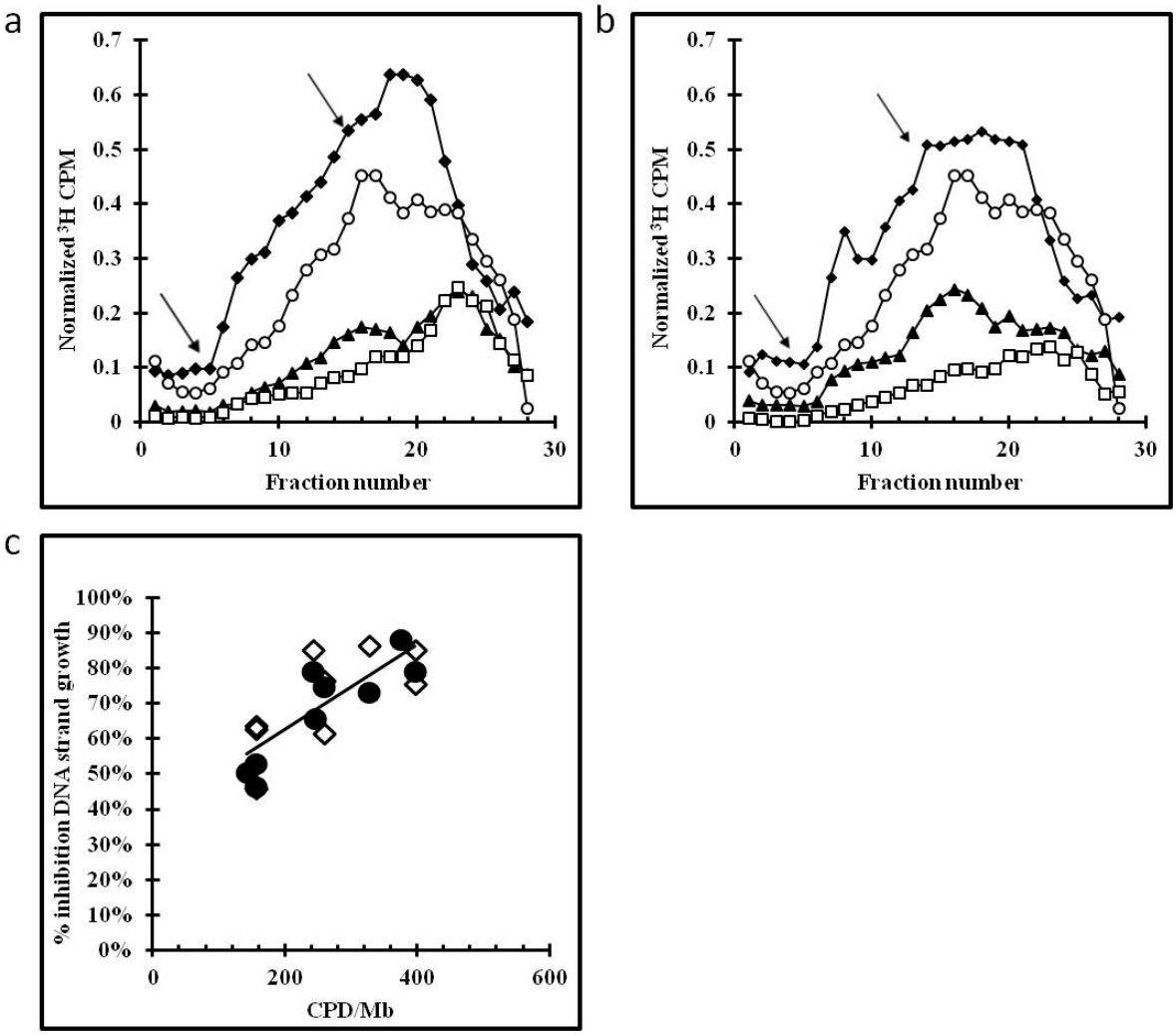

Figure 2.6 Inhibition of DNA strand growth by UVC or UVA. Representative velocity sedimentation analysis of nascent DNA from NHF1 cells exposed to high fluences of **a)** UVC (5, 7.5, 8, 10, or 12 J/m^2) or **b)** UVA (18.3, 27.4, 29.2, 36.5, or 41.6 kJ/m^2). Fluences were chosen to induce equal CPD densities (156, 242, 259, 328, or 397 CPD/Mb, respectively). **c)** Inhibition of DNA strand growth (calculated from the area under curve between the two arrows as compared to sham irradiated) is shown as a function of CPD burden for NHF1 exposed to UVA (closed circles) or UVC (open diamonds). There was no statistical difference in the % inhibition of DNA strand growth by UVA or UVC (linear regression analysis, p=0.59).

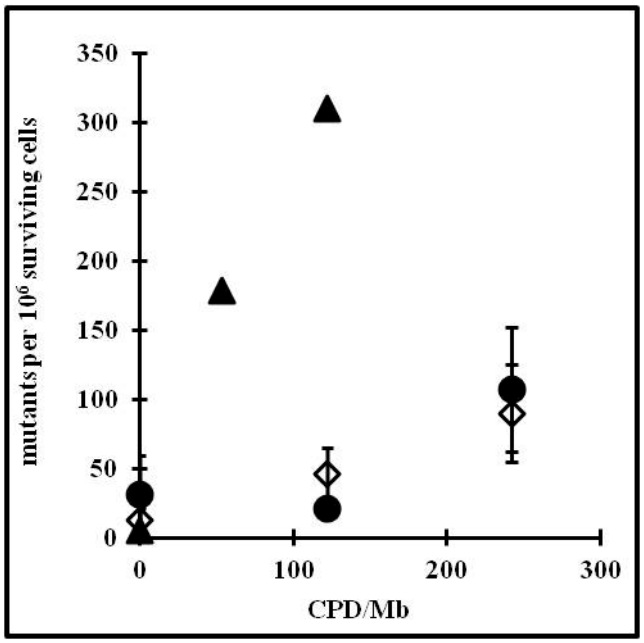

Figure 2.7 UVA or UVC-induced mutation frequency at the *HPRT* locus. *HPRT* mutation frequency in 2359XPV cells (closed triangles, n=1) or NHF1 exposed to UVA (closed circles, n=4) or UVC (open diamonds, n=4) expressed as mutants per 10^6 surviving cells ± SEM. The mutation frequency induced by UVA was not statistically different from that induced by UVC (p=0.2 and 0.69 for 122 or 242 CPD/Mb respectively, Wilcoxon rank-sum test).

Discussion

The health effects of prolonged skin exposures to the sun have been connected mechanistically to the cellular DNA damage induced by UVR. However, there is still controversy over which wavelengths are most dangerous and whether or not exposure primarily to UVA (for example through tanning beds) carries the same risks as sunlight, which also includes wavelengths within the UVB range. The properties of different wavelengths of UVR, in particular skin penetration and efficiency of inducing different types of cellular damage (including those triggering inflammation) have made the detailed investigation of this complex issue quite difficult.

This study focused specifically on DNA damage caused by UVR in cultured human fibroblasts and the attendant biological responses, both shortly after irradiation (activation of the intra-S checkpoint, inhibition of DNA synthesis), as well as the resulting cytotoxicity and frequency of *HPRT* mutations in the surviving populations. Biological effects produced by UVR cannot be compared on the basis of the incident fluence alone, which are often measured at a single wavelength, while the source spectral profiles can vary widely. Therefore, in order to compare biological responses to the UVR sources used in this study, DNA damage dosimetry curves for CPD (**Figure 2.1**) and 6-4PP (**Figure 2.2**) were produced. CPD densities per J/m^2 indicated that UVC was approximately 284 and 3654 times more efficient than UVB and UVA, respectively, in producing this type of DNA lesion. It is well established that short wavelength UVR produces CPD in either irradiated cells or purified DNA in solution more efficiently than long wavelength UVR (Clingen *et al.*, 1995; Douki *et al.*, 1999; Enninga *et al.*, 1986; Kuluncsics *et al.*, 1999). The relative amounts of UVA-induced CPD reported here are higher than other reported values, but this is not surprising given that the lamp used emits ~5.7% of its radiant energy in the UVB range. UVC was also more efficient in producing 6-4PP; after normalization to the CPD density in

the same sample, the density of 6-4 PP per CPD was 1.3 and 2 times higher in DNA from cells exposed to UVC than in those exposed to the UVB and UVA sources, respectively (**Figure 2.2**). This relative 6-4PP production is similar to values reported in human dermal fibroblasts, where UVC induced 1.4 times more 6-4PP per CPD than did irradiation with a narrow-band UVB source (Clingen *et al.*, 1995); but, it is lower than observed in DNA from mouse embryonic fibroblasts, where UVC produced 5.4 times more 6-4PP per CPD than did a monochromatic source of UVB (305nm) (Besaratinia *et al.*, 2011). It is also expected that the 6-4PP density measured in NHF1 exposed to the UVA lamp was produced by UVB wavelengths emitted by this source, as it is generally believed that 6-4PP are not produced by wavelengths greater than 310nm (Besaratinia *et al.*, 2011; Douki *et al.*, 2003; Pfeifer and Besaratinia, 2012).

Survival curves generated using the UVA, UVB, and UVC lamps and constructed against CPD densities suggest that this type of DNA damage was primarily responsible for the induced cytotoxicity, regardless of the radiation source (**Figure 2.3**). The estimated D_0 values were not statistically different, and the CPD densities correlated better with the overall survival than the 6-4PP densities; although 8-oxo-dG was not detected above background, it is possible that the slightly reduced survival observed after UVA irradiation could be due to oxidative damage to other cellular components. Other studies have reported a wavelength-dependent increase in cytotoxicity, with longer wavelengths causing higher inactivation of colony formation, when compared on the basis of equivalent dimer densities (Enninga *et al.*, 1986), or that cytotoxicity in cultured cells irradiated with UVC or UVB correlated best with the 6-4PP density (Clingen *et al.*, 1995). The study reported here, as well as those cited above used the same narrow-band UVB source and were performed with normal human dermal fibroblasts; so the differences described are not likely to be due to different cell types or UVR sources.

CPD density was well correlated with the activation of the intra-S checkpoint in fibroblasts exposed to UVA and UVC. Phosphorylation of CHK1 at S345 (**Figure 2.4**), inhibition of replicon initiation (**Figure 2.5**), and inhibition of DNA strand growth (**Figure 2.6**) were all adequately described by CPD density. The observation that CPD density, and not the 6-4PP density, correlated best with these endpoints is consistent with a model that the CPD, as the most abundant lesion induced by UVR, is the primary UV-induced DNA damage encountered by DNA replication forks, thus initially creating a majority of genome sites where the activation of ATR/CHK1 takes place to trigger the intra-S checkpoint responses.

The time course of inhibition of DNA synthesis and the lesion repair kinetics in human fibroblasts have been used to suggest that CPD were not likely to be predominantly responsible for intra-S phase checkpoint activation. The maximal CHK1 phosphorylation signal and inhibition of DNA synthesis are both reported to occur 45-120 min following UVC irradiation and to recover to basal levels within 6 h post-irradiation (Chen *et al.*, 2009; Kaufmann and Cleaver, 1981). While significant numbers of CPD remain after DNA synthesis has recovered, the kinetics of 6-4PP repair closely match this time course, with more than 80% of the 6-4PP being removed within 6 h post–irradiation (Courdavault *et al.*, 2005). The data presented here, however, are more consistent with the CPD being the lesion primarily responsible for checkpoint activation, and that recovery of DNA synthesis occurs even in the presence of persisting CPD. This interpretation is supported by data showing that UV-induced γ-H2AX foci, also a marker of ATR activation, are formed within the first hour post-irradiation, continue to accumulate 48 h post irradiation, and are reduced by 50% upon CPD photoreactivation (Garinis *et al.*, 2005; Ward and Chen, 2001). Thus, it is plausible that the decay in checkpoint signaling is related not to repair of the less frequent 6-4PP (although it could be a contributing factor), but to the efficiency of translesion synthesis

(TLS) across UV-induced CPD; indeed, TLS-defective XP-V fibroblasts display delayed intra-S phase checkpoint recovery following UV-irradiation (Bi *et al.*, 2005) despite having normal rates of nucleotide excision repair (Boyer *et al.*, 1990; Tung *et al.*, 1996).

Other studies have examined the influence of long wavelength UVR on the intra-S checkpoint. Irradiation of SV40-transformed normal human fibroblasts and AT-fibroblasts showed that both displayed inhibition of DNA synthesis following irradiation with UVA or UVC (Girard *et al.*, 2008). Treatment with 5 mM caffeine (an ATM and ATR inhibitor) abrogated this inhibition in both cell types following irradiation with UVC but not with UVA, suggesting that the ATR/CHK1 pathway is dispensable to UVA-induced inhibition of DNA synthesis. However, these studies also reported a relatively low production of CPD (less than 2 TT CPD/Mb) at UVA fluences that caused both significant cytotoxicity and inhibition of DNA synthesis; these findings led the authors to conclude that DNA damage (TT CPD, 8-oxo-dG, or strand breaks) was not contributing to inhibition of DNA synthesis despite evidence that CHK1 was being activated. Instead, they suggested that the inhibition of DNA synthesis could be explained by UVA-induced ROS causing oxidation of replication proteins. Such an effect is less likely in the studies reported here, since our UVA irradiation conditions appear to have produced significantly lower levels of UVA-induced ROS (**Table 2.1**).

No differences in mutation frequencies at the *HPRT* locus were observed in NHF1 cells irradiated with UVA or UVC when compared on an equal CPD basis (**Figure 2.7**). These data suggest that in this model system, the CPD is the UVR-induced photolesion predominantly contributing to mutagenesis. It is also noteworthy that formation of 8-oxo-dG was not detectable (**Table 2.1**) at levels above background, suggesting that oxidative damage to DNA did not likely contribute significantly to UVR-induced mutagenesis. The data presented here are at odds with other findings examining the effect of UVR wavelength on mutagenesis. Human fibroblasts irradiated with longer wavelengths of UVR displayed higher

mutation frequencies than those irradiated with short wavelength UVR when compared on the basis of equal T4 endonuclease sensitive sites, a common marker for CPD (Enninga *et al.*, 1986). Authors suggested that either long wavelength UVR produced additional DNA damage that contributed to mutagenesis, or interfered with the efficient repair or lesion bypass of CPD. Approximately two-fold higher mutation frequencies were observed in a shuttle vector carried by human embryonic kidney cells when cultures were irradiated with equitoxic fluences of UVA as compared to UVB (Robert *et al.*, 1996b). Mutation frequency in primary neonatal human fibroblasts was also higher in cells irradiated with UVA as compared to roughly equitoxic fluences of UVB (Kappes *et al.*, 2006), but quantitative toxicity and dosimetry data were not provided. Each of these studies relied upon the use of different UVR sources, possibly accounting for some of the divergence in the results. Furthermore, the lack of dosimetry data in some cases makes comparisons between the studies difficult, and emphasizes the utility of quantitative DNA damage markers.

The observation of similar mutation frequencies in NHF1 irradiated with UVA and UVC are consistent with other research examining the mutation spectrum induced by different wavelengths of UVR. The C:G→T:A transition and the CC:GG→TT:AA tandem mutations are considered UV signatures arising from replication past CPD and 6-4PP (Ziegler *et al.*, 1993). Sequencing of the *HPRT* gene in primary neonatal fibroblasts showed that C:G→T:A transitions were by far the most abundant UV-induced mutation induced by either UVA or UVB, and that these tended to occur in pyrimidine rich hotspots (Kappes *et al.*, 2006). In addition, most of these mutational hotspots were shared by cells irradiated with UVA or UVB, suggesting that these mutations were formed by a common mechanism. Similarly, C:G→T:A transitions at dipyrimidine sites were also the most common base pair change found in mutants isolated from the epidermis of transgenic mice harboring λ-phage-based *lacZ* mutational reporter genes after irradiation with UVA or UVB (Ikehata *et al.*,

2008). These findings support the conclusion that the CPD is the primary lesion associated with UVR-induced mutagenesis.

One limitation of the current analysis is the use of dermal fibroblasts that are not the target of UVR carcinogenesis in skin. We have compared the effects of UVC, UVB and UVA on human dermal melanocytes. We found that melanocytes displayed levels of phosphorylation of checkpoint kinases in response to UVR similar to fibroblasts (see Supplemental Material **Figure S2.1**). Normal human melanocytes were also found to repair CPD and 6-4PP with kinetics similar to fibroblasts (see Supplemental Material **Figure S2.2** and (Gaddameedhi *et al.*, 2010)). Thus, the radiobiological responses reported here for fibroblasts are likely to hold true for melanocytes.

Taken together, the results described in this paper constitute strong evidence that CPD density is the most predictive biomarker for the biological effects derived from UVR exposure. We recognize that the broad-spectrum UVA lamp used in this study emits ~5.7% UVB wavelengths (based on manufacturer's spectral output curves), but emphasize that this percentage is similar to that present in natural sunlight and that similar UVA sources are increasingly utilized in biological research. This UVB representation is expected to have contributed to the abundance and relative proportions of CPD and 6-4PP, and thus also to the biological responses measured in the fibroblasts irradiated with the UVA lamp. Therefore, the importance of including quantitative DNA damage dosimetry to studies examining UVR-induced biological responses cannot be emphasized enough.

Support

This work has been supported by National Institutes of Health awards (RO1 ES015856 to MCS, T32 ES007126 to the UNC Curriculum in Toxicology for the support of CDS, P30 CA16086 to the Lineberger Comprehensive Cancer Center, P30 ES10126 to the

Center for Environmental Health and Susceptibility). We would like to acknowledge Bruna Brylawski and Jenna Brophy for technical help and Dr. Dennis Simpson for the information in Supplemental material **Figure S2.1**.

Materials and methods

Cell culture

The normal human fibroblast cell line NHF1-hTERT was derived from neonatal foreskin fibroblasts (Boyer *et al.*, 1991) and immortalized by ectopic expression of the catalytic subunit of human telomerase (Heffernan *et al.*, 2002). The xeroderma pigmentosum variant (XPV) cell line GM02359-hTERT (XP115L0) was derived in the laboratory of Dr. Roger A. Shultz (University of Texas Southwestern Medical Center, Dallas, TX; (Ouellette *et al.*, 2000)) and clone 1B (Cordeiro-Stone *et al.*, 2002) was compared with NHF1 in the studies reported here. Cells were cultured in Minimum Essential Medium (MEM) supplemented with 2 mM L-glutamine and 10% fetal calf serum. GM02359-hTERT cells were additionally supplemented with 1x MEM non-essential amino acids (Gibco). All cell cultures were maintained at 37°C in humidified 95% air and 5% CO_2.

Irradiation

Cells were rinsed in phosphate buffered saline (PBS) prior to irradiation and all cell culture plates were irradiated with lids removed. See **Figure S2.3** for the relative emission spectra for each lamp used. UVC irradiation was performed with a germicidal fluorescent lamp (Sylvania G8T5, 90% emission at 254 nm). UVB irradiations were performed with two Philips TL20W/01 NB-UVB fluorescent lamps emitting between 300 and 315 nm, with a maximum emission at 312 nm. UVA irradiations were performed with four Houvalite F20T12BL/HO PUVA lamps, emitting between 300 and 400 nm, with a maximum emission at 350 nm. UVC irradiations were performed with no liquid in the plates, while PBS was

used to cover the cultures during UVB and UVA exposures (as detailed below). Sham irradiated plates were handled the same way minus the exposure to UVR. These control plates were covered with aluminum foil and placed in the irradiation chamber along with those exposed to the highest fluence used in the experiment. Lamp irradiance was measured using a UVX Digital Radiometer (UVP, LLC) and the following sensors: UVX-25 (250-290nm range, calibrated at 254 nm), UVX-31 (280-340 nm range, calibrated at 310 nm) and UVX-36 (335-380 nm range, calibrated at 365 nm).

Cytoxicity

UVR-induced inhibition of [^{3}H]-thymidine incorporation was measured as an index of cytotoxicity, as described previously (Kaufmann *et al.*, 2003; Yamada *et al.*, 2000). This short-term assay for inhibition of cell proliferation yields results in close agreement with those based on reduction of efficiency of colony formation (Kaufmann *et al.*, 2003). Logarithmically growing cells were seeded in 6-well plates at 1000 cells per well. The following day, cells were rinsed with PBS and irradiated with increasing fluences of the specified UVR sources; 500 µL or 1 mL PBS were used to cover cells in each well during irradiation with UVB or UVA, respectively. Approximately 72 h post-irradiation, cells were pulse labeled for 60 min at 37°C in medium containing 2 µCi/mL [^{3}H]-thymidine. Afterwards, the plates were placed on ice and the wells rinsed 2x with cold PBS. Cells were then fixed in 5% trichloroacetic acid (TCA) for 30 min and rinsed 2x with 5% TCA and 2x with 95% ethanol. Fixed cells were allowed to dry overnight and then dissolved for 1 h in 1 mL of 0.3 M sodium hydroxide. Equal volumes of solubilized cells were analyzed by liquid scintillation counting.

Immuno-slot blot quantification of CPD

Cell cultures were irradiated in 10-cm dishes after rinsing and removing the liquid from the plates (UVC), or while covered with 2 mL (UVB) or 6 mL (UVA) PBS. DNA from irradiated cells was purified using a Qiagen DNeasy Blood and Tissue kit, using RNase A to remove RNA in the samples and CPD quantified as published (Karbaschi *et al.*, 2012). After denaturation at 100°C for 10 min, 200 ng of DNA was combined with an equal volume of 2 M ammonium acetate and placed on ice. Each DNA sample was spotted onto a nitrocellulose membrane (equilibrated in 1 M ammonium acetate) in triplicate, using a Minifold slot-blot manifold (Schleicher & Shuell). Membranes were then washed in 5x Saline Sodium-Citrate (SSC) buffer for 15 min in a 37°C water bath, and dried in a vacuum oven for 30 min at 80°C. After blocking in 5% powdered milk in TBST (0.5% Tween-20, 10 mM Tris-HCl, 10 mM NaCl, pH 7.4), membranes were probed with mouse anti-CPD antibody (Cosmo-Bio, NMDND001). Following secondary antibody application (HRP-conjugated, GE Healthcare), enhanced chemiluminescence (ECL) was used to detect on film the antibody-dependent signal from each DNA band. Densitometry of film bands was performed using an Alpha Innotech Fluor-Chem HD2. Each membrane contained a standard curve prepared from UVC-irradiated calf thymus DNA in which the CPD density had previously been determined by radioimmunoassay (RIA).

Radioimmunoassay

DNA damage was quantified using RIA. RIA is a competitive binding assay between radiolabeled DNA and sample DNA for antisera raised against UV-irradiated DNA. DNA damage frequencies in samples used for the standard curve were determined using HPLC tandem mass spectrometry (Thierry Douki, CEA, Grenoble). These details, as well as those

concerning the specificities of the RIAs and standards used for quantification, are described in (Berton and Mitchell, 2012; Mitchell, 1996; Mitchell, 2006).

Western blotting and antibodies

Cells were harvested by trypsinization 1 h after irradiation, pelleted and flash frozen in liquid nitrogen. Cell pellets were resuspended in urea lysis buffer (8 M urea, 5 M NaH_2PO_4, 1 M Tris-HCl pH 8) for 30 min on ice and then clarified by centrifugation at 16000 x g and 4°C. Protein concentrations were determined using the Bio-Rad Protein Assay kit. Protein lysates were combined with equal volumes of loading buffer (125 mM Tris pH 6.8, 20% glycerol, 10% β-mercaptoethanol, 4% sodium dodecyl sulfate, 0.05% bromo-phenol blue) and equal amounts of protein were loaded onto BioRad Criterion-TGX 4-15% gradient gels (run for approximately 150-200 V for 2-4 h). Size-separated proteins were transferred (100 mA, overnight) onto a nitrocellulose membrane, and blocked in 5% powdered milk in TBST. The following antibodies were used: rabbit anti-P-CHK1 S345 (2348s Cell Signaling), mouse anti-CHK1 (SC-8408, Santa Cruz), goat anti-ACTIN (SC-1616, Santa Cruz). Following incubation with secondary antibody (HRP-conjugated, GE Healthcare), bands were visualized on film by ECL. Densitometry of film bands was performed using an Alpha Innotech Fluor-Chem HD2**.**

Velocity sedimentation

The steady-state size distribution of nascent DNA was determined 45 min after UV irradiation by centrifugation in an alkaline sucrose density gradient as previously described (Day *et al.*, 2011; Kaufmann *et al.*, 1980b). Cells were uniformly pre-labeled by incubation with 5-10 nCi/mL [^{14}C]-thymidine for at least 36 h during logarithmic growth. Medium containing [^{14}C]-thymidine was removed overnight and cells treated the following day. Cells for alkaline sucrose gradient experiments were grown in 60 mm dishes and covered with 2

mL PBS during UVA irradiations. After UV-irradiation, cells were incubated for 30 min in reserved medium and then pulse-labeled with 25 µCi/mL [^{3}H]-thymidine for 15 min. Cells were washed, then scraped on ice into 0.1 M NaCl, 0.01 M EDTA (pH 8) and 0.5 ml added to an equal volume of lysis buffer (1 M NaOH, 0.02 M EDTA) on top of an alkaline sucrose gradient (5-20% sucrose in 0.4 M NaOH, 2 M NaCl, 0.01 M EDTA). These gradients were left under fluorescent lighting for 45 min and then centrifuged in a Beckman SW32Ti rotor at 25000 rpm and 20°C for 5 h. Gradients were fractioned into equal volumes through a hole punched in the bottom of the centrifuge tube and acid-precipitable material filtered onto glass microfiber filters (Whatman GF/C 24mm), which were then analyzed by liquid scintillation counting. All experiments included cells pre-labeled with [^{14}C]-thymidine, but not pulse-labeled with [^{3}H]-thymidine, which were used to measure the ^{14}C CPM values detected in the ^{3}H channel (spillover) during liquid scintillation counting. Normalized ^{3}H CPM were the counts in each fraction detected in the ^{3}H channel, corrected for the ^{14}C spillover, and divided by the total ^{14}C in the gradient (proportional to the number of cells analyzed).

HAT selection

Cells used for mutagenesis experiments were preselected for functional HPRT by expanding cultures for 10-14 days in medium supplemented with 1 x HAT (Bassett *et al.*, 2004). The 100x lyophilized HAT solution contains 10 mM sodium hypoxanthine, 40 M aminopterin, and 1.6 mM thymidine. Aliquots of HAT selected cells were frozen and stored and a new aliquot was used for every *HPRT* mutagenesis experiment. Cell cultures were expanded in normal medium without HAT for 10-14 days prior to mutagenesis experiments.

Mutagenesis

Cells were plated at 5x10^{5} per 10-cm dish (2 dishes per treatment) and irradiated the following day. Cell cultures were irradiated after rinsing and removing the liquid from the

plates (UVC), or while covered with 6 mL PBS (UVA). These cultures were maintained in logarithmic growth for 4-6 population doublings prior to selection. *HPRT* mutants were selected by plating $4x10^4$ cells per 10-cm dish (55 dishes per treatment) in medium containing 40 μM 6-thioguanine. Colony forming efficiency was determined at the time of mutant selection by plating 400 cells per dish in medium lacking 6-thioguanine. After 2 weeks, colonies were fixed in 3:1 methanol:acetic acid and stained with 0.05% crystal violet. Colonies with more than 50 cells were counted. Mutation frequencies were calculated from the number of plates without any mutant colonies, using the Poisson distribution as follows: [-ln (number of plates without 6-thioguanine resistant colonies/total number of plates)]/[(number of cells plated for selection) x (colony-forming efficiency at time of selection)].

Statistical methods

Statistical comparisons were performed in order to determine whether 6-4PP density, cytotoxicity, CHK1 phosphorylation, inhibition of replicon initiation, inhibition of DNA strand growth, and mutagenicity varied significantly between different sources of ultraviolet radiation. The linear regression model was used to carry out the data analysis for estimating various parameters of interest with appropriate 95% confidence intervals, and hypothesis testing. Specifically, the linear model was used to model the density of 6-4PP and the inhibition of DNA strand growth as response variables with the density of CPD, the radiation source, and their interactions as covariates. Wald statistics were used to determine the statistical significance of the comparisons. The Wilcoxon rank sum test was used to do the

group-wise comparison at different CPD levels at various sources of UVR for cell survival percentage, normalized ratios of P-CHK1 to total CHK1, inhibition of replicon initiation, and the mutation frequencies. Exact test statistics were used to determine the statistical significance of the comparisons. All statistical analyses were performed using SAS 9.3 (SAS Institute Inc., Cary, NC).

Supplemental material

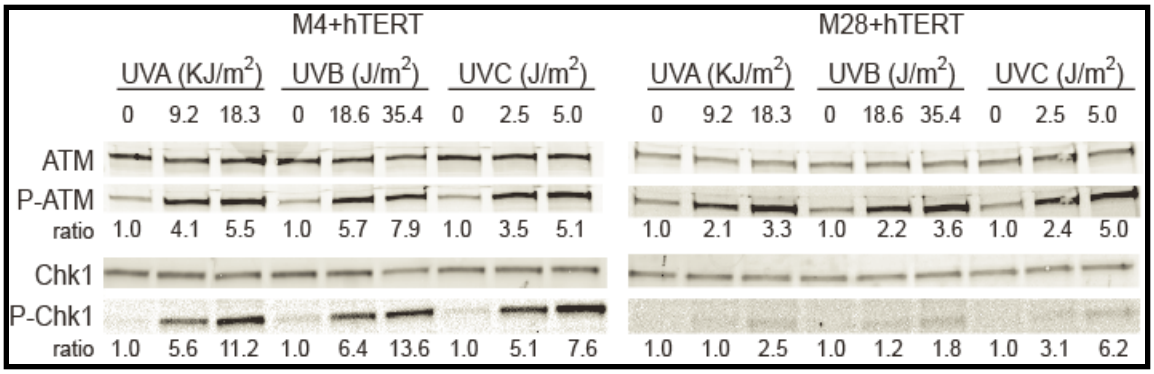

Figure S2.1 Activation of the intra-S checkpoint by UV-induced DNA damage in normal human melanocytes. Activation of checkpoint kinases by UVR-induced DNA damage in normal human melanocytes. Lightly pigmented NHM4+TERT and heavily pigmented NHM28+TERT melanocytes were sham-treated or irradiated with UVC, UVB (a broad-band source emitting 280-370 nm, peak emission at 316 nm) or UVA using fluences pre-determined to induce equal CPD densities in human fibroblasts. After 30-min incubation, cells were harvested for immunoblot analysis of the phosphorylation status of ATM (P-ATM, Cell Signaling 4526; ATM, Santa Cruz SC-7230) and CHK1. P-ATM/ATM and P-Chk1/Chk1 ratios were normalized to the sham-treated control. The lower ratios determined for the M28+hTERT melanocytes are expected to be due to an attenuation of the DNA damage burden in these heavily pigmented cells. Experiment performed by Dr. Dennis Simpson.

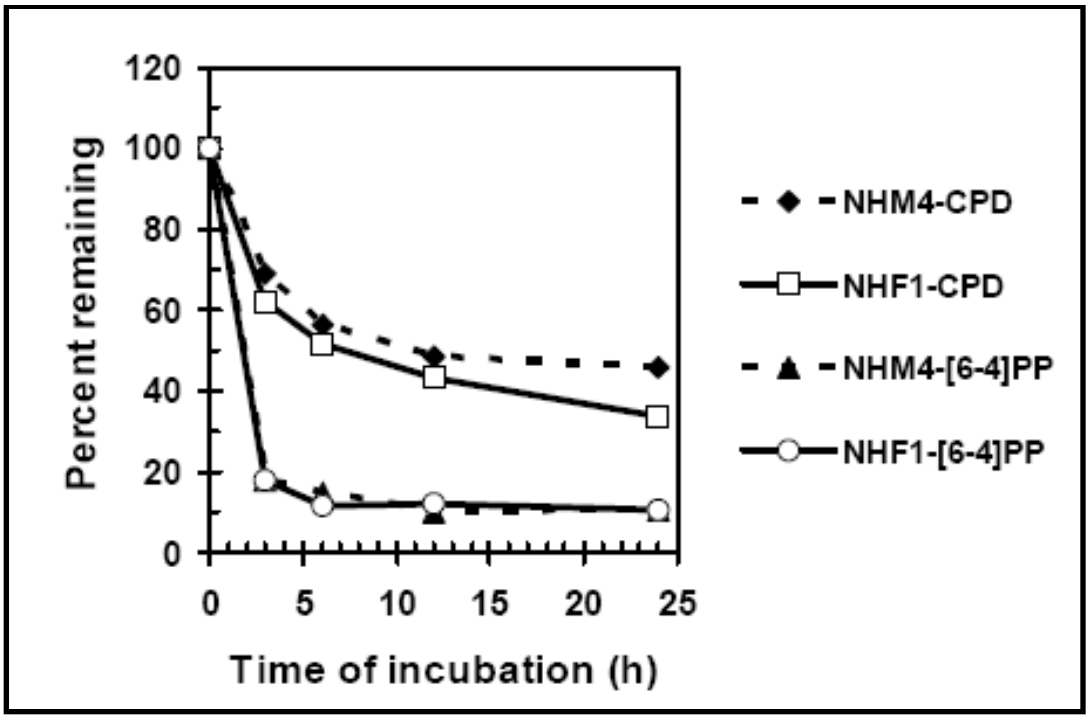

Figure S2.2 Repair of CPD or 6-4PP in NHF1 and NHM4. Confluent cultures of NHF1 or NHM4 were irradiated with 12 J/m^2 UVC and harvested 0, 3, 6, 12, or 24 h post irradiation (experiment performed in the laboratory of Dr. William Kaufmann). DNA was purified and CPD and 6-4PP were quantified by RIA in the laboratory of Dr. David Mitchell.

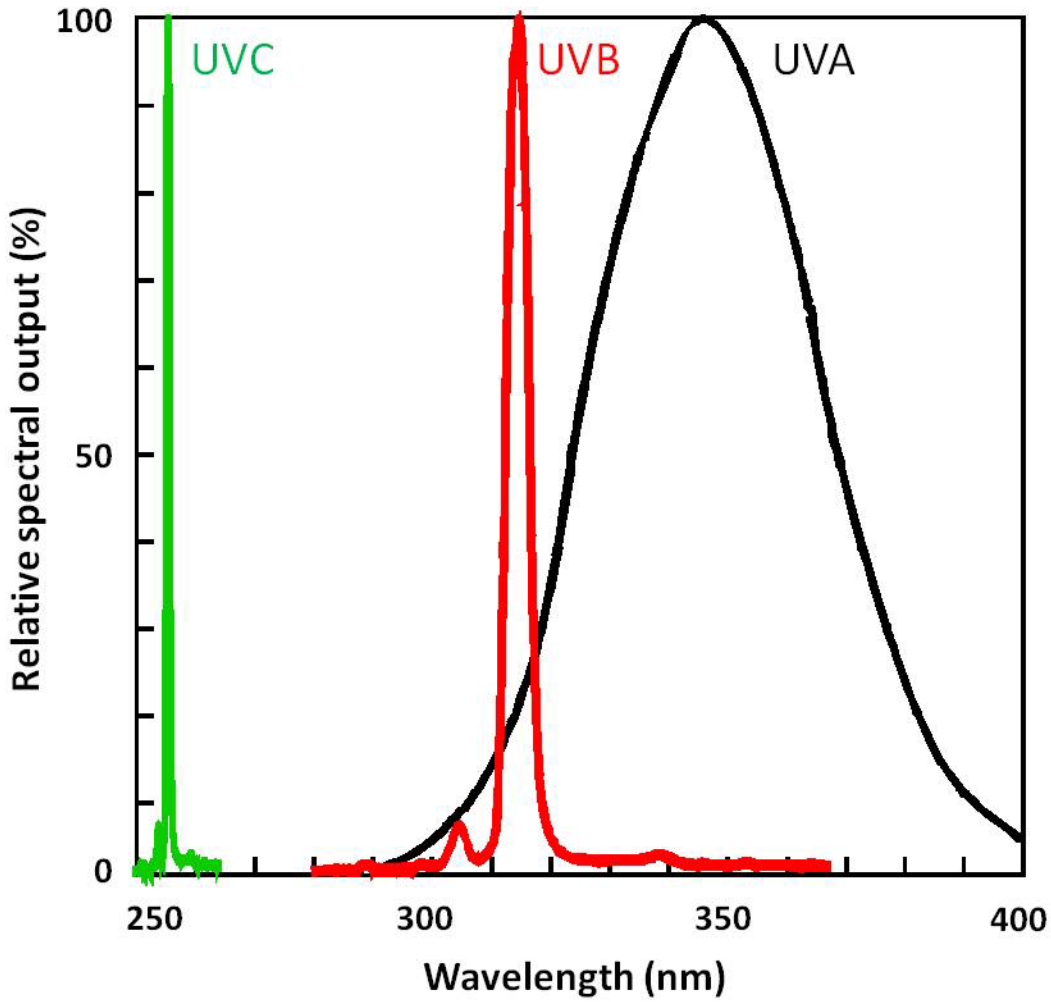

Figure S2.3 Relative spectral output for UVA, UVB, and UVC sources used in these experiments. UVC irradiation was performed with a germicidal fluorescent lamp (Sylvania G8T5, 90% emission at 254 nm). UVB irradiations were performed with two Philips TL20W/01 NB-UVB fluorescent lamps emitting between 300 and 315 nm, with a maximum emission at 312 nm. UVA irradiations were performed with four Houvalite F20T12BL/HO PUVA lamps, emitting between 300 and 400 nm, with a maximum emission at 350 nm.

CHAPTER 3

IS ACTIVATION OF THE INTRA-S CHECKPOINT IN HUMAN FIBROBLASTS AN IMPORTANT FACTOR IN PROTECTION AGAINST UV-INDUCED MUTAGENESIS?[2]

Introduction

The capacity to replicate and segregate the entire genome with high fidelity is a hallmark of normal division cycles. Furthermore, preventing replication of damaged DNA decreases the potential for mutations (Konze-Thomas *et al.*, 1982). Cellular DNA constantly experiences damage, both as a consequence of normal cellular metabolism and respiration, and as a result of environmental insults. In order to cope with such genomic damage, cells have evolved a network of DNA damage responses (DDR) (Giglia-Mari *et al.*, 2011), consisting of DNA repair mechanisms, damage tolerance pathways, and cell cycle checkpoints.

Cell cycle checkpoints are systems in place to recognize damaged DNA, or aberrant DNA structures, and activate signaling cascades designed to halt or slow progression through the cell cycle, thus maximizing the time to repair such damage before DNA is replicated or segregated to progeny. Indeed, checkpoint failures have been shown to result in chromosomal abnormalities, developmental defects, and predisposition to cancer (Kastan and Bartek, 2004; Kerzendorfer and O'Driscoll, 2009). Upon sensing damaged DNA, cell

[2] Christopher D. Sproul, Shangbang Rao, Joseph G. Ibrahim, William K. Kaufmann, Marila Cordeiro-Stone, prepared as manuscript for submission to *Carcinogenesis*

cycle checkpoints inhibit progression out of the G_1 and G_2 phases of the cell cycle, while the intra-S checkpoint slows progression through S-phase (Kastan and Bartek, 2004).

The intra-S checkpoint can be divided into two main signaling cascades that respond to different forms of DNA damage. The first recognizes double strand breaks in DNA, such as those induced by ionizing radiation (IR). The intra-S checkpoint response to IR requires the proteins ATM, MRE-11, RAD50 and NBS1 and involves activation of the checkpoint kinases CHK1 and CHK2, promoting proteolytic degradation of CDC25A. Loss of the CDC25A phosphatase prevents removal of the inhibitory phosphorylation at tyr15 of CDK2, thus maintaining this kinase inactive, and preventing CDC45 loading and initiation at new replication origins (Kastan and Bartek, 2004). ATM also maintains the intra-S checkpoint response by signaling through the cohesion subunits Smc1 and Smc3 (Kastan and Bartek, 2004; Kaufmann, 2009). The second main signaling cascade recognizes bulky DNA adducts, such as those induced by ultraviolet (UV) radiation or benzo[a]pyrene diolepoxide. This checkpoint response to UV was found to require the activity of checkpoint proteins ataxia telangiectasia and Rad3-related (ATR) kinase, and its target CHK1, to act on downstream substrate(s) to inhibit the firing of new origins of replication (Chastain *et al.*, 2006; Heffernan *et al.*, 2002; Miao *et al.*, 2003) and to slow down rates of DNA chain elongation (Petermann *et al.*, 2006; Seiler *et al.*, 2007; Unsal-Kacmaz *et al.*, 2007). At sub-lethal fluences of UV, the ATR/CHK1 pathway has been shown not to depend on degradation of CDC25A, but rather it has been proposed to act on the DBF4-dependent kinase to prevent CDC45-dependent activation of the MCM helicase, thus inhibiting new replicon initiation (Heffernan *et al.*, 2007; Lee *et al.*, 2012).

It is well established that loss of functional ATM increases IR-induced mutation frequency (Xue *et al.*, 2009) and predisposes mammals to lymphomas and other malignancies (Reiman *et al.*, 2011). Although *ATM* is widely recognized as a tumor-

suppressor gene, it is unclear whether this function depends primarily on the activation of the ATM-dependent intra-S checkpoint or on ATM's role in other DNA damage responses. In contrast, loss of *Atr* causes embryonic lethality in mice (Brown and Baltimore, 2000; de Klein *et al.*, 2000), while Seckel syndrome is a consequence of an *ATR* hypomorphic splice mutation. Seckel syndrome manifests as a developmental disease, with patients exhibiting dwarfism, microcephaly, and mental retardation, but cancer is not typically associated with the disorder (Kerzendorfer and O'Driscoll, 2009). Abrogation of the ATR/CHK1 pathway has clearly been shown to inhibit the intra-S checkpoint to UV (Heffernan *et al.*, 2002; Miao *et al.*, 2003), and to lead to an increase in chromosomal instability (Smith-Roe *et al.*, 2013). Despite these observations, it is less clear whether abrogation of the ATR/CHK1-dependent S-phase checkpoint influences mutagenesis. To address this question, we employed siRNA-mediated depletion of ATR or CHK1, or pharmacological inhibition of CHK1 kinase function, to inactivate the intra-S checkpoint and measured mutation frequency at the *HPRT* locus in UV-irradiated human fibroblasts. The results described here support the conclusion that in the presence or absence of the rapid activation of intra-S checkpoint responses, UV-irradiated normal human fibroblasts acquire the same burden of mutations.

Results

Depletion of ATR or CHK1 abrogated the intra-S phase checkpoint triggered by UV

The activation of the intra-S checkpoint in UV-irradiated NHF1 was assessed by examining changes in the steady-state distribution of sizes of nascent DNA pulse-labeled with ^{3}H-thymidine. Responses were compared in populations pre-treated with a non-targeted control (NTC) siRNA and those with siRNA-mediated depletion of ATR or CHK1. **Figure 3.1a** illustrates the siRNA-mediated depletion of ATR, which in the irradiated cells was accompanied by a severe reduction in phosphorylation of its substrate CHK1, a known mediator of UV-induced S-phase checkpoint activation (Chastain *et al.*, 2006; Heffernan *et al.*, 2002; Miao *et al.*, 2003). Velocity sedimentation analyses showed that fibroblasts pre-treated with the NTC-siRNA (**Figure 3.1b**) displayed a stereotypical reduction in the abundance of small molecular weight (MW) nascent DNA when exposed to a low fluence of UVC. The selective reduction in abundance of this size class of origin-proximal, newly synthesized DNA represents a functional indicator of the inhibition of initiation of replication origins that were scheduled to fire post-irradiation (Kaufmann *et al.*, 1980a; Kaufmann and Cleaver, 1981; Miao *et al.*, 2003). Depletion of ATR (**Figure 3.1c**) interfered with this selective inhibition of the synthesis of small MW nascent DNA, thus demonstrating the abrogation of the intra-S checkpoint response of inhibition of replicon initiation. Similarly, inhibition of this S-phase checkpoint response was confirmed following siRNA-mediated depletion of CHK1 (**Figure 3.2**).

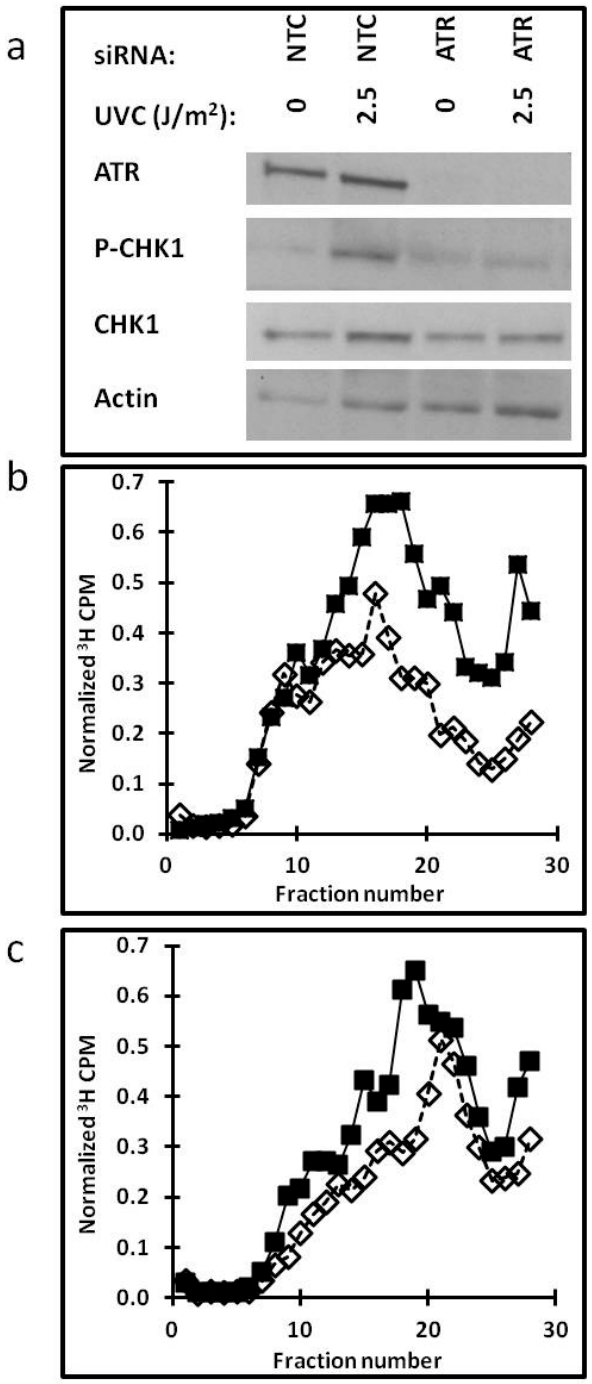

Figure 3.1 Depletion of ATR abrogates the intra-S checkpoint response: a) NHF1 cells were electroporated with NTC or ATR siRNA and UV-irradiated (sham or 2.5 J/m^2) 48 h following electroporation. Cells were harvested and protein extracts examined by immunoblotting 1 h after irradiation. **b and c)** Velocity sedimentation analysis of nascent DNA from NHF1 cells exposed to UVC (sham-closed squares or 2.5 J/m^2-open diamonds) 48 h post-electroporation with **b)** NTC or **c)** ATR siRNA; the irradiated cells were incubated for 30 min and then pulse labeled with ^{3}H-thymidine for 15 min.

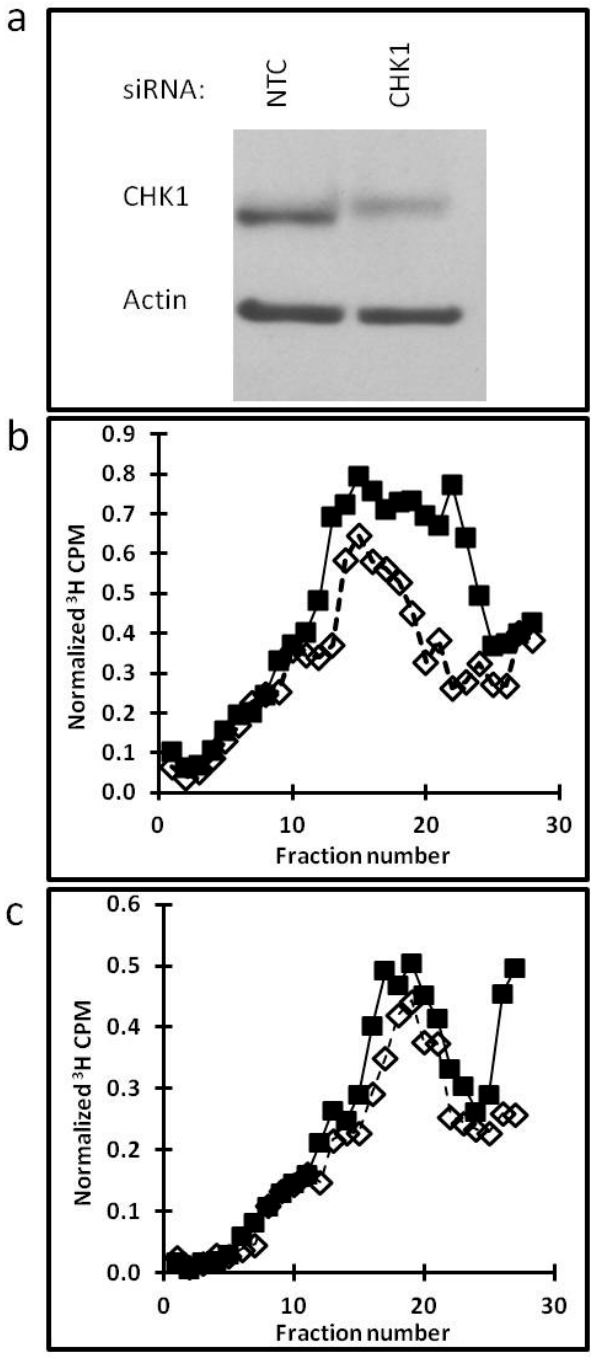

Figure 3.2 Depletion of CHK1 abrogates the intra-S checkpoint response: a) NHF1 cells were electroporated with NTC or CHK1 siRNA. Cells were harvested 24 h later and protein extracts examined by immunoblotting. **b and c)** Velocity sedimentation analysis of nascent DNA from NHF1 cells exposed to UVC (sham-closed squares or 2.5 J/m^2-open diamonds), following electroporation with **b)** NTC or **c)** CHK1 siRNA. Cells were irradiated 24 h post-electroporation and 30 min later were pulse labeled with ^{3}H-thymidine for 15 min.

Depletion of ATR or CHK1 did not increase the UV-induced mutation frequency at the *HPRT* locus

Mutation frequency at the *HPRT* locus was measured in NHF1 cells following depletion of ATR or CHK1 and irradiation with increasing fluences of UVC (**Figure 3.3**). In cultured fibroblasts treated with the NTC-siRNA, UV induced the formation of 6-thioguanine resistant mutant colonies at frequencies above the background (measured in the sham-irradiated populations) ($p<0.05$ for sham vs. 7.5 J/m^2, one-sided Wilcoxon rank-sum test, or by linear regression of all fluences). As a pre-validation of the adopted methodology, under the laboratory conditions used in this study, NHF1 cultures were treated with siRNA targeting the translesion synthesis (TLS) DNA polymerase η (Choi and Pfeifer, 2005b); an elevated recovery of *HPRT* mutant colonies was observed, as compared to the NTC siRNA-treated population, even at fluences ≤ 4 J/m^2 (see Supplemental material**, Figure S3.1**). In contrast, cells depleted of CHK1 or ATR did not display mutation frequencies higher than those treated with control siRNA (**Figure 3.3**).

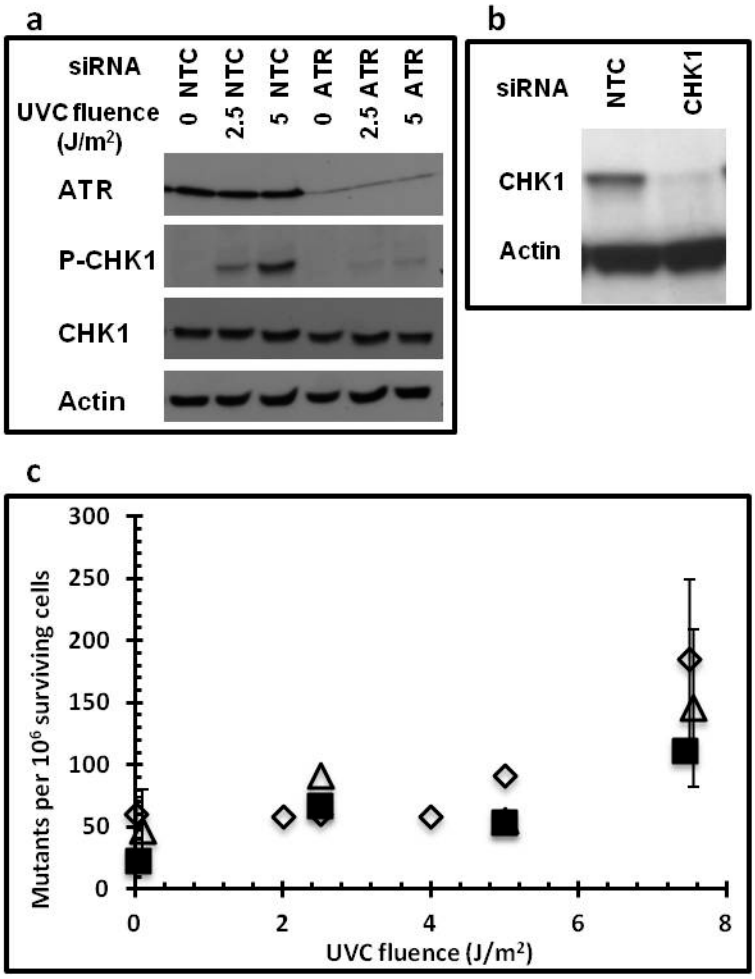

Figure 3.3 Depletion of ATR or CHK1 does not increase UV-induced mutation frequency at the *HPRT* locus: a) Depletion of ATR in cells used for mutagenesis experiment. NHF1 cells were electroporated with NTC or ATR siRNA and irradiated (sham, 2.5, or 5 J/m^2) 48 h following electroporation. Cells were harvested and protein extracts examined by immunoblotting 1 h after irradiation. **b)** Depletion of CHK1 in cells used for mutagenesis experiment. NHF1 cells were electroporated with NTC or CHK1 siRNA. Cells were harvested 24 h later and protein extracts examined by immunoblotting. **c)** UV-induced (0, 2.5, 5, or 7.5 J/m^2) *HPRT* mutation frequencies in NHF1 following depletion of ATR (open triangle) or CHK1 (closed squares) or NTC (open diamonds) expressed as mutants per 10^6 surviving cells ± SEM. Values for sham or 7.5 J/m^2 were slightly offset on figure to allow for clear illustration of error bars. In NTC-treated cells, UV induced a mutation frequency statistically higher than that measured in the sham-irradiated cells ($p<0.05$ for sham vs. 7.5 J/m^2, one-sided Wilcoxon rank-sum test, or by linear regression of all fluences). Depletion of ATR or CHK1 did not cause a significant difference in UV-induced mutation frequency ($p=0.86$ and 0.63, respectively, Wilcoxon rank-sum test).

Pharmacological inhibition of CHK1 with TCS2312 abrogated the UV-induced intra-S phase checkpoint

The results described above were confirmed by experiments in which an alternative approach was employed to inactivate the intra-S checkpoint. Instead of depleting the cells of the two major kinases involved in the activation of this checkpoint, a CHK1 inhibitor (TCS2312) was used to block the signaling pathway while retaining normal cellular protein levels. First, the effect of increasing concentrations of this inhibitor on overall DNA synthesis rates was measured. The lowest concentrations inhibiting DNA synthesis were tested for their effects on the intra-S checkpoint response of inhibition of replicon initiation (see Supplemental material**, Figures S3.2-S3.4**). As was observed following depletion of ATR or CHK1, treatment of fibroblasts with 1 µM TCS2312 reversed the UV-induced selective inhibition of small MW nascent DNA observed in the control population irradiated with 1 or 2.5 J/m^2 UVC, indicating a blockage in the S-phase checkpoint signaling cascade (**Figure 3.4** and Supplemental material, **Figure S3.4**).

CHK1 inhibition did not increase the UV-induced mutation frequency at the HPRT locus

Mutation frequencies at the *HPRT* locus were measured in NHF1 cells following treatment with 1 µM TCS2312 and irradiation with 0, 2.5, 5, or 7.5 J/m^2 UVC (**Figure 3.5**). NHF1 cells irradiated in the presence or absence of inhibitor formed 6-thioguanine resistant mutant colonies in a fluence-dependent manner ($p<0.005$, linear regression analysis). Despite abrogation of the S-phase checkpoint through pharmacological inhibition of CHK1, *HPRT* mutation frequencies were no different than those observed in cells not receiving the inhibitor.

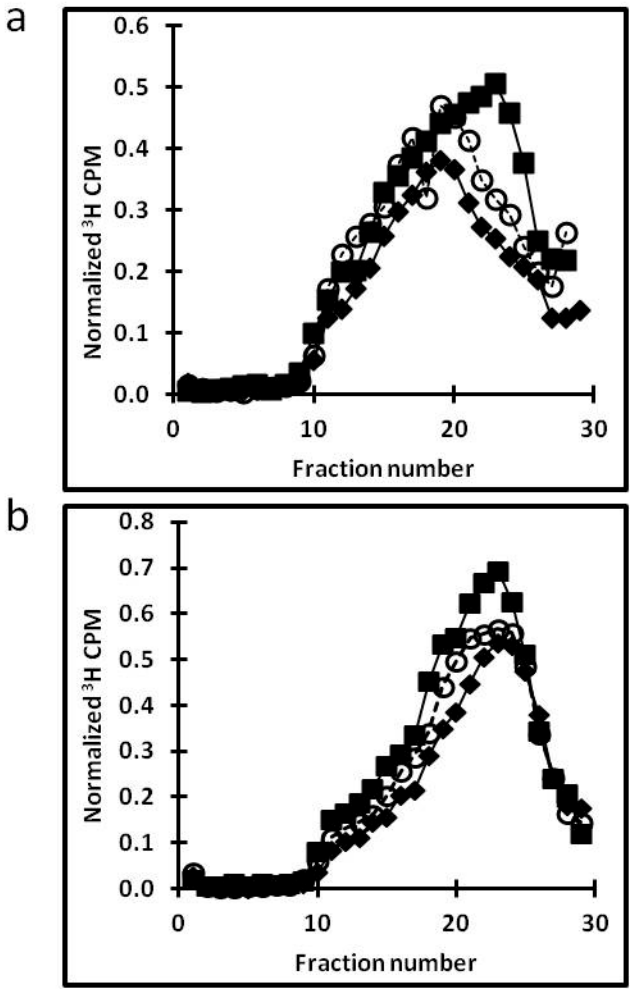

Figure 3.4 CHK1 inhibitor TCS2312 abrogates the intra-S checkpoint response: Velocity sedimentation analysis of nascent DNA from NHF1 cells treated with the CHK1 inhibitor TCS2312. Cells were treated with **a)** vehicle or **b)** 1 µM TCS2312 30 min prior to irradiation with 0 (closed squares), 1 (open circles), or 2.5 (closed diamonds) J/m^2 and inhibitor remained until cells were harvested. Cells were pulse-labeled with ^{3}H-thymidine (15 min) 30 min post-irradiation.

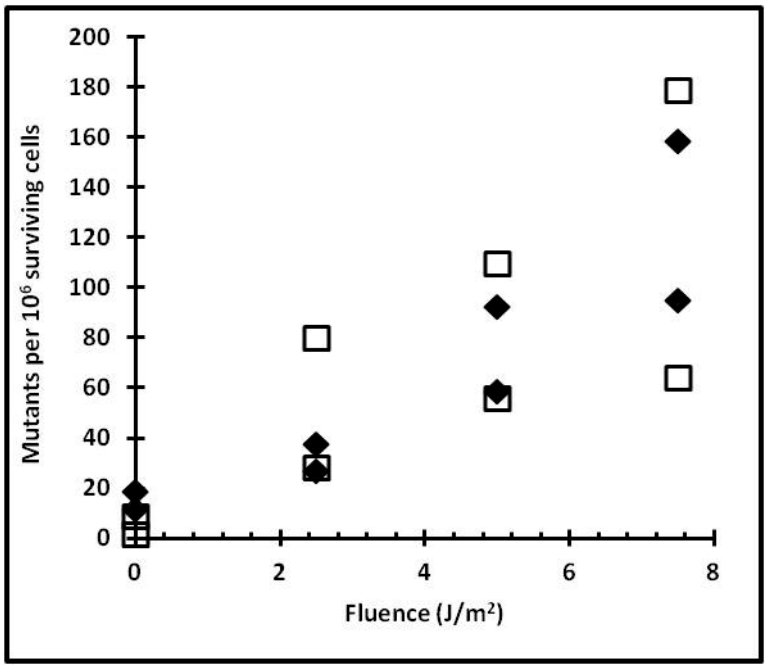

Figure 3.5 CHK1 inhibitor TCS2312 does not increase UV-induced mutation frequency at the *HPRT* locus: UV-induced (0, 2.5, 5, or 7.5 J/m^2) *HPRT* mutation frequencies in NHF1 following treatment with vehicle (closed diamonds) or 1 µM TCS2312 (open squares) expressed as mutants per 10^6 surviving cells (2 experiments, all points shown). In both vehicle and TCS2312 treated cells, UV induced a fluence-dependent increase in mutation frequency ($p<0.005$, linear regression analysis). The UV-induced mutation frequency was not different between cells treated with vehicle or inhibitor ($p=0.97$, linear regression analysis)

Colony forming efficiency and UV-induced cytotoxicity following ATR/CHK1 depletion or CHK1 inhibition

In the course of performing the mutagenesis studies described above, colony forming assays were done in each experiment to assess the effect of siRNA-mediated depletion of CHK1 or ATR, or inhibition of CHK1, on overall cell survival and on UV-induced cytotoxicity. Depletion of either ATR ($p=0.03$, one-sided Wilcoxon rank-sum test) or CHK1 ($p=0.01$, one-sided Wilcoxon rank-sum test) decreased colony forming efficiency in the absence of UV by 63% or 40%, respectively, as compared to the colony forming efficiency of NTC siRNA-treated cells; similarly, inhibition of CHK1 by TCS2312 reduced colony forming efficiency by 51% compared to the vehicle treated cells (**Figure 3.6a**). Loss of ATR or CHK1 (**Figure 3.6b**), or treatment with TCS2312 (**Figure3.6c**), also sensitized NHF1 to UV-induced cytotoxicity ($p<0.0001$ for both siRNA depletions, $p<0.001$ for inhibitor, by linear regression analysis).

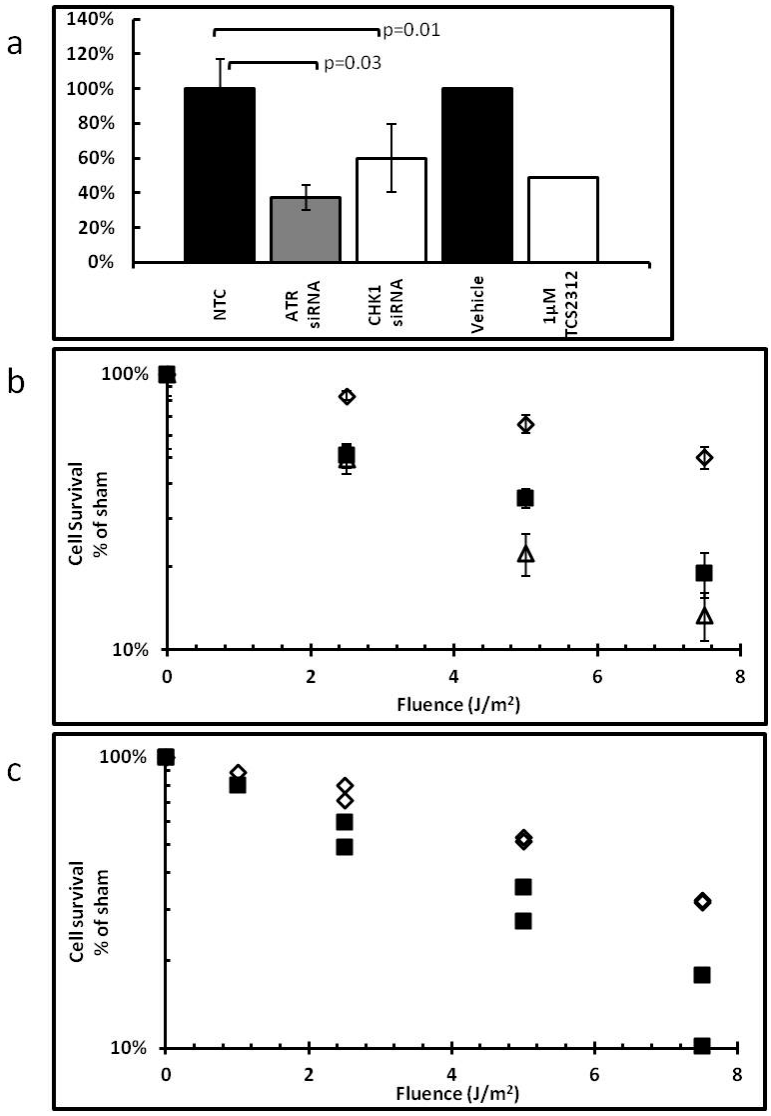

Figure 3.6 Influence of ATR or CHK1 depletion, or CHK1 inhibition, on colony forming efficiency or UV-induced cytotoxicity: a) Colony forming efficiency of cells depleted of CHK1 (n=4) or ATR (n=6), or treated with 1 µM TCS2312 (n=2) as compared with either the NTC (n=10) or vehicle (n=2) treated cells. Depletion of ATR (p=0.03, one-sided Wilcoxon rank-sum test) or CHK1 (p=0.01, one-sided Wilcoxon rank-sum test) decreased colony forming efficieny from that of NTC treated cells. **b)** UV-induced cytotoxicity of NHF1 after siRNA-mediated depletion of NTC (open diamonds), ATR (open triangles) or CHK1 (closed squares) as measured by colony forming efficiency (n=3-9, ± SEM). Depletion of ATR or CHK1 increased UV-induced cytotoxicity ($p<0.0001$ for both depletions, linear regression analysis). **c)** UV-induced cytotoxicity of NHF1 after treatment with vehicle (closed diamonds), or 1 µM TCS2312 (open squares) as measured by colony forming efficiency (2 experiments, all points shown). The UV-induced cytotoxicity in cells treated with inhibitor was greater than that of vehicle treated cells ($p<0.001$, linear regression analysis).

Discussion

Nucleotide excision repair, DNA polymerase η-dependent translesion synthesis (TLS), and cell cycle checkpoints are known to minimize the consequences of UV-induced DNA damage. Xeroderma pigmentosum (XP) is a genetic disorder characterized by dramatic UV sensitivity and a >1000-fold predisposition to skin cancers in areas exposed to solar radiation (Cleaver, 2005). XP is primarily caused by mutations in nucleotide excision repair genes, highlighting the importance of this pathway in protecting against UV-induced mutagenesis and carcinogenesis (Lehmann *et al.*, 2011). Similarly, XP patients of the variant complementation group (XPV) lack functional DNA polymerase η, which is required for efficient synthesis across UV-induced photoproducts (Masutani *et al.*, 1999). XPV patients also display increased sensitivity to sunlight, with patients typically developing skin cancers between the ages of 20 and 30 (Kannouche and Stary, 2003). To date it has not been established that aberrant cell cycle checkpoints contribute directly to UV-induced carcinogenesis. Although not proven to be cancer drivers, there is evidence that the G1 and G2 checkpoints are defective in some melanoma cell lines (Carson *et al.*, 2012; Kaufmann *et al.*, 2008; Omolo *et al.*, 2013), but there is no evidence that the intra-S checkpoint is abrogated in cancers. The prevailing paradigm has been that checkpoints decrease the probability that damaged DNA will be replicated, allowing time for nucleotide excision repair to remove template lesions. The intra-S checkpoint, in particular, has been hypothesized to minimize mutagenesis by inhibiting the replication of damaged DNA (Kaufmann, 2009), or by improving the efficiency of TLS across DNA photoproducts by facilitating PCNA ubiquitination (Bi *et al.*, 2005; Kaufmann, 2009; Yang and Zou, 2009) and recruitment of DNA polymerase η (Gohler *et al.*, 2011; Speroni *et al.*, 2012).

Absent or malfunctioning components of the IR-induced DDR that regulate cell cycle checkpoint pathways lead to a number of human disorders, including ataxia telangiectasia

(AT), AT-like disorder, Nijmegen breakage syndrome, and Li Fraumeni syndrome. Mutations in *ATM*, *NBS1*, *MRE11* and *CHK2* have been linked to increased cancer susceptibility, and ATM-deficient cells have been shown to be hypermutable in response to IR (Xue *et al.*, 2009). The proteins coded by these genes are involved in multiple facets of the IR-induced DDR, including double strand break repair and multiple cell cycle checkpoints (Kastan and Bartek, 2004); hence, it is not clear if loss of the intra-S checkpoint contributes to the increase in susceptibility to malignancy. Mutations identified as causing Seckel syndrome, either in *ATR*, *ATRIP*, or *PCNT*, result in impaired UV-induced DDR (Alderton *et al.*, 2004; Griffith *et al.*, 2008; Ogi *et al.*, 2012), but elevated cancer risk is not typically associated with this disease. It is unclear whether a malfunctioning ATR/CHK1-dependent intra-S checkpoint results in increased mutation frequencies in cells exposed to agents that induce bulky DNA lesions (e.g. UV or benzo[a]pyrene diolepoxide). Results shown here confirmed that upon depletion of ATR or CHK1 the intra-S checkpoint was not activated by UV. Similarly, pharmacologic inhibition of the CHK1 kinase abrogated the UV-induced inhibition of replicon initiation. However, the UV-induced mutation frequency at the *HPRT* locus was not increased relative to matched controls. These results suggest that loss of ATR/CHK1 signaling, at least during the first S phase following UV exposure when cells must cope with the highest density of DNA photoproducts, does not result in higher mutation frequencies, even at a locus (*HPRT*) where point mutations, as well as small or large deletions, result in the same phenotype (6-thioguanine resistance).

To date, little information is available regarding the role of the ATR/CHK1 pathway as a tumor suppressor. However, some insight can be derived from research describing germline or somatic mutations that are presumed to affect this pathway, or by examining data from animal models targeting ATR/CHK1. A germline mutation in the FAT domain of *ATR* in an autosomal-dominant oropharyngeal cancer syndrome (Tanaka *et al.*, 2012), or a

mutation in the checkpoint mediator *CLSPN* in the germline of a familial breast cancer case (Zhang *et al.*, 2009), did not impair intra-S checkpoint activation as measured by CHK1 phosphorylation. Somatic mutations in *ATR* and *CHK1* have also been reported in endometrial, colorectal, and stomach cancers, particularly in mismatch repair deficient cells with microsatellite instability (MSI) (Lewis *et al.*, 2007; Menoyo *et al.*, 2001; Vassileva *et al.*, 2002). It is unclear whether or not these mutations compromise the activation of the intra-S checkpoint, and whether they are cancer drivers or passenger mutations. One MSI+ colon cancer cell line, heterozygous for an *ATR* truncation mutation, was shown to be impaired in the UV-induced phosphorylation of CHK1 and the late-S/G2 arrest induced by topotecan (Lewis *et al.*, 2005). In this same study, chronic myelogenous leukemia cells transiently transfected with an *ATR* truncation mutant allele displayed a similar phenotype while retaining expression of endogenous ATR, suggesting that the truncation mutation acts in a dominant negative manner. We cannot rule out the possibility that a dominant negative ATR or CHK1 could influence UV-induced mutation frequency. However, such a mechanism would most likely not depend on the inhibition of CHK1 kinase activity, as we did not observe a change in UV-induced mutation frequency upon pharmacological inhibition of CHK1 kinase.

Animal models for *ATR* or *CHK1* heterozygosity have also shown enhanced tumorigenesis (Brown and Baltimore, 2000; Fang *et al.*, 2004; Gilad *et al.*, 2010; Liu *et al.*, 2000; Tho *et al.*, 2012) or tumor progression (Tho *et al.*, 2012). The reported effects, however, often require synergistic combination with a cancer-driver mutation. For example, loss of one allele of *Chk1* or *p53* in mouse mammary tissue did not result in tumor formation, but when combined, the loss of one allele at each locus resulted in 60% tumor formation (Fishler *et al.*, 2010). Similarly, *Atr+/- ,Mlh-/-* mice developed cancer at much higher rates (71%) than their *Atr+/-* (0%) or *Mlh-/-* (17%) littermates (Fang *et al.*, 2004). It is known that

Atr and *Chk1* knockout mice are not viable (Brown and Baltimore, 2000; de Klein *et al.*, 2000; Liu *et al.*, 2000) and that loss of either protein enhances cytotoxicity; therefore, the tumorigenic effects described above might depend on a threshold of expression of these proteins. The implications to our findings would be that below this threshold, cell survival is compromised to the point that enhanced mutagenesis may not be observed in our *in vitro* system. It has yet to be determined if moderately depleted levels of ATR or CHK1, such as those observed in heterozygous knockout animals, would allow cell survival at the cost of genomic instability and increased mutagenesis.

There is evidence that intra-S checkpoint signaling affects TLS (Bi *et al.*, 2005; Gohler *et al.*, 2011; Speroni *et al.*, 2012; Yang *et al.*, 2008), and it is conceivable that intra-S checkpoint inhibition is also inhibiting efficient TLS. Because mutagenesis requires replication of the damaged DNA, error-prone TLS is considered a prominent driver of UV-induced mutagenesis. Thus, even if intra-S checkpoint inhibition was allowing newly fired replication forks to encounter UV-induced DNA damage sites, TLS would be required to replicate across the photolesions, and to potentially induce mutations. If ATR or CHK1 were important for efficient bypass synthesis (in addition to their known checkpoint functions), it stands to reason that the depletion of these enzymes might inhibit TLS and reduce mutation frequency. It has been suggested that ATR, CHK1, and other components of the replication fork protection complex, not only operate cooperatively to activate the intra-S checkpoint, but that they possess separate functions for preservation of intrinsic chromosomal stability (Smith-Roe *et al.*, 2013); also that loss of ATR or CHK1 increases genomic instability at common fragile sites (Casper *et al.*, 2002; Durkin *et al.*, 2006). Common fragile sites tend to be replicated late in S phase; the formation of secondary structures within the fragile sites is thought to slow progression of replication forks (Durkin *et al.*, 2006; Durkin and Glover, 2007). It is of note that the active *HPRT* gene is replicated early in S-phase (Schmidt and

Migeon, 1990). Perhaps the primary function of the intra-S checkpoint proteins is to preserve genomic stability at difficult to replicate regions and/or regions replicated late in S-phase, and that inhibition of replicon initiation in response to UV is not of primary importance in minimizing UV-induced mutations in regions of the genome that are replicated more easily or early in S-phase.

The results reported here show that severe depletion of ATR/CHK1 did not increase UV-induced mutagenesis, perhaps as a consequence of preferential cytotoxicity in cells most depleted of CHK1 or ATR, or decreased TLS efficiency. There has been increasing interest in developing ATR or CHK1 kinase inhibitors as therapeutics designed to sensitize cancer cells to the cytotoxic effects of clinical drugs (Chen *et al.*, 2012). Our results agree with many others showing that CHK1 inhibition sensitizes cells to DNA damaging agents, including cisplatin in non-small cell lung carcinoma cells (Mack *et al.*, 2003) and camptothecin in colon cancer cells (Furuta *et al.*, 2006). An attractive idea has been that some cancer cells are selectively sensitive to ATR/CHK1 inhibition in combination with DNA damaging agents, perhaps because of loss of the p53-dependent G1 checkpoint (Toledo *et al.*, 2011). Although our results indicate that loss of ATR/CHK1 or inhibition of CHK1 does not increase UV-induced mutagenesis, it remains to be determined if this would hold true for other DNA-damaging chemotherapeutics. If so, our results would suggest that the combination of ATR/CHK1 inhibitors and chemotherapy would have the additional advantage of not enhancing the probability of drug resistant clones or secondary, chemotherapy-induced cancers emerging from an increase in mutagenesis.

Materials and methods

Cell culture and UV treatment

The normal human fibroblast cell line NHF1-hTERT was derived from neonatal foreskin fibroblasts (Boyer *et al.*, 1991) and immortalized by ectopic expression of the catalytic subunit of human telomerase (Heffernan *et al.*, 2002). Cells were cultured in minimum essential medium (GIBCO) supplemented with 10% fetal calf serum and 2 mM L-glutamine, and were maintained in humidified 95% air and 5% CO_2 at 37°C. For UV irradiations, cells were rinsed in phosphate buffered saline, all extra liquid removed, and the culture plates irradiated without the lids. Irradiation was performed with a fluorescent germicidal lamp emitting primarily 254 nm UVC (Sylvania G8T5, 90% emission at 254 nm). Control plates were treated under identical conditions, but were not exposed to UV (sham controls). Lamp irradiance was measured using a UVX Digital Radiometer (Ultra-Violet Products Inc.) using the UVX-25 sensor (250-290 nm range, calibrated at 254 nm).

Protein depletion

siRNA was introduced by electroporation (100 pmol siRNA per 10^6 cells), using the normal human dermal fibroblast kit VDP-1001 (Lonza) and program U-23 on a Nucleofector 2b electroporation device (Lonza). ON-TARGET plus duplex siRNAs were purchased from Dharmacon: NTC (D-001210-2), CHK1 (J-003255), and ATR SMART pool (L-003202). Experiments were conducted 24 h post electroporation with CHK1 or 48 h post-electroporation with ATR.

CHK1 inhibitor TCS2312

The CHK1 inhibitor TCS2312 (Tocris) was dissolved in sterile water (1 mM stock solution) and added to cell culture medium at the indicated concentrations. For velocity

sedimentation experiments, inhibitor was added 30 min prior to irradiation and kept in the medium during the subsequent 30 min incubation and the 15 min ^{3}H-thymidine pulse-labeling period. For mutagenesis and cytotoxicity experiments, inhibitor was added 30 min prior to irradiation and removed six hours after the UV exposure, at which time the cells were rinsed with buffered saline and fed with fresh culture medium.

Western blotting and antibodies

One hour after irradiation, cells were harvested by trypsinization, pelleted and flash frozen in liquid nitrogen. Frozen pellets were resuspended in lysis buffer (8 M urea, 5 M NaH_2PO_4, 1 M Tris-HCl pH 8) on ice for 30 min and then clarified by centrifugation (16000 x g and 4°C). The Bio-Rad Protein Assay kit was used to determine protein concentration. Equal volumes of loading buffer (125 mM Tris pH 6.8, 20% glycerol, 10% β-mercaptoethanol, 4% sodium dodecyl sulfate, 0.05% bromo-phenol blue) were combined with protein lysates and samples were boiled for 5 min. Equal amounts of protein were loaded onto BioRad Criterion-TGX 4-15% gradient gels (approximately 150-200 V, 2-4 h). Size-separated proteins were transferred overnight (100 mA) onto a nitrocellulose membrane. After blocking in 5% powdered milk in TBST (0.5% Tween-20, 10 mM Tris-HCl, 10 mM NaCl, pH=7.4), primary antibodies were applied. The following antibodies were used: rabbit anti-P-CHK1 S345 (Cell Signaling), mouse anti-CHK1, goat anti-ATR, and goat anti-Actin (Santa Cruz). Following application of HRP-conjugated secondary antibody (Amersham), bands were visualized on film by enhanced chemiluminescence (ECL). An Alpha Innotech Fluor-Chem HD2 was used to measure the densitometry of film bands.

Velocity sedimentation

As previously described (Day *et al.*, 2011; Kaufmann *et al.*, 1980b), the steady-state size distribution of nascent DNA was determined by centrifugation in an alkaline sucrose

density-gradient 45 min after UV irradiation. Cells were uniformly pre-labeled during logarithmic growth by incubation with ^{14}C-thymidine (5-10 nCi/mL) for at least 36 h. Medium containing ^{14}C-thymidine was removed overnight and cells treated the following day. Thirty minutes after UV-irradiation, cells were incubated with 25 µCi/mL ^{3}H-thymidine for 15 min. Cells were rinsed in PBS then scraped on ice into 0.1 M NaCl, 0.01 M EDTA (pH 8) and then passed through a 22G needle 5x. An equal volume of lysis buffer (1 M NaOH, 0.02 M EDTA) was added to 0.5 mL of lysed cells and the mixture added on top of an alkaline sucrose gradient (5-20% sucrose in 0.4 M NaOH, 2 M NaCl, 0.01 M EDTA). These gradients were left under fluorescent lighting for 45 min and then centrifuged in a Beckman SW32Ti rotor for 5 h at 25000 rpm and 20°C. Gradients were fractioned through a hole punched in the bottom of the centrifuge tube and acid-precipitable material filtered onto a glass microfiber filter (Whatman GF/C 24mm). The glass microfiber filters were then analyzed by liquid scintillation counting. All experiments included cells pre-labeled with ^{14}C-thymidine but not pulse-labeled with ^{3}H-thymidine. These samples were used to measure the ^{14}C CPM values detected in the ^{3}H channel during liquid scintillation counting. Normalized ^{3}H CPM were the ^{3}H CPM in each fraction, corrected for the ^{14}C spillover, and normalized to the total ^{14}C in the gradient, which is proportional to the number of cells.

HAT selection

Pre-selection for functional HPRT in cells used for mutagenesis experiments was performed by expanding cultures in medium supplemented with 1 x HAT (100x lyophilized HAT contains 10 mM sodium hypoxanthine, 40 M aminopterin, and 1.6 mM thymidine) for 10-14 days (Bassett *et al.*, 2004). New aliquots of frozen and stored HAT selected cells were used for every *HPRT* mutagenesis experiment. Cell cultures were expanded in normal medium without HAT for 10-14 days prior to mutagenesis experiments.

Mutagenesis

Mutagenesis experiments were performed by plating electroporated cells at $1x10^6$ per dish or $5x10^5$ for cells to be treated with vehicle/inhibitor (2 plates per condition). Cells were irradiated 24 h (CHK1 or inhibitor experiments) or 48 h post-electroporation (ATR). After irradiation, cells were maintained in logarithmic growth for 4-6 population doublings. *HPRT* mutants were selected by plating $4x10^4$ cells per 10-cm dish (55 dishes per treatment) in medium containing 40 µM 6-thioguanine. At the time of selection, colony forming efficiency was determined by plating 400 cells per dish in medium lacking 6-thioguanine. Approximately two weeks post-seeding, all selective and colony forming efficiency plates were fixed in 3:1 methanol:acetic acid and stained with 0.05% crystal violet, and colonies with more than 50 cells were counted. Mutation frequencies were calculated from the number of plates without any mutant colonies, using the Poisson distribution as follows: [-ln (number of plates without 6-thioguanine resistant colonies/total number of plates)]/[(number of cells plated for selection) x (colony-forming efficiency at time of selection)].

Cytotoxicity experiments

Concurrent with the mutagenesis experiments, cytotoxicity was determined by colony forming assay at the time of treatment. Cells depleted of CHK1 (and their matched NTC controls) were plated at a density of 1000 cells per 10-cm dish and irradiated 24 h after electroporation. Cells depleted of ATR (and their matched NTC controls) were left in culture for 24 h post-electroporation and re-seeded at a density of 500 cells per 10-cm dish, and irradiated 48 h after electroporation. Cells treated with 1 µM TCS2312 or vehicle were seeded at a density of 500 cells per 10-cm dish and irradiated 30 min after the addition of inhibitor. The inhibitor remained on the cultures for 6 h post-irradiation. These cell densities

resulted in approximately 100 colonies per dish for the vehicle or NTC-treated, sham-irradiated plates, and 3-6 plates per condition were counted. Plates were fed weekly and colonies fixed in 3:1 methanol:acetic acid and stained with 0.05% crystal violet approximately two weeks later. Colonies with more than 50 cells were counted.

Statistical methods

Statistical comparisons were performed in order to determine whether UVC induced mutation frequencies, UV-induced cytotoxicity, or colony forming efficiency following siRNA-mediated depletion of ATR or CHK1, or pharmacological inhibition of CHK1, varied significantly from the NTC or vehicle controls. The linear regression model was used to carry out data analysis for estimating various parameters of interest with appropriate 95% confidence intervals, and hypothesis testing. Specifically, the linear model was used to model the mutation frequency and cell survival percentage as response variables, using UVC fluence level and siRNA-mediated protein depletion or inhibitor treatment as covariates. The interaction effect between covariates was also considered to make the model more flexible. Wald statistics were used to determine the statistical significance of the comparisons. The Wilcoxon rank sum test was used to do group-wise comparisons at different UVC fluences and with different protein depletions to test for statistical differences in mutation frequency or colony forming efficiency. Exact test statistics were used to determine the statistical significance of the comparisons. All statistical analyses were performed using SAS 9.3 (SAS Institute Inc., Cary, NC).

.

Supplemental material

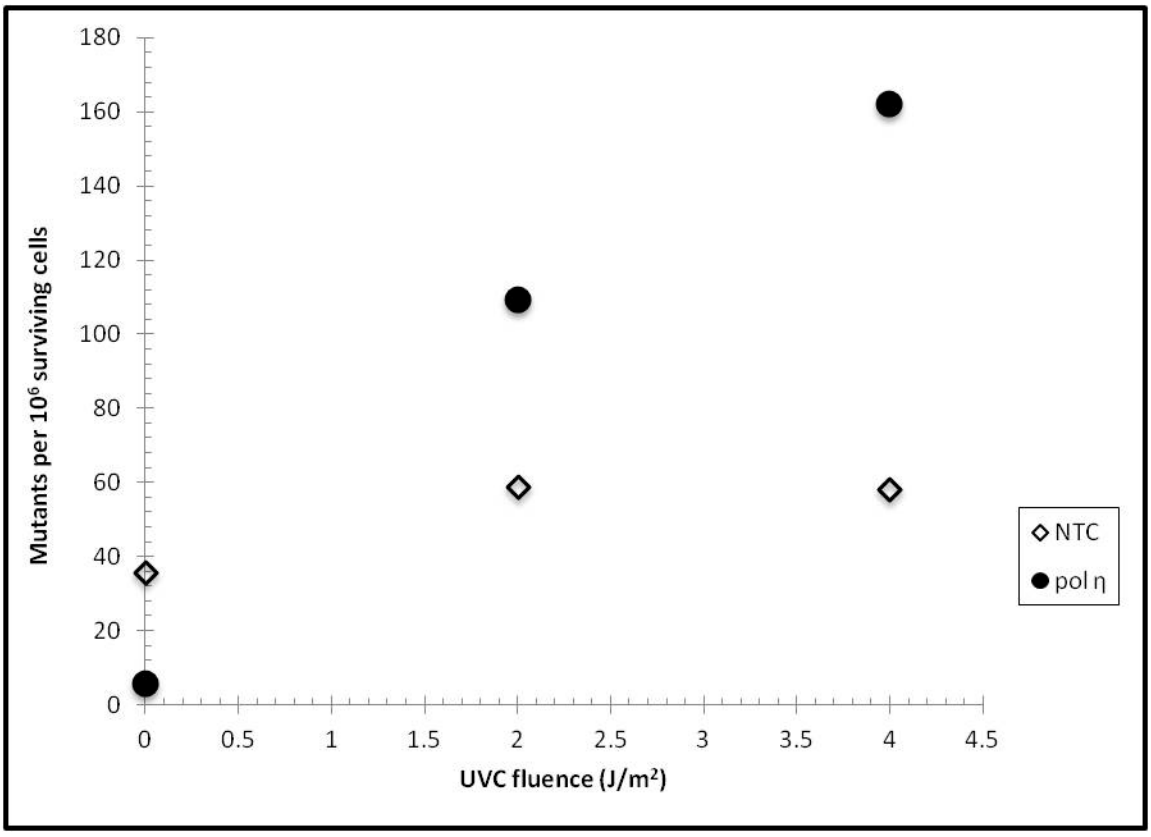

Figure S3.1 Depletion of DNA polymerase η increases UV-induced mutagenesis. siRNA mediated depletion of DNA polymerase η (Dharmacon ON-TARGET J-006454-09, closed circles) increased UV-induced (2, or 4 J/m^2) mutation frequency at the *HPRT* locus compared to cells treated with NTC siRNA (open diamonds). Cells were irradiated 24 h post-electroporation, n=1.

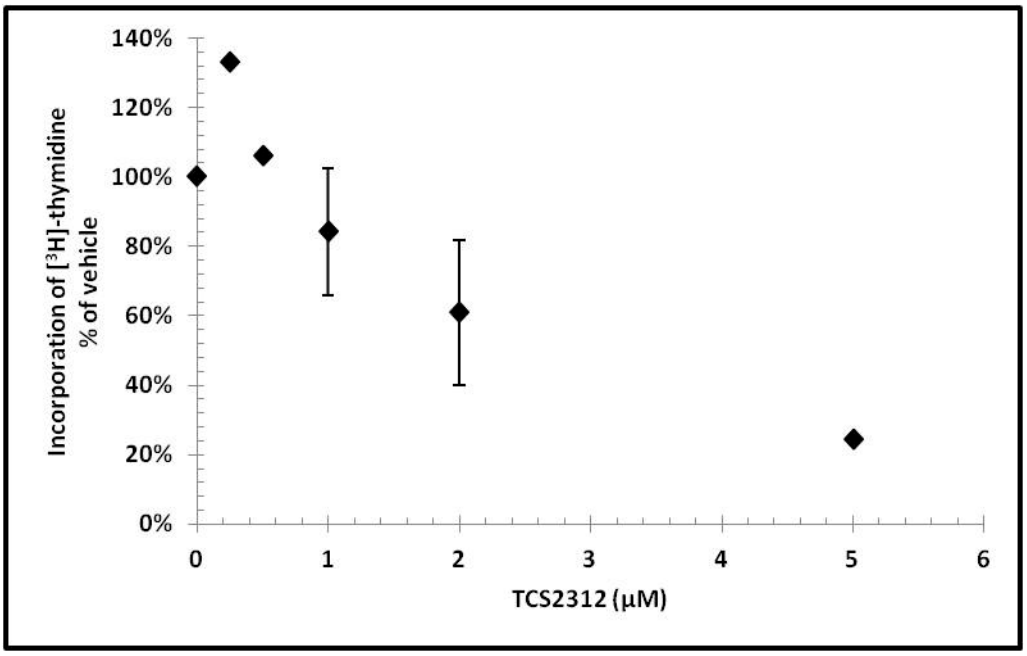

Figure S3.2 Inhibition of DNA synthesis by TCS2312. NHF1 were uniformly pre-labeled in medium containing 5 nCi/mL ^{14}C-thymidine for ~48 h prior to replating in 6-well plates. Indicated concentrations of TCS2312 were added to the medium for 1 h prior to pulse labeling for 15 min with 10 µCi/mL ^{3}H-thymidine. Cells were then rinsed twice in ice cold phosphate buffered saline and fixed in cold 5% trichloroacetic acid for 30 min. After fixing, wells were rinsed twice with 5% trichloroacetic acid and twice with 95% ethanol. Cells were then dissolved in 0.3 N sodium hydroxide and analyzed by liquid scintillation counting.

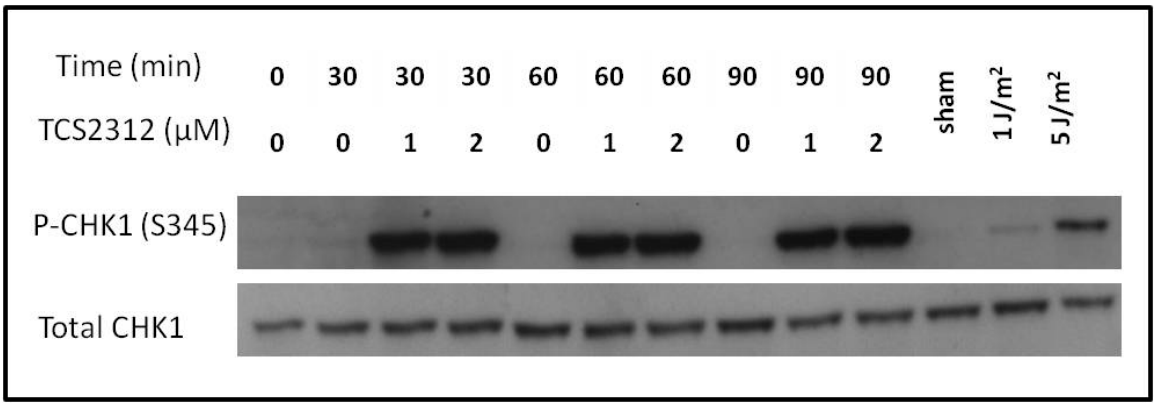

Figure S3.3 Inhibition of CHK1 kinase activity enhances CHK1 phosphorylation. NHF1 were treated with 0, 1, or 2 μM TCS2312 for 30, 60, or 90 min and P-CHK1 (S345) analyzed by immunoblotting. P-CHK1 levels in UV-irradiated NHF1 (45 min post-irradiation) included for comparison.

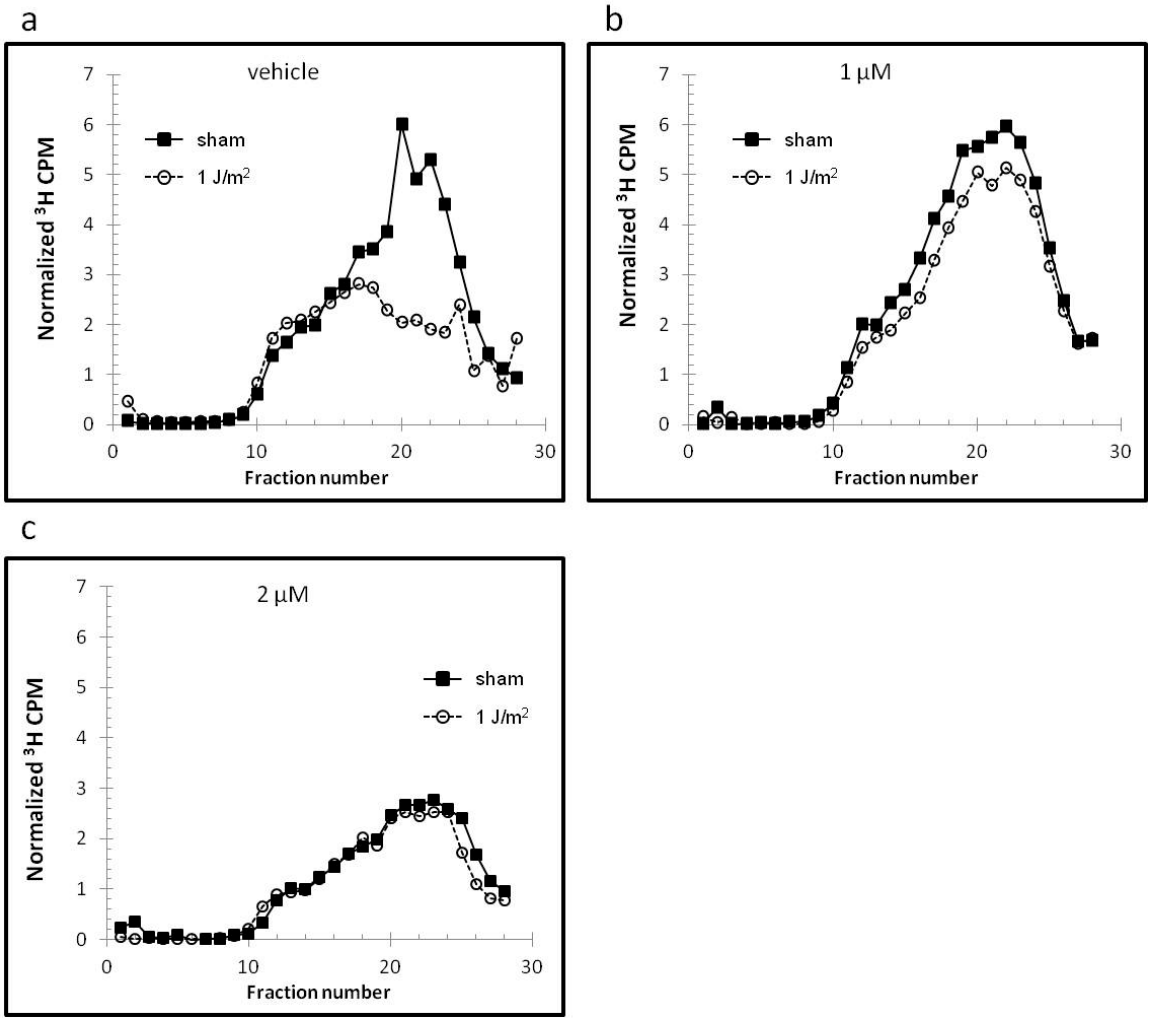

Figure S3.4 Velocity sedimentation analysis of nascent DNA from NHF1 cells treated with the CHK1 inhibitor TCS2312. Cells were treated with **a)** 0, **b)** 1, or **c)** 2 µM TCS2312 30 min prior to irradiation with 0 (closed squares) or 1 J/m^2 (open circles) and inhibitor remained until cells were harvested. Cells were pulse-labeled with ^{3}H-thymidine (15 min) 30 min post-irradiation.

CHAPTER 4

CONCLUSIONS AND FUTURE DIRECTIONS

Much research has been devoted to examining the mechanisms of skin cancers and UV-induced carcinogenesis. Many risk factors for developing skin cancers have been proposed, including tobacco use, immunosuppression, HPV infections, chemical exposures (dioxins, PAH, coal tars, pesticides, arsenic), and certain genetic disorders (XP, Bloom syndrome, Fanconi anemia). However, it has become widely accepted that exposure to solar UVR is the primary etiological cause of both NMSC and melanomas. The primary mechanism of UVR-induced skin carcinogenesis is thought to involve its ability to act as a direct mutagen. It has been clearly demonstrated that UVR is genotoxic and multiple forms of UVR-induced DNA damage have been identified. Despite the fact that UVR has been extensively studied and that much is known about UV-induced skin cancers, there remain many unanswered questions. What are the contributions of different wavelengths to UV-induced skin carcinogenesis? What role does skin inflammation (erythema) play? Which particular UV-induced DNA lesion(s) is/are responsible for mutagenesis? Are there other genetic or environmental factors that influence susceptibility to UV-induced skin cancers? Are tanning bed exposures safe? These have been difficult questions to answer due to the highly complex nature of UV-induced skin cancers. UVR includes a broad spectrum of wavelengths that penetrate skin differently, cause multiple and different forms of DNA damage as well as other forms of cellular damage, and induce potentially varying biological responses. These characteristics make studying UVR not unlike elucidating the carcinogenic effect of chemical mixtures. It has been a challenge to elucidate the importance of the contributions from different components of UVR to skin carcinogenesis. In an attempt to answer some of these questions, investigators have looked to model systems to break down complex biological responses to UVR into individual components and attempt

to examine the relative contribution of these components to the final outcomes. While models have become increasingly specific in order to address isolated systems, it is also important to recognize the aggregate effect of combining these individual components to recapitulate real world UVR exposures and biological responses.

Early studies examining the wavelength dependence of UVR-induced cytotoxicity and mutagenicity indicated that perhaps there was a relationship between these biological outcomes and wavelength. Enninga *et al* reported that cytotoxicity and mutation frequency at the *HPRT* locus increased in normal human fibroblasts as wavelength increased, when compared on the basis of equal T4 endonuclease sensitive sites (Enninga *et al.*, 1986). The authors concluded that either 1) repair systems are inhibited by longer wavelengths, 2) a different spectrum of pyrimidine dimers was induced by longer wavelengths, or 3) other types of lethal and mutagenic lesions are produced by longer wavelengths of UVR. While some of these explanations are supported by experimental evidence, other studies have not confirmed the main findings. Subsequent experiments producing survival curves with different wavelength lamps indicated that human fibroblasts were more sensitive to UVC than they were to a narrow band UVB lamp, when compared on the basis of CPD density measured by immunostaining of exposed cells (Clingen *et al.*, 1995). Mutagenesis studies have also yielded divergent results. Mutation frequencies in a shuttle vector containing the *lacZ* gene were examined in UVA- or UVB-irradiated 293 transformed human embryonic kidney cells (Robert *et al.*, 1996a). These authors did not employ dosimetry, but instead relied upon cytotoxicity to normalize results and allow comparisons of mutation frequency between the two sources of UVR. Their results showed that at 10% cell survival, mutation frequencies were equal for UVA- or UVB-irradiated cells. Only when irradiated with fluences resulting in less than 10% cell survival, fluences that many would consider biologically irrelevant, did they observe a modestly higher mutation frequency in UVA-irradiated cells.

Other research concluded that the mutation frequency at the *HPRT* locus of UVA irradiated NHF was 3.5 times higher than an “equitoxic” fluence of UVB, although cell survival values for these fluences were not reported and dosimetry was not performed (Kappes *et al.*, 2006).

The results reported here suggest that we did find a slight increase in cytotoxicity for NHF1 irradiated with UVA as compared to those irradiated with UVB or UVC inducing equal CPD densities. We could speculate that UVA is inducing additional damage to DNA above the measured CPD densities (see below) or other cellular compartments, for instance ROS-mediated oxidative damage to cellular proteins and lipids. Although UVA displayed enhanced cytotoxicity (over that of UVB or UVC) when analyzed by linear regression analysis, there was no statistically significant decrease in the D_0 value for UVA-irradiated cells, suggesting that any such difference was minimal. In addition, we did not find a difference in the UV-induced mutation frequency between cells irradiated with UVA or UVB at fluences inducing equal CPD densities. It should be noted that our UVA lamps emitted approximately 5.7% of their radiant output in the UVB range and it is possible that this UVB component significantly contributed to the biological effect measured here, including a substantial proportion of the measured CPD and 6-4PP. Thus, it is also possible that a pure UVA source could less efficiently produce CPD and more efficiently induce oxidative damage to DNA, thereby altering the mutation frequency per CPD and the mutational spectrum as well. Although perhaps not ideal for such mechanistic studies, the proportion of UVB in our UVA source is not unlike that found in terrestrial sunlight. Even in studies where differences in mutation frequencies were noted, mutation spectrum analysis still provides little support for the role of UV-induced oxidative DNA damage in mutagenesis (Ikehata *et al.*, 2008; Kappes and Runger, 2005; Kappes *et al.*, 2006).

Similarly, we found no evidence that UVA-induced oxidative DNA damage was contributing to activation of the intra-S checkpoint. When normalized on the basis of CPD density, both UVC and UVA irradiated NHF1 displayed nearly identical activation of intra-S checkpoint signaling (phosphorylation of CHK1), inhibition of replicon initiation (after low dose UVR), and inhibition of DNA strand growth (after higher fluences of UVR). Dose-response curves for the generation of 6-4PP indicate that these lesions are produced in less abundance than are CPD, and that shorter wavelengths of UVR more efficiently produce 6-4PP than longer wavelengths, even when normalized on the basis of CPD density. It has been suggested that a 6-4PP represents a stronger block to the replication machinery than does a CPD, perhaps as a consequence of a more complex TLS bypass mechanism (Gibbs *et al.*, 2005; Li *et al.*, 2002). UVC induced 2 and 1.3 times as many 6-4PP per CPD than did UVA or UVB, with no difference in intra-S checkpoint function. Thus, it seems unlikely that 6-4PP contribute more to intra-S checkpoint activation than do the much more abundant CPD, since if this were the case it would be expected that all measures of intra-S checkpoint function would have been higher in cells irradiated with UVC. We cannot rule out that different experimental systems or other cell types (with variable antioxidant capabilities) might have generated measurable UVA-induced oxidative damage and that such damage could influence DNA synthesis. However, we did not detect 8-oxo-dG in UVA-irradiated NHF1 and must conclude that ROS were not produced in levels high enough to affect DNA synthesis under our experimental conditions.

In an attempt to break down the complexity of *in vivo* responses to solar radiation, the studies employed here have utilized cellular models to examine specific biological responses to UVR. While valuable tools for breaking down complex issues into mechanistic research questions, these simplifications can come at the cost of potentially overlooking important considerations. For instance, the research models employed here examined

dermal fibroblasts growing in a monolayer. This is neither the target cell of solar radiation-induced carcinogenesis nor do they model the structure and cellular interactions of real skin. These could be important considerations when accounting for both “dose”, e.g. incident radiance and the penetration of different wavelengths of UVR, the antioxidant potential of different cell types, or the role(s) of melanin in protecting and/or sensitizing skin cells to carcinogenesis; or when examining the “response”, e.g., potential differences in DNA damage repair capacity, or differences in the magnitude of other biological endpoints being measured. Thus, future studies may consider utilizing cell types and systems that better model *in vivo* exposures. Indeed, advances in melanocyte and keratinocyte culturing are continuously allowing researchers to more easily use these target cells in experiments (see **Figures S2.1** and **S2.2**). Similarly, researchers are creating model systems that better mimic natural skin and using these systems to address important biological questions (Ikuta *et al.*, 2006; Li *et al.*, 2011).

The work presented in Chapter 3 questioned the long-standing dogma that the ATR-dependent intra-S checkpoint serves as a protective measure to minimize mutations induced by agents that cause helix-distorting DNA lesions, such as UVR. Initially, it seemed that this would be an easy hypothesis to support experimentally; it seemed obvious that inhibiting the intra-S checkpoint response would increase UV-induced mutagenesis. What were projected to be preliminary experiments en route to investigating other scientific questions turned out to be much more complex. Contrary to expectations, intra-S checkpoint inhibition did not increase UV-induced mutation frequency at the *HPRT* locus, either by depletion of ATR or CHK1, or by pharmacological inhibition of CHK1 kinase function. It is clear that these proteins are important to the intra-S checkpoint response, and that this response can be inhibited by depletion of the proteins or by inhibiting their signaling cascade. Given that ATR and CHK1 are essential proteins, it is also clear that they perform

vital cellular functions. Our results lead to the conclusions that either 1) the intra-S checkpoint does protect against UV-induced mutagenesis and that our model system was not suited to elucidating this role or 2) the intra-S checkpoint does not protect against UV-induced mutagenesis and that the vital role of these essential proteins is independent of the intra-S checkpoint response to UVR.

There are several possible explanations for the lack of increased mutation frequency observed in NHF1 after inhibition of the intra-S checkpoint. One possibility is that abrogation of the intra-S checkpoint may reduce the efficiency of TLS. There is some evidence that proteins vital to intra-S checkpoint responses might also influence TLS. H2199 human lung carcinoma cells depleted of ATR, or expressing a kinase-dead CHK1 showed lower BPDE-induced PCNA ubiquitination and lower association between PCNA and Polκ (Bi *et al.*, 2005). ATR was also shown to phosphorylate chromatin-bound Pol η in response to UVR, perhaps facilitating Pol η loading onto PCNA (Gohler *et al.*, 2011). Finally, CHK1 has been implicated in damage-induced PCNA ubiquitination (Bi *et al.*, 2005; Yang *et al.*, 2008; Yang and Zou, 2009); and CHK1-PCNA interactions and subsequent release of CHK1 from chromatin were shown to be important in Pol η-mediated replication of damaged DNA (Speroni *et al.*, 2012). These data suggest that intra-S checkpoint proteins are important for efficient TLS across damaged template DNA. Because mutagenesis requires replication of the damaged template, error-prone TLS is considered a prominent driver of UV-induced mutagenesis. Thus, even if intra-S checkpoint inhibition was allowing newly fired replication forks to encounter UV-induced DNA damage sites, TLS would be required to replicate across the photolesions, and to potentially induce mutations. If ATR or CHK1 were important for efficient bypass synthesis (in addition to their known checkpoint functions), it stands to reason that the depletion of these enzymes might inhibit TLS and reduce mutation frequency, even if abrogation of the intra-S checkpoint function were allowing a greater

number of replication forks to encounter DNA damage sites. That pharmacological inhibition of CHK1 kinase function did not affect mutation frequency is more difficult to explain with this model, since it is not clear whether CHK1 kinase activity is required for efficient TLS. It has been reported that expression of kinase dead CHK1 inhibited BPDE-induced PCNA ubiquitination in H1299 cells (Bi *et al.*, 2005) or that it did not inhibit UV or HU-induced PCNA ubiquitination in HeLa cells (despite that depletion of CHK1 did) (Yang *et al.*, 2008); thus, it is less clear if inhibition of CHK1 kinase activity would both abrogate the intra-S checkpoint response and inhibit efficient TLS.

It has also been suggested that RFPC proteins function not only to cooperatively activate the intra-S checkpoint, but that they possess separate functions for preservation of intrinsic chromosomal stability (Smith-Roe *et al.*, 2013), and that loss of ATR or CHK1 increases genomic instability at common fragile sites (Casper *et al.*, 2002; Durkin *et al.*, 2006). Common fragile sites tend to be replicated late in S phase, possibly due to a lack of proximal replication origins and due to the formation of secondary structure within the fragile site, thought to slow progression of replication forks (Durkin *et al.*, 2006; Durkin and Glover, 2007). One possibility is that the primary function of the RFPC proteins is to preserve genomic stability at such difficult to replicate regions, and that inhibition of replicon initiation in response to UVR is not of primary importance in minimizing UV-induced mutations in regions of the genome that are replicated more easily. Cells depleted of ATR do accumulate chromosomal breaks despite apparently normal progression through the S phase (Smith-Roe *et al.*, 2013), supporting the role of ATR in preserving genomic stability in late-replicating and difficult to replicate regions of the genome. Indeed, differences in mutation frequency following intra-S checkpoint inhibition might be observed in regions of the genome containing fragile sites. Another possibility is that the intra-S checkpoint serves to protect late replicating genes and that because the active *HPRT* gene is replicated early in S-phase

(Schmidt and Migeon, 1990), activation of the checkpoint does not inhibit the firing of *HPRT*-replicating origins. Examining the UV-induced mutation frequency, following checkpoint inhibition, in a locus that is replicated late in S phase might yield different results than observed in our experiments. These two possibilities may be interdependent; temporal/spatial regulation of DNA replication and the proteins involved in the intra-S checkpoint may serve to protect regions of the genome that are inherently more difficult to replicate; such heterochromatic regions and regions with a high degree of secondary structure are typically replicated late in S phase (reviewed in (Herrick, 2011)).

Perturbations to other DNA damage responses, including DNA repair systems and cell cycle checkpoints, have been identified in human cancers, and there is strong evidence that such alterations contribute to a mutator phenotype in cancers and pre-cancers (Carson *et al.*, 2012; Kerzendorfer and O'Driscoll, 2009; Omolo *et al.*, 2013). To date, there is little evidence that a misfunctioning intra-S checkpoint contributes directly to carcinogenesis. Seckel syndrome patients, germline mutations in RFPC genes, somatic RFPC gene mutations found in cancers, and heterozygous *ATR* or *CHK1* mouse models, all provide starting points for further examining the role of the ATR-dependent intra-S checkpoint in protecting against carcinogenesis. Further mechanistic investigation is needed to determine if these alterations are abrogating intra-S checkpoint response, and if they contribute to mutagenicity and/or carcinogenicity.

Interestingly, although cells derived from Seckel patients have been shown to be sensitive to UV (O'Driscoll *et al.*, 2003), display chromosomal instability at common fragile sites (Casper *et al.*, 2004), and to have reduced HU-induced CHK1 phosphorlyation (O'Driscoll *et al.*, 2007), there is no published information examining intra-S checkpoint function in Seckel patients. Velocity sedimentation experiments or DNA fiber spreading experiments with Seckel-derived cells could determine if mutations associated with Seckel

syndrome affect intra-S checkpoint function. Furthermore, it has not been established that cells derived from Seckel patients are hypermutable.

Germline mutations in *ATR* (Tanaka *et al.*, 2012) or *CLSPN* (Zhang *et al.*, 2009) have been identified in human cancers, but it is unclear whether these mutations affect intra-S checkpoint function. Although no functional assessments of checkpoint function were reported, neither of these studies observed decreased CHK1 phosphorylation in response to hydroxyurea (*ATR*) or to UV (*CLSPN*). Again, it is unclear if these germline mutations affect mutagenesis. The authors reported that the A6431G mutation in the FAT domain of ATR reduced basal p53 levels and also reduced HU-induced increases in p53 levels, leading them to speculate that this germline mutation was promoting tumorigenesis by reducing p53 signaling via disruption of ATR-AIMP3 (aminoacyl tRNA synthetase interacting multifunctional protein 3) interactions (Tanaka *et al.*, 2012).

Somatic *ATR* and *CHK1* mutations have also been described in endometrial, colorectal, and stomach cancers, particularly in mismatch repair deficient cells with microsatellite instability (Lewis *et al.*, 2005; Lewis *et al.*, 2007; Menoyo *et al.*, 2001; Vassileva *et al.*, 2002), and may have defective intra-S checkpoint signaling and impaired S-phase arrest in response to topotecan (Lewis *et al.*, 2005). It would be interesting to determine if the dominant negative mutation in *ATR* (truncation mutation in codon 776 or 778 of exon 10) prevents UV-induced inhibition of replicon initiation or DNA strand growth, or produces an elevated UV-induced mutation frequency.

Finally, mouse models for Atr or Chk1 deficiency have been utilized (homozygous deletion of either gene is embryonic lethal) to examine the effect of heterozygous deletion of either gene on carcinogenesis (Brown and Baltimore, 2000; Fang *et al.*, 2004; Fishler *et al.*, 2010; Gilad *et al.*, 2010; Liu *et al.*, 2000; Tho *et al.*, 2012). There is indication that loss of

one *Atr* allele reduces UV-induced survival and aphidicolin-induced Chk1 phosphorylation (Fang *et al.*, 2004), suggesting that loss of one allele is sufficient to inhibit intra-S checkpoint signaling. However, no functional assessment of Atr-dependent DNA damage-induced inhibition of replicon initiation has been performed in cells derived from $Atr^{+/-}$ mice. It is also not clear if the increased tumor incidence observed in some $Atr^{+/-}$ or $Chk^{+/-}$ mouse models is due to elevated mutation frequencies in the cells with the heterozygous deletions, relative to the +/+ genotypes at these loci.

It is noteworthy that Seckel patients do not display elevated cancer risks (Kerzendorfer and O'Driscoll, 2009), and that it has been difficult to identify somatic or germline mutations that both abrogate intra-S checkpoint function and clearly contribute to carcinogenesis. ATR and CHK1 are both essential proteins (Brown and Baltimore, 2000; Liu *et al.*, 2000), and depletion of many RFPC proteins drastically reduces cell survival (Smith-Roe *et al.*, 2013), indicating that these proteins have essential functions. These essential functions may very well be separate from the intra-S checkpoint response, or alternatively, the UV-induced checkpoint response is merely a secondary observation in a system designed to maintain genomic stability during the well regulated replication of a complex genome. Although much research is still needed, these observations, along with the data presented here question whether inhibition of the intra-S checkpoint alone is a plausible mechanism for inducing a mutator phenotype in cancer cells. It has even been suggested that the UVA component of UVR might itself inhibit DNA damage responses (Kappes *et al.*, 2006; Runger and Kappes, 2008), including the intra-S checkpoint (de Laat *et al.*, 1997; Runger and Kappes, 2008), potentially contributing to the enhanced mutagenesis that some

investigators have reported with longer wavelengths of UVR. Within the limitations of our model system, not only did we fail to observe UVA-induced inhibition of the intra-S checkpoint or an increased mutation frequency in UVA-irradiated cells, but we also cannot conclude that intra-S checkpoint inhibition increases UV-induced mutation frequency.

REFERENCES

Agar, N.S., Halliday, G.M., Barnetson, R.S., Ananthaswamy, H.N., Wheeler, M., Jones, A.M., 2004. The basal layer in human squamous tumors harbors more UVA than UVB fingerprint mutations: a role for UVA in human skin carcinogenesis, Proc. Natl. Acad. Sci. U. S. A. 101, 4954-4959. doi: 10.1073/pnas.0401141101.

Alderton, G.K., Joenje, H., Varon, R., Borglum, A.D., Jeggo, P.A., O'Driscoll, M., 2004. Seckel syndrome exhibits cellular features demonstrating defects in the ATR-signalling pathway, Hum. Mol. Genet. 13, 3127-3138. doi: 10.1093/hmg/ddh335.

Barnes, J.W., Tischkau, S.A., Barnes, J.A., Mitchell, J.W., Burgoon, P.W., Hickok, J.R., Gillette, M.U., 2003. Requirement of mammalian Timeless for circadian rhythmicity, Science 302, 439-442. doi: 10.1126/science.1086593.

Bassett, E., King, N.M., Bryant, M.F., Hector, S., Pendyala, L., Chaney, S.G., Cordeiro-Stone, M., 2004. The role of DNA polymerase eta in translesion synthesis past platinum-DNA adducts in human fibroblasts, Cancer Res. 64, 6469-6475. doi: 10.1158/0008-5472.CAN-04-1328.

Beckman, R.A., Loeb, L.A., 2005. Genetic instability in cancer: theory and experiment, Semin. Cancer Biol. 15, 423-435. doi: 10.1016/j.semcancer.2005.06.007.

Bentley, N.J., Holtzman, D.A., Flaggs, G., Keegan, K.S., DeMaggio, A., Ford, J.C., Hoekstra, M., Carr, A.M., 1996. The Schizosaccharomyces pombe rad3 checkpoint gene, EMBO J. 15, 6641-6651.

Berton, T.R., Mitchell, D.L., 2012. Quantification of DNA photoproducts in mammalian cell DNA using radioimmunoassay, Methods Mol. Biol. 920, 177-187. doi: 10.1007/978-1-61779-998-3_13; 10.1007/978-1-61779-998-3_13.

Besaratinia, A., Pfeifer, G.P., 2008. Sunlight ultraviolet irradiation and BRAF V600 mutagenesis in human melanoma, Hum. Mutat. 29, 983-991. doi: 10.1002/humu.20802; 10.1002/humu.20802.

Besaratinia, A., Synold, T.W., Xi, B., Pfeifer, G.P., 2004. G-to-T transversions and small tandem base deletions are the hallmark of mutations induced by ultraviolet a radiation in mammalian cells, Biochemistry 43, 8169-8177. doi: 10.1021/bi049761v.

Besaratinia, A., Yoon, J.I., Schroeder, C., Bradforth, S.E., Cockburn, M., Pfeifer, G.P., 2011. Wavelength dependence of ultraviolet radiation-induced DNA damage as determined by laser irradiation suggests that cyclobutane pyrimidine dimers are the principal DNA lesions produced by terrestrial sunlight, FASEB J. 25, 3079-3091. doi: 10.1096/fj.11-187336.

Bi, X., Slater, D.M., Ohmori, H., Vaziri, C., 2005. DNA polymerase kappa is specifically required for recovery from the benzo[a]pyrene-dihydrodiol epoxide (BPDE)-induced S-phase checkpoint, J. Biol. Chem. 280, 22343-22355. doi: 10.1074/jbc.M501562200.

Boyer, J.C., Kaufmann, W.K., Brylawski, B.P., Cordeiro-Stone, M., 1990. Defective postreplication repair in xeroderma pigmentosum variant fibroblasts, Cancer Res. 50, 2593-2598.

Boyer, J.C., Kaufmann, W.K., Cordeiro-Stone, M., 1991. Role of postreplication repair in transformation of human fibroblasts to anchorage independence, Cancer Res. 51, 2960-2964.

Brash, D.E., Rudolph, J.A., Simon, J.A., Lin, A., McKenna, G.J., Baden, H.P., Halperin, A.J., Ponten, J., 1991. A role for sunlight in skin cancer: UV-induced p53 mutations in squamous cell carcinoma, Proc. Natl. Acad. Sci. U. S. A. 88, 10124-10128.

Brash, D.E., Ziegler, A., Jonason, A.S., Simon, J.A., Kunala, S., Leffell, D.J., 1996. Sunlight and sunburn in human skin cancer: p53, apoptosis, and tumor promotion, J. Investig. Dermatol. Symp. Proc. 1, 136-142.

Brown, E.J., Baltimore, D., 2000. ATR disruption leads to chromosomal fragmentation and early embryonic lethality, Genes Dev. 14, 397-402.

Cadet, J., Sage, E., Douki, T., 2005. Ultraviolet radiation-mediated damage to cellular DNA, Mutat. Res. 571, 3-17. doi: 10.1016/j.mrfmmm.2004.09.012.

Carson, C., Omolo, B., Chu, H., Zhou, Y., Sambade, M.J., Peters, E.C., Tompkins, P., Simpson, D.A., Thomas, N.E., Fan, C., Sarasin, A., Dessen, P., Shields, J.M., Ibrahim, J.G., Kaufmann, W.K., 2012. A prognostic signature of defective p53-dependent G1 checkpoint function in melanoma cell lines, Pigment Cell. Melanoma Res. 25, 514-526. doi: 10.1111/j.1755-148X.2012.01010.x; 10.1111/j.1755-148X.2012.01010.x.

Casper, A.M., Durkin, S.G., Arlt, M.F., Glover, T.W., 2004. Chromosomal instability at common fragile sites in Seckel syndrome, Am. J. Hum. Genet. 75, 654-660. doi: 10.1086/422701.

Casper, A.M., Nghiem, P., Arlt, M.F., Glover, T.W., 2002. ATR regulates fragile site stability, Cell 111, 779-789.

Chastain, P.D.,2nd, Heffernan, T.P., Nevis, K.R., Lin, L., Kaufmann, W.K., Kaufman, D.G., Cordeiro-Stone, M., 2006. Checkpoint regulation of replication dynamics in UV-irradiated human cells, Cell. Cycle 5, 2160-2167.

Chen, B., Simpson, D.A., Zhou, Y., Mitra, A., Mitchell, D.L., Cordeiro-Stone, M., Kaufmann, W.K., 2009. Human papilloma virus type16 E6 deregulates CHK1 and sensitizes human fibroblasts to environmental carcinogens independently of its effect on p53, Cell. Cycle 8, 1775-1787.

Chen, T., Stephens, P.A., Middleton, F.K., Curtin, N.J., 2012. Targeting the S and G2 checkpoint to treat cancer, Drug Discov. Today 17, 194-202. doi: 10.1016/j.drudis.2011.12.009; 10.1016/j.drudis.2011.12.009.

Choi, J.H., Pfeifer, G.P., 2005a. The role of DNA polymerase eta in UV mutational spectra, DNA Repair (Amst) 4, 211-220. doi: 10.1016/j.dnarep.2004.09.006.

Choi, J.H., Pfeifer, G.P., 2005b. The role of DNA polymerase eta in UV mutational spectra, DNA Repair (Amst) 4, 211-220. doi: 10.1016/j.dnarep.2004.09.006.

Cleaver, J.E., 2005. Cancer in xeroderma pigmentosum and related disorders of DNA repair, Nat. Rev. Cancer. 5, 564-573. doi: 10.1038/nrc1652.

Cliby, W.A., Roberts, C.J., Cimprich, K.A., Stringer, C.M., Lamb, J.R., Schreiber, S.L., Friend, S.H., 1998. Overexpression of a kinase-inactive ATR protein causes sensitivity to DNA-damaging agents and defects in cell cycle checkpoints, EMBO J. 17, 159-169. doi: 10.1093/emboj/17.1.159.

Clingen, P.H., Arlett, C.F., Cole, J., Waugh, A.P., Lowe, J.E., Harcourt, S.A., Hermanova, N., Roza, L., Mori, T., Nikaido, O., 1995. Correlation of UVC and UVB cytotoxicity with the induction of specific photoproducts in T-lymphocytes and fibroblasts from normal human donors, Photochem. Photobiol. 61, 163-170.

Cordeiro-Stone, M., Frank, A., Bryant, M., Oguejiofor, I., Hatch, S.B., McDaniel, L.D., Kaufmann, W.K., 2002. DNA damage responses protect xeroderma pigmentosum variant from UVC-induced clastogenesis, Carcinogenesis 23, 959-965.

Cortez, D., Guntuku, S., Qin, J., Elledge, S.J., 2001. ATR and ATRIP: partners in checkpoint signaling, Science 294, 1713-1716. doi: 10.1126/science.1065521.

Costanzo, V., Robertson, K., Ying, C.Y., Kim, E., Avvedimento, E., Gottesman, M., Grieco, D., Gautier, J., 2000. Reconstitution of an ATM-dependent checkpoint that inhibits chromosomal DNA replication following DNA damage, Mol. Cell 6, 649-659.

Courdavault, S., Baudouin, C., Charveron, M., Canguilhem, B., Favier, A., Cadet, J., Douki, T., 2005. Repair of the three main types of bipyrimidine DNA photoproducts in human keratinocytes exposed to UVB and UVA radiations, DNA Repair (Amst) 4, 836-844. doi: 10.1016/j.dnarep.2005.05.001.

Courdavault, S., Baudouin, C., Charveron, M., Favier, A., Cadet, J., Douki, T., 2004. Larger yield of cyclobutane dimers than 8-oxo-7,8-dihydroguanine in the DNA of UVA-irradiated human skin cells, Mutat. Res. 556, 135-142. doi: 10.1016/j.mrfmmm.2004.07.011.

Dahle, J., Brunborg, G., Svendsrud, D.H., Stokke, T., Kvam, E., 2008. Overexpression of human OGG1 in mammalian cells decreases ultraviolet A induced mutagenesis, Cancer Lett. 267, 18-25. doi: 10.1016/j.canlet.2008.03.002; 10.1016/j.canlet.2008.03.002.

Danpure, H.J., Tyrrell, R.M., 1976. Oxygen-dependence of near UV (365 NM) lethality and the interaction of near UV and X-rays in two mammalian cell lines, Photochem. Photobiol. 23, 171-177.

Day, T.A., Sproul, C., Cordeiro-Stone, M., Vaziri, C., 2011. Analyzing DNA replication dynamics of genotoxin-treated cells using velocity sedimentation, Methods Mol. Biol. 782, 159-170. doi: 10.1007/978-1-61779-273-1_11; 10.1007/978-1-61779-273-1_11.

De Fabo, E.C., Noonan, F.P., Fears, T., Merlino, G., 2004. Ultraviolet B but not ultraviolet A radiation initiates melanoma, Cancer Res. 64, 6372-6376. doi: 10.1158/0008-5472.CAN-04-1454.

de Klein, A., Muijtjens, M., van Os, R., Verhoeven, Y., Smit, B., Carr, A.M., Lehmann, A.R., Hoeijmakers, J.H., 2000. Targeted disruption of the cell-cycle checkpoint gene ATR leads to early embryonic lethality in mice, Curr. Biol. 10, 479-482.

de Laat, A., Kroon, E.D., de Gruijl, F.R., 1997. Cell cycle effects and concomitant p53 expression in hairless murine skin after longwave UVA (365 nm) irradiation: a comparison with UVB irradiation, Photochem. Photobiol. 65, 730-735.

Dore, J.F., Chignol, M.C., 2012. Tanning salons and skin cancer, Photochem. Photobiol. Sci. 11, 30-37. doi: 10.1039/c1pp05186e; 10.1039/c1pp05186e.

Douki, T., Perdiz, D., Grof, P., Kuluncsics, Z., Moustacchi, E., Cadet, J., Sage, E., 1999. Oxidation of guanine in cellular DNA by solar UV radiation: biological role, Photochem. Photobiol. 70, 184-190.

Douki, T., Reynaud-Angelin, A., Cadet, J., Sage, E., 2003. Bipyrimidine photoproducts rather than oxidative lesions are the main type of DNA damage involved in the genotoxic effect of solar UVA radiation, Biochemistry 42, 9221-9226. doi: 10.1021/bi034593c.

Drobetsky, E.A., Turcotte, J., Chateauneuf, A., 1995. A role for ultraviolet A in solar mutagenesis, Proc. Natl. Acad. Sci. U. S. A. 92, 2350-2354.

Drouin, R., Therrien, J.P., 1997. UVB-induced cyclobutane pyrimidine dimer frequency correlates with skin cancer mutational hotspots in p53, Photochem. Photobiol. 66, 719-726.

Durkin, S.G., Arlt, M.F., Howlett, N.G., Glover, T.W., 2006. Depletion of CHK1, but not CHK2, induces chromosomal instability and breaks at common fragile sites, Oncogene 25, 4381-4388. doi: 10.1038/sj.onc.1209466.

Durkin, S.G., Glover, T.W., 2007. Chromosome fragile sites, Annu. Rev. Genet. 41, 169-192. doi: 10.1146/annurev.genet.41.042007.165900.

Enninga, I.C., Groenendijk, R.T., Filon, A.R., van Zeeland, A.A., Simons, J.W., 1986. The wavelength dependence of u.v.-induced pyrimidine dimer formation, cell killing and mutation induction in human diploid skin fibroblasts, Carcinogenesis 7, 1829-1836.

Fang, Y., Tsao, C.C., Goodman, B.K., Furumai, R., Tirado, C.A., Abraham, R.T., Wang, X.F., 2004. ATR functions as a gene dosage-dependent tumor suppressor on a mismatch repair-deficient background, EMBO J. 23, 3164-3174. doi: 10.1038/sj.emboj.7600315.

Fishler, T., Li, Y.Y., Wang, R.H., Kim, H.S., Sengupta, K., Vassilopoulos, A., Lahusen, T., Xu, X., Lee, M.H., Liu, Q., Elledge, S.J., Ried, T., Deng, C.X., 2010. Genetic instability and mammary tumor formation in mice carrying mammary-specific disruption of Chk1 and p53, Oncogene 29, 4007-4017. doi: 10.1038/onc.2010.163; 10.1038/onc.2010.163.

Focarelli, M.L., Soza, S., Mannini, L., Paulis, M., Montecucco, A., Musio, A., 2009. Claspin inhibition leads to fragile site expression, Genes Chromosomes Cancer 48, 1083-1090. doi: 10.1002/gcc.20710; 10.1002/gcc.20710.

Furuta, T., Hayward, R.L., Meng, L.H., Takemura, H., Aune, G.J., Bonner, W.M., Aladjem, M.I., Kohn, K.W., Pommier, Y., 2006. p21CDKN1A allows the repair of replication-mediated DNA double-strand breaks induced by topoisomerase I and is inactivated by the checkpoint kinase inhibitor 7-hydroxystaurosporine, Oncogene 25, 2839-2849. doi: 10.1038/sj.onc.1209313.

Gaddameedhi, S., Kemp, M.G., Reardon, J.T., Shields, J.M., Smith-Roe, S.L., Kaufmann, W.K., Sancar, A., 2010. Similar nucleotide excision repair capacity in melanocytes and melanoma cells, Cancer Res. 70, 4922-4930. doi: 10.1158/0008-5472.CAN-10-0095; 10.1158/0008-5472.CAN-10-0095.

Gailani, M.R., Stahle-Backdahl, M., Leffell, D.J., Glynn, M., Zaphiropoulos, P.G., Pressman, C., Unden, A.B., Dean, M., Brash, D.E., Bale, A.E., Toftgard, R., 1996. The role of the human homologue of Drosophila patched in sporadic basal cell carcinomas, Nat. Genet. 14, 78-81. doi: 10.1038/ng0996-78.

Garinis, G.A., Mitchell, J.R., Moorhouse, M.J., Hanada, K., de Waard, H., Vandeputte, D., Jans, J., Brand, K., Smid, M., van der Spek, P.J., Hoeijmakers, J.H., Kanaar, R., van der Horst, G.T., 2005. Transcriptome analysis reveals cyclobutane pyrimidine dimers as a major source of UV-induced DNA breaks, EMBO J. 24, 3952-3962. doi: 10.1038/sj.emboj.7600849.

Garland, C.F., Garland, F.C., Gorham, E.D., 1993. Rising trends in melanoma. An hypothesis concerning sunscreen effectiveness, Ann. Epidemiol. 3, 103-110.

Gibbs, P.E., McDonald, J., Woodgate, R., Lawrence, C.W., 2005. The relative roles in vivo of Saccharomyces cerevisiae Pol eta, Pol zeta, Rev1 protein and Pol32 in the bypass and mutation induction of an abasic site, T-T (6-4) photoadduct and T-T cis-syn cyclobutane dimer, Genetics 169, 575-582. doi: 10.1534/genetics.104.034611.

Giglia-Mari, G., Zotter, A., Vermeulen, W., 2011. DNA damage response, Cold Spring Harb Perspect. Biol. 3, a000745. doi: 10.1101/cshperspect.a000745; 10.1101/cshperspect.a000745.

Gilad, O., Nabet, B.Y., Ragland, R.L., Schoppy, D.W., Smith, K.D., Durham, A.C., Brown, E.J., 2010. Combining ATR suppression with oncogenic Ras synergistically increases genomic instability, causing synthetic lethality or tumorigenesis in a dosage-dependent manner, Cancer Res. 70, 9693-9702. doi: 10.1158/0008-5472.CAN-10-2286; 10.1158/0008-5472.CAN-10-2286.

Gilchrest, B.A., Eller, M.S., Geller, A.C., Yaar, M., 1999. The pathogenesis of melanoma induced by ultraviolet radiation, N. Engl. J. Med. 340, 1341-1348. doi: 10.1056/NEJM199904293401707.

Girard, P.M., Pozzebon, M., Delacote, F., Douki, T., Smirnova, V., Sage, E., 2008. Inhibition of S-phase progression triggered by UVA-induced ROS does not require a functional DNA damage checkpoint response in mammalian cells, DNA Repair (Amst) 7, 1500-1516. doi: 10.1016/j.dnarep.2008.05.004.

Gohler, T., Sabbioneda, S., Green, C.M., Lehmann, A.R., 2011. ATR-mediated phosphorylation of DNA polymerase eta is needed for efficient recovery from UV damage, J. Cell Biol. 192, 219-227. doi: 10.1083/jcb.201008076; 10.1083/jcb.201008076.

Goloudina, A., Yamaguchi, H., Chervyakova, D.B., Appella, E., Fornace, A.J.,Jr, Bulavin, D.V., 2003. Regulation of human Cdc25A stability by Serine 75 phosphorylation is not sufficient to activate a S phase checkpoint, Cell. Cycle 2, 473-478.

Gotter, A.L., Suppa, C., Emanuel, B.S., 2007. Mammalian TIMELESS and Tipin are evolutionarily conserved replication fork-associated factors, J. Mol. Biol. 366, 36-52. doi: 10.1016/j.jmb.2006.10.097.

Griffith, E., Walker, S., Martin, C.A., Vagnarelli, P., Stiff, T., Vernay, B., Al Sanna, N., Saggar, A., Hamel, B., Earnshaw, W.C., Jeggo, P.A., Jackson, A.P., O'Driscoll, M., 2008. Mutations in pericentrin cause Seckel syndrome with defective ATR-dependent DNA damage signaling, Nat. Genet. 40, 232-236. doi: 10.1038/ng.2007.80.

Gueranger, Q., Stary, A., Aoufouchi, S., Faili, A., Sarasin, A., Reynaud, C.A., Weill, J.C., 2008. Role of DNA polymerases eta, iota and zeta in UV resistance and UV-induced mutagenesis in a human cell line, DNA Repair (Amst) 7, 1551-1562. doi: 10.1016/j.dnarep.2008.05.012; 10.1016/j.dnarep.2008.05.012.

Hanahan, D., Weinberg, R.A., 2011. Hallmarks of cancer: the next generation, Cell 144, 646-674. doi: 10.1016/j.cell.2011.02.013; 10.1016/j.cell.2011.02.013.

Hanahan, D., Weinberg, R.A., 2000. The hallmarks of cancer, Cell 100, 57-70.

Hannuksela-Svahn, A., Sigurgeirsson, B., Pukkala, E., Lindelof, B., Berne, B., Hannuksela, M., Poikolainen, K., Karvonen, J., 1999. Trioxsalen bath PUVA did not increase the risk of squamous cell skin carcinoma and cutaneous malignant melanoma in a joint analysis of 944 Swedish and Finnish patients with psoriasis, Br. J. Dermatol. 141, 497-501.

Hassepass, I., Voit, R., Hoffmann, I., 2003. Phosphorylation at serine 75 is required for UV-mediated degradation of human Cdc25A phosphatase at the S-phase checkpoint, J. Biol. Chem. 278, 29824-29829. doi: 10.1074/jbc.M302704200.

Heffernan, T.P., Simpson, D.A., Frank, A.R., Heinloth, A.N., Paules, R.S., Cordeiro-Stone, M., Kaufmann, W.K., 2002. An ATR- and Chk1-dependent S checkpoint inhibits replicon initiation following UVC-induced DNA damage, Mol. Cell. Biol. 22, 8552-8561.

Heffernan, T.P., Unsal-Kacmaz, K., Heinloth, A.N., Simpson, D.A., Paules, R.S., Sancar, A., Cordeiro-Stone, M., Kaufmann, W.K., 2007. Cdc7-Dbf4 and the human S checkpoint response to UVC, J. Biol. Chem. 282, 9458-9468. doi: 10.1074/jbc.M611292200.

Herrick, J., 2011. Genetic variation and DNA replication timing, or why is there late replicating DNA? Evolution 65, 3031-3047. doi: 10.1111/j.1558-5646.2011.01407.x; 10.1111/j.1558-5646.2011.01407.x.

Hill, B.H., 1976. Immunosuppressive drug therapy as a potentiator of skin tumours in five patients with lymphoma, Australas. J. Dermatol. 17, 46-48.

Hocker, T., Tsao, H., 2007. Ultraviolet radiation and melanoma: a systematic review and analysis of reported sequence variants, Hum. Mutat. 28, 578-588. doi: 10.1002/humu.20481.

Hoxtell, E.O., Mandel, J.S., Murray, S.S., Schuman, L.M., Goltz, R.W., 1977. Incidence of skin carcinoma after renal transplantation, Arch. Dermatol. 113, 436-438.

Ichihashi, M., Ueda, M., Budiyanto, A., Bito, T., Oka, M., Fukunaga, M., Tsuru, K., Horikawa, T., 2003. UV-induced skin damage, Toxicology 189, 21-39.

Ikehata, H., Kawai, K., Komura, J., Sakatsume, K., Wang, L., Imai, M., Higashi, S., Nikaido, O., Yamamoto, K., Hieda, K., Watanabe, M., Kasai, H., Ono, T., 2008. UVA1 genotoxicity is mediated not by oxidative damage but by cyclobutane pyrimidine dimers in normal mouse skin, J. Invest. Dermatol. 128, 2289-2296. doi: 10.1038/jid.2008.61.

Ikehata, H., Kudo, H., Masuda, T., Ono, T., 2003. UVA induces C-->T transitions at methyl-CpG-associated dipyrimidine sites in mouse skin epidermis more frequently than UVB, Mutagenesis 18, 511-519.

Ikehata, H., Ono, T., 2011. The mechanisms of UV mutagenesis, J. Radiat. Res. 52, 115-125.

Ikuta, S., Sekino, N., Hara, T., Saito, Y., Chida, K., 2006. Mouse epidermal keratinocytes in three-dimensional organotypic coculture with dermal fibroblasts form a stratified sheet resembling skin, Biosci. Biotechnol. Biochem. 70, 2669-2675.

Jares, P., Donaldson, A., Blow, J.J., 2000. The Cdc7/Dbf4 protein kinase: target of the S phase checkpoint? EMBO Rep. 1, 319-322. doi: 10.1093/embo-reports/kvd076.

Jiang, Y., Rabbi, M., Kim, M., Ke, C., Lee, W., Clark, R.L., Mieczkowski, P.A., Marszalek, P.E., 2009. UVA generates pyrimidine dimers in DNA directly, Biophys. J. 96, 1151-1158. doi: 10.1016/j.bpj.2008.10.030.

Kannouche, P., Stary, A., 2003. Xeroderma pigmentosum variant and error-prone DNA polymerases, Biochimie 85, 1123-1132.

Kappes, U.P., Luo, D., Potter, M., Schulmeister, K., Runger, T.M., 2006. Short- and long-wave UV light (UVB and UVA) induce similar mutations in human skin cells, J. Invest. Dermatol. 126, 667-675. doi: 10.1038/sj.jid.5700093.

Kappes, U.P., Runger, T.M., 2005. No major role for 7,8-dihydro-8-oxoguanine in ultraviolet light-induced mutagenesis, Radiat. Res. 164, 440-445.

Karbaschi, M., Brady, N.J., Evans, M.D., Cooke, M.S., 2012. Immuno-slot blot assay for detection of UVR-mediated DNA damage, Methods Mol. Biol. 920, 163-175. doi: 10.1007/978-1-61779-998-3_12; 10.1007/978-1-61779-998-3_12.

Kastan, M.B., Bartek, J., 2004. Cell-cycle checkpoints and cancer, Nature 432, 316-323. doi: 10.1038/nature03097.

Kaufmann, W.K., 2009. The human intra-S checkpoint response to UVC-induced DNA damage, Carcinogenesis . doi: 10.1093/carcin/bgp230.

Kaufmann, W.K., Cleaver, J.E., 1981. Mechanisms of inhibition of DNA replication by ultraviolet light in normal human and xeroderma pigmentosum fibroblasts, J. Mol. Biol. 149, 171-187.

Kaufmann, W.K., Cleaver, J.E., Painter, R.B., 1980a. Ultraviolet radiation inhibits replicon initiation in S phase human cells, Biochim. Biophys. Acta 608, 191-195.

Kaufmann, W.K., Cleaver, J.E., Painter, R.B., 1980b. Ultraviolet radiation inhibits replicon initiation in S phase human cells, Biochim. Biophys. Acta 608, 191-195.

Kaufmann, W.K., Heffernan, T.P., Beaulieu, L.M., Doherty, S., Frank, A.R., Zhou, Y., Bryant, M.F., Zhou, T., Luche, D.D., Nikolaishvili-Feinberg, N., Simpson, D.A., Cordeiro-Stone, M., 2003. Caffeine and human DNA metabolism: the magic and the mystery, Mutat. Res. 532, 85-102.

Kaufmann, W.K., Nevis, K.R., Qu, P., Ibrahim, J.G., Zhou, T., Zhou, Y., Simpson, D.A., Helms-Deaton, J., Cordeiro-Stone, M., Moore, D.T., Thomas, N.E., Hao, H., Liu, Z., Shields, J.M., Scott, G.A., Sharpless, N.E., 2008. Defective cell cycle checkpoint functions in melanoma are associated with altered patterns of gene expression, J. Invest. Dermatol. 128, 175-187. doi: 10.1038/sj.jid.5700935.

Kaufmann, W.K., Paules, R.S., 1996. DNA damage and cell cycle checkpoints, FASEB J. 10, 238-247.

Kerzendorfer, C., O'Driscoll, M., 2009. Human DNA damage response and repair deficiency syndromes: linking genomic instability and cell cycle checkpoint proficiency, DNA Repair (Amst) 8, 1139-1152. doi: 10.1016/j.dnarep.2009.04.018; 10.1016/j.dnarep.2009.04.018.

Kim, S.I., Pfeifer, G.P., Besaratinia, A., 2007. Mutagenicity of ultraviolet A radiation in the lacI transgene in Big Blue mouse embryonic fibroblasts, Mutat. Res. 617, 71-78. doi: 10.1016/j.mrfmmm.2006.12.003.

Konze-Thomas, B., Hazard, R.M., Maher, V.M., McCormick, J.J., 1982. Extent of excision repair before DNA synthesis determines the mutagenic but not the lethal effect of UV radiation, Mutat. Res. 94, 421-434.

Kuluncsics, Z., Perdiz, D., Brulay, E., Muel, B., Sage, E., 1999. Wavelength dependence of ultraviolet-induced DNA damage distribution: involvement of direct or indirect mechanisms and possible artefacts, J. Photochem. Photobiol. B. 49, 71-80. doi: 10.1016/S1011-1344(99)00034-2.

Kumagai, A., Dunphy, W.G., 2000. Claspin, a novel protein required for the activation of Chk1 during a DNA replication checkpoint response in Xenopus egg extracts, Mol. Cell 6, 839-849.

Lee, A.Y., Chiba, T., Truong, L.N., Cheng, A.N., Do, J., Cho, M.J., Chen, L., Wu, X., 2012. Dbf4 is direct downstream target of ataxia telangiectasia mutated (ATM) and ataxia telangiectasia and Rad3-related (ATR) protein to regulate intra-S-phase checkpoint, J. Biol. Chem. 287, 2531-2543. doi: 10.1074/jbc.M111.291104; 10.1074/jbc.M111.291104.

Lee, D.H., Pfeifer, G.P., 2003. Deamination of 5-methylcytosines within cyclobutane pyrimidine dimers is an important component of UVB mutagenesis, J. Biol. Chem. 278, 10314-10321. doi: 10.1074/jbc.M212696200.

Lee, J., Kumagai, A., Dunphy, W.G., 2007. The Rad9-Hus1-Rad1 checkpoint clamp regulates interaction of TopBP1 with ATR, J. Biol. Chem. 282, 28036-28044. doi: 10.1074/jbc.M704635200.

Lehmann, A.R., McGibbon, D., Stefanini, M., 2011. Xeroderma pigmentosum, Orphanet J. Rare Dis. 6, 70-1172-6-70. doi: 10.1186/1750-1172-6-70; 10.1186/1750-1172-6-70.

Leman, A.R., Noguchi, C., Lee, C.Y., Noguchi, E., 2010. Human Timeless and Tipin stabilize replication forks and facilitate sister-chromatid cohesion, J. Cell. Sci. 123, 660-670. doi: 10.1242/jcs.057984; 10.1242/jcs.057984.

Lewis, K.A., Bakkum-Gamez, J., Loewen, R., French, A.J., Thibodeau, S.N., Cliby, W.A., 2007. Mutations in the ataxia telangiectasia and rad3-related-checkpoint kinase 1 DNA damage response axis in colon cancers, Genes Chromosomes Cancer 46, 1061-1068. doi: 10.1002/gcc.20486.

Lewis, K.A., Mullany, S., Thomas, B., Chien, J., Loewen, R., Shridhar, V., Cliby, W.A., 2005. Heterozygous ATR mutations in mismatch repair-deficient cancer cells have functional significance, Cancer Res. 65, 7091-7095. doi: 10.1158/0008-5472.CAN-05-1019.

Ley, R.D., 1997. Ultraviolet radiation A-induced precursors of cutaneous melanoma in Monodelphis domestica, Cancer Res. 57, 3682-3684.

Li, L., Fukunaga-Kalabis, M., Herlyn, M., 2011. The three-dimensional human skin reconstruct model: a tool to study normal skin and melanoma progression, J. Vis. Exp. (54). pii: 2937. doi, 10.3791/2937. doi: 10.3791/2937; 10.3791/2937.

Li, Z., Zhang, H., McManus, T.P., McCormick, J.J., Lawrence, C.W., Maher, V.M., 2002. hREV3 is essential for error-prone translesion synthesis past UV or benzo[a]pyrene diol epoxide-induced DNA lesions in human fibroblasts, Mutat. Res. 510, 71-80.

Liu, P., Barkley, L.R., Day, T., Bi, X., Slater, D.M., Alexandrow, M.G., Nasheuer, H.P., Vaziri, C., 2006. The Chk1-mediated S-phase checkpoint targets initiation factor Cdc45 via a Cdc25A/Cdk2-independent mechanism, J. Biol. Chem. 281, 30631-30644. doi: 10.1074/jbc.M602982200.

Liu, Q., Guntuku, S., Cui, X.S., Matsuoka, S., Cortez, D., Tamai, K., Luo, G., Carattini-Rivera, S., DeMayo, F., Bradley, A., Donehower, L.A., Elledge, S.J., 2000. Chk1 is an essential kinase that is regulated by Atr and required for the G(2)/M DNA damage checkpoint, Genes Dev. 14, 1448-1459.

Liu, S., Shiotani, B., Lahiri, M., Marechal, A., Tse, A., Leung, C.C., Glover, J.N., Yang, X.H., Zou, L., 2011. ATR autophosphorylation as a molecular switch for checkpoint activation, Mol. Cell 43, 192-202. doi: 10.1016/j.molcel.2011.06.019; 10.1016/j.molcel.2011.06.019.

Loeb, L.A., 1991. Mutator phenotype may be required for multistage carcinogenesis, Cancer Res. 51, 3075-3079.

Mack, P.C., Gandara, D.R., Lau, A.H., Lara, P.N.,Jr, Edelman, M.J., Gumerlock, P.H., 2003. Cell cycle-dependent potentiation of cisplatin by UCN-01 in non-small-cell lung carcinoma, Cancer Chemother. Pharmacol. 51, 337-348. doi: 10.1007/s00280-003-0571-6.

Mailand, N., Falck, J., Lukas, C., Syljuasen, R.G., Welcker, M., Bartek, J., Lukas, J., 2000. Rapid destruction of human Cdc25A in response to DNA damage, Science 288, 1425-1429.

Marrot, L., Meunier, J.R., 2008. Skin DNA photodamage and its biological consequences, J. Am. Acad. Dermatol. 58, S139-48. doi: 10.1016/j.jaad.2007.12.007.

Masutani, C., Kusumoto, R., Yamada, A., Dohmae, N., Yokoi, M., Yuasa, M., Araki, M., Iwai, S., Takio, K., Hanaoka, F., 1999. The XPV (xeroderma pigmentosum variant) gene encodes human DNA polymerase eta, Nature 399, 700-704. doi: 10.1038/21447.

Matsuda, T., Bebenek, K., Masutani, C., Hanaoka, F., Kunkel, T.A., 2000. Low fidelity DNA synthesis by human DNA polymerase-eta, Nature 404, 1011-1013. doi: 10.1038/35010014.

Matsumura, Y., Ananthaswamy, H.N., 2004. Toxic effects of ultraviolet radiation on the skin, Toxicol. Appl. Pharmacol. 195, 298-308. doi: 10.1016/j.taap.2003.08.019.

Matsunaga, T., Hieda, K., Nikaido, O., 1991. Wavelength dependent formation of thymine dimers and (6-4) photoproducts in DNA by monochromatic ultraviolet light ranging from 150 to 365 nm, Photochem. Photobiol. 54, 403-410.

Menoyo, A., Alazzouzi, H., Espin, E., Armengol, M., Yamamoto, H., Schwartz, S.,Jr, 2001. Somatic mutations in the DNA damage-response genes ATR and CHK1 in sporadic stomach tumors with microsatellite instability, Cancer Res. 61, 7727-7730.

Miao, H., Seiler, J.A., Burhans, W.C., 2003. Regulation of cellular and SV40 virus origins of replication by Chk1-dependent intrinsic and UVC radiation-induced checkpoints, J. Biol. Chem. 278, 4295-4304. doi: 10.1074/jbc.M204264200.

Mitchell, D., Fernandez, A., 2012. The photobiology of melanocytes modulates the impact of UVA on sunlight-induced melanoma, Photochem. Photobiol. Sci. 11, 69-73. doi: 10.1039/c1pp05146f; 10.1039/c1pp05146f.

Mitchell, D.L., 2006. Quantification of photoproducts in mammalian cell DNA using radioimmunoassay, Methods Mol. Biol. 314, 239-249. doi: 10.1385/1-59259-973-7:239.

Mitchell, D.L., 1996. Radioimmunoassay of DNA Damaged by Ultraviolet Light. In: Pfeifer, G.P. (Ed.), Technologies for Detection of DNA Damage and Mutations. Plenum Press, New York, pp. 73-73-86.

Mitchell, D.L., Fernandez, A.A., Nairn, R.S., Garcia, R., Paniker, L., Trono, D., Thames, H.D., Gimenez-Conti, I., 2010. Ultraviolet A does not induce melanomas in a Xiphophorus hybrid fish model, Proc. Natl. Acad. Sci. U. S. A. 107, 9329-9334. doi: 10.1073/pnas.1000324107; 10.1073/pnas.1000324107.

Mitchell, D.L., Jen, J., Cleaver, J.E., 1991. Relative induction of cyclobutane dimers and cytosine photohydrates in DNA irradiated in vitro and in vivo with ultraviolet-C and ultraviolet-B light, Photochem. Photobiol. 54, 741-746.

Mordes, D.A., Glick, G.G., Zhao, R., Cortez, D., 2008. TopBP1 activates ATR through ATRIP and a PIKK regulatory domain, Genes Dev. 22, 1478-1489. doi: 10.1101/gad.1666208; 10.1101/gad.1666208.

Mouret, S., Baudouin, C., Charveron, M., Favier, A., Cadet, J., Douki, T., 2006. Cyclobutane pyrimidine dimers are predominant DNA lesions in whole human skin exposed to UVA radiation, Proc. Natl. Acad. Sci. U. S. A. 103, 13765-13770. doi: 10.1073/pnas.0604213103.

Nam, E.A., Zhao, R., Glick, G.G., Bansbach, C.E., Friedman, D.B., Cortez, D., 2011. Thr-1989 phosphorylation is a marker of active ataxia telangiectasia-mutated and Rad3-related (ATR) kinase, J. Biol. Chem. 286, 28707-28714. doi: 10.1074/jbc.M111.248914; 10.1074/jbc.M111.248914.

Noguchi, E., Noguchi, C., McDonald, W.H., Yates, J.R.,3rd, Russell, P., 2004. Swi1 and Swi3 are components of a replication fork protection complex in fission yeast, Mol. Cell. Biol. 24, 8342-8355. doi: 10.1128/MCB.24.19.8342-8355.2004.

O'Driscoll, M., Dobyns, W.B., van Hagen, J.M., Jeggo, P.A., 2007. Cellular and clinical impact of haploinsufficiency for genes involved in ATR signaling, Am. J. Hum. Genet. 81, 77-86. doi: 10.1086/518696.

O'Driscoll, M., Ruiz-Perez, V.L., Woods, C.G., Jeggo, P.A., Goodship, J.A., 2003. A splicing mutation affecting expression of ataxia-telangiectasia and Rad3-related protein (ATR) results in Seckel syndrome, Nat. Genet. 33, 497-501. doi: 10.1038/ng1129.

Oe, T., Nakajo, N., Katsuragi, Y., Okazaki, K., Sagata, N., 2001. Cytoplasmic occurrence of the Chk1/Cdc25 pathway and regulation of Chk1 in Xenopus oocytes, Dev. Biol. 229, 250-261. doi: 10.1006/dbio.2000.9968.

Ogi, T., Walker, S., Stiff, T., Hobson, E., Limsirichaikul, S., Carpenter, G., Prescott, K., Suri, M., Byrd, P.J., Matsuse, M., Mitsutake, N., Nakazawa, Y., Vasudevan, P., Barrow, M., Stewart, G.S., Taylor, A.M., O'Driscoll, M., Jeggo, P.A., 2012. Identification of the first ATRIP-deficient patient and novel mutations in ATR define a clinical spectrum for ATR-ATRIP Seckel Syndrome, PLoS Genet. 8, e1002945. doi: 10.1371/journal.pgen.1002945; 10.1371/journal.pgen.1002945.

Omolo, B., Carson, C., Chu, H., Zhou, Y., Simpson, D.A., Hesse, J.E., Paules, R.S., Nyhan, K.C., Ibrahim, J.G., Kaufmann, W.K., 2013. A prognostic signature of G 2 checkpoint function in melanoma cell lines, Cell. Cycle 12, 1071-1082. doi: 10.4161/cc.24067; 10.4161/cc.24067.

Ouellette, M.M., McDaniel, L.D., Wright, W.E., Shay, J.W., Schultz, R.A., 2000. The establishment of telomerase-immortalized cell lines representing human chromosome instability syndromes, Hum. Mol. Genet. 9, 403-411.

Painter, R.B., 1985. Inhibition and recovery of DNA synthesis in human cells after exposure to ultraviolet light, Mutat. Res. 145, 63-69.

Painter, R.B., Young, B.R., 1980. Radiosensitivity in ataxia-telangiectasia: a new explanation, Proc. Natl. Acad. Sci. U. S. A. 77, 7315-7317.

Perdiz, D., Grof, P., Mezzina, M., Nikaido, O., Moustacchi, E., Sage, E., 2000. Distribution and repair of bipyrimidine photoproducts in solar UV-irradiated mammalian cells. Possible role of Dewar photoproducts in solar mutagenesis, J. Biol. Chem. 275, 26732-26742. doi: 10.1074/jbc.M001450200.

Petermann, E., Maya-Mendoza, A., Zachos, G., Gillespie, D.A., Jackson, D.A., Caldecott, K.W., 2006. Chk1 requirement for high global rates of replication fork progression during normal vertebrate S phase, Mol. Cell. Biol. 26, 3319-3326. doi: 10.1128/MCB.26.8.3319-3326.2006.

Pfeifer, G.P., Besaratinia, A., 2012. UV wavelength-dependent DNA damage and human non-melanoma and melanoma skin cancer, Photochem. Photobiol. Sci. 11, 90-97. doi: 10.1039/c1pp05144j.

Reiman, A., Srinivasan, V., Barone, G., Last, J.I., Wootton, L.L., Davies, E.G., Verhagen, M.M., Willemsen, M.A., Weemaes, C.M., Byrd, P.J., Izatt, L., Easton, D.F., Thompson, D.J., Taylor, A.M., 2011. Lymphoid tumours and breast cancer in ataxia telangiectasia; substantial protective effect of residual ATM kinase activity against childhood tumours, Br. J. Cancer 105, 586-591. doi: 10.1038/bjc.2011.266; 10.1038/bjc.2011.266.

Robert, C., Muel, B., Benoit, A., Dubertret, L., Sarasin, A., Stary, A., 1996a. Cell survival and shuttle vector mutagenesis induced by ultraviolet A and ultraviolet B radiation in a human cell line, J. Invest. Dermatol. 106, 721-728.

Robert, C., Muel, B., Benoit, A., Dubertret, L., Sarasin, A., Stary, A., 1996b. Cell survival and shuttle vector mutagenesis induced by ultraviolet A and ultraviolet B radiation in a human cell line, J. Invest. Dermatol. 106, 721-728.

Rochette, P.J., Lacoste, S., Therrien, J.P., Bastien, N., Brash, D.E., Drouin, R., 2009. Influence of cytosine methylation on ultraviolet-induced cyclobutane pyrimidine dimer formation in genomic DNA, Mutat. Res. 665, 7-13. doi: 10.1016/j.mrfmmm.2009.02.008; 10.1016/j.mrfmmm.2009.02.008.

Runger, T.M., 2011. Is UV-induced mutation formation in melanocytes different from other skin cells? Pigment Cell. Melanoma Res. 24, 10-12. doi: 10.1111/j.1755-148X.2010.00802.x; 10.1111/j.1755-148X.2010.00802.x.

Runger, T.M., Kappes, U.P., 2008. Mechanisms of mutation formation with long-wave ultraviolet light (UVA), Photodermatol. Photoimmunol. Photomed. 24, 2-10. doi: 10.1111/j.1600-0781.2008.00319.x.

Sage, E., Girard, P.M., Francesconi, S., 2012. Unravelling UVA-induced mutagenesis, Photochem. Photobiol. Sci. 11, 74-80. doi: 10.1039/c1pp05219e.

Sancar, A., Lindsey-Boltz, L.A., Unsal-Kacmaz, K., Linn, S., 2004. Molecular mechanisms of mammalian DNA repair and the DNA damage checkpoints, Annu. Rev. Biochem. 73, 39-85. doi: 10.1146/annurev.biochem.73.011303.073723.

Savitsky, K., Bar-Shira, A., Gilad, S., Rotman, G., Ziv, Y., Vanagaite, L., Tagle, D.A., Smith, S., Uziel, T., Sfez, S., Ashkenazi, M., Pecker, I., Frydman, M., Harnik, R., Patanjali, S.R., Simmons, A., Clines, G.A., Sartiel, A., Gatti, R.A., Chessa, L., Sanal, O., Lavin, M.F., Jaspers, N.G., Taylor, A.M., Arlett, C.F., Miki, T., Weissman, S.M., Lovett, M., Collins, F.S., Shiloh, Y., 1995. A single ataxia telangiectasia gene with a product similar to PI-3 kinase, Science 268, 1749-1753.

Schmidt, M., Migeon, B.R., 1990. Asynchronous replication of homologous loci on human active and inactive X chromosomes, Proc. Natl. Acad. Sci. U. S. A. 87, 3685-3689.

Schuch, A.P., da Silva Galhardo, R., de Lima-Bessa, K.M., Schuch, N.J., Menck, C.F., 2009. Development of a DNA-dosimeter system for monitoring the effects of solar-ultraviolet radiation, Photochem. Photobiol. Sci. 8, 111-120. doi: 10.1039/b810085c; 10.1039/b810085c.

Sehgal, A., Price, J.L., Man, B., Young, M.W., 1994. Loss of circadian behavioral rhythms and per RNA oscillations in the Drosophila mutant timeless, Science 263, 1603-1606.

Seiler, J.A., Conti, C., Syed, A., Aladjem, M.I., Pommier, Y., 2007. The intra-S-phase checkpoint affects both DNA replication initiation and elongation: single-cell and -DNA fiber analyses, Mol. Cell. Biol. 27, 5806-5818. doi: 10.1128/MCB.02278-06.

Setlow, R.B., Grist, E., Thompson, K., Woodhead, A.D., 1993. Wavelengths effective in induction of malignant melanoma, Proc. Natl. Acad. Sci. U. S. A. 90, 6666-6670.

Shackelford, R.E., Kaufmann, W.K., Paules, R.S., 1999. Cell cycle control, checkpoint mechanisms, and genotoxic stress, Environ. Health Perspect. 107 Suppl 1, 5-24.

Shann, Y.J., Hsu, M.T., 2001. Cloning and characterization of liver-specific isoform of Chk1 gene from rat, J. Biol. Chem. 276, 48863-48870. doi: 10.1074/jbc.M108253200.

Smith-Roe, S.L., Patel, S.S., Zhou, Y., Simpson, D.A., Rao, S., Ibrahim, J.G., Cordeiro-Stone, M., Kaufmann, W.K., 2013. Separation of intra-S checkpoint protein contributions to DNA replication fork protection and genomic stability in normal human fibroblasts, Cell. Cycle 12, 332-345. doi: 10.4161/cc.23177; 10.4161/cc.23177.

Snellman, E., Strozyk, M., Segerback, D., Klimenko, T., Hemminki, K., 2003. Effect of the spectral range of a UV lamp on the production of cyclobutane pyrimidine dimers in human skin in situ, Photodermatol. Photoimmunol. Photomed. 19, 281-286.

Speroni, J., Federico, M.B., Mansilla, S.F., Soria, G., Gottifredi, V., 2012. Kinase-independent function of checkpoint kinase 1 (Chk1) in the replication of damaged DNA, Proc. Natl. Acad. Sci. U. S. A. 109, 7344-7349. doi: 10.1073/pnas.1116345109; 10.1073/pnas.1116345109.

Stary, A., Kannouche, P., Lehmann, A.R., Sarasin, A., 2003. Role of DNA polymerase eta in the UV mutation spectrum in human cells, J. Biol. Chem. 278, 18767-18775. doi: 10.1074/jbc.M211838200.

Stern, R.S., Nichols, K.T., Vakeva, L.H., 1997. Malignant melanoma in patients treated for psoriasis with methoxsalen (psoralen) and ultraviolet A radiation (PUVA). The PUVA Follow-Up Study, N. Engl. J. Med. 336, 1041-1045.

Takai, H., Tominaga, K., Motoyama, N., Minamishima, Y.A., Nagahama, H., Tsukiyama, T., Ikeda, K., Nakayama, K., Nakanishi, M., Nakayama, K., 2000. Aberrant cell cycle checkpoint function and early embryonic death in Chk1(-/-) mice, Genes Dev. 14, 1439-1447.

Takeda, T., Ogino, K., Tatebayashi, K., Ikeda, H., Arai, K., Masai, H., 2001. Regulation of initiation of S phase, replication checkpoint signaling, and maintenance of mitotic chromosome structures during S phase by Hsk1 kinase in the fission yeast, Mol. Biol. Cell 12, 1257-1274.

Tanaka, A., Weinel, S., Nagy, N., O'Driscoll, M., Lai-Cheong, J.E., Kulp-Shorten, C.L., Knable, A., Carpenter, G., Fisher, S.A., Hiragun, M., Yanase, Y., Hide, M., Callen, J., McGrath, J.A., 2012. Germline mutation in ATR in autosomal- dominant oropharyngeal cancer syndrome, Am. J. Hum. Genet. 90, 511-517. doi: 10.1016/j.ajhg.2012.01.007; 10.1016/j.ajhg.2012.01.007.

Tewari, A., Sarkany, R.P., Young, A.R., 2012. UVA1 induces cyclobutane pyrimidine dimers but not 6-4 photoproducts in human skin in vivo, J. Invest. Dermatol. 132, 394-400. doi: 10.1038/jid.2011.283; 10.1038/jid.2011.283.

Tho, L.M., Libertini, S., Rampling, R., Sansom, O., Gillespie, D.A., 2012. Chk1 is essential for chemical carcinogen-induced mouse skin tumorigenesis, Oncogene 31, 1366-1375. doi: 10.1038/onc.2011.326; 10.1038/onc.2011.326.

Thomas, N.E., Berwick, M., Cordeiro-Stone, M., 2006. Could BRAF mutations in melanocytic lesions arise from DNA damage induced by ultraviolet radiation? J. Invest. Dermatol. 126, 1693-1696. doi: 10.1038/sj.jid.5700458.

Tibbetts, R.S., Cortez, D., Brumbaugh, K.M., Scully, R., Livingston, D., Elledge, S.J., Abraham, R.T., 2000. Functional interactions between BRCA1 and the checkpoint kinase ATR during genotoxic stress, Genes Dev. 14, 2989-3002.

Toledo, L.I., Murga, M., Fernandez-Capetillo, O., 2011. Targeting ATR and Chk1 kinases for cancer treatment: a new model for new (and old) drugs, Mol. Oncol. 5, 368-373. doi: 10.1016/j.molonc.2011.07.002; 10.1016/j.molonc.2011.07.002.

Tommasi, S., Denissenko, M.F., Pfeifer, G.P., 1997. Sunlight induces pyrimidine dimers preferentially at 5-methylcytosine bases, Cancer Res. 57, 4727-4730.

Tung, B.S., McGregor, W.G., Wang, Y.C., Maher, V.M., McCormick, J.J., 1996. Comparison of the rate of excision of major UV photoproducts in the strands of the human HPRT gene of normal and xeroderma pigmentosum variant cells, Mutat. Res. 362, 65-74.

Unsal-Kacmaz, K., Chastain, P.D., Qu, P.P., Minoo, P., Cordeiro-Stone, M., Sancar, A., Kaufmann, W.K., 2007. The human Tim/Tipin complex coordinates an Intra-S checkpoint response to UV that slows replication fork displacement, Mol. Cell. Biol. 27, 3131-3142. doi: 10.1128/MCB.02190-06.

Unsal-Kacmaz, K., Makhov, A.M., Griffith, J.D., Sancar, A., 2002. Preferential binding of ATR protein to UV-damaged DNA, Proc. Natl. Acad. Sci. U. S. A. 99, 6673-6678. doi: 10.1073/pnas.102167799.

Unsal-Kacmaz, K., Mullen, T.E., Kaufmann, W.K., Sancar, A., 2005. Coupling of human circadian and cell cycles by the timeless protein, Mol. Cell. Biol. 25, 3109-3116. doi: 10.1128/MCB.25.8.3109-3116.2005.

Vassileva, V., Millar, A., Briollais, L., Chapman, W., Bapat, B., 2002. Genes involved in DNA repair are mutational targets in endometrial cancers with microsatellite instability, Cancer Res. 62, 4095-4099.

Ward, I.M., Chen, J., 2001. Histone H2AX is phosphorylated in an ATR-dependent manner in response to replicational stress, J. Biol. Chem. 276, 47759-47762. doi: 10.1074/jbc.C100569200.

Webb, R.B., Malina, M.M., 1970. Mutagenic effects of near ultraviolet and visible radiant energy on continuous cultures of escherichia coli, Photochem. Photobiol. 12, 457-468.

Wright, J.A., Keegan, K.S., Herendeen, D.R., Bentley, N.J., Carr, A.M., Hoekstra, M.F., Concannon, P., 1998. Protein kinase mutants of human ATR increase sensitivity to UV and ionizing radiation and abrogate cell cycle checkpoint control, Proc. Natl. Acad. Sci. U. S. A. 95, 7445-7450.

Xiao, Z., Chen, Z., Gunasekera, A.H., Sowin, T.J., Rosenberg, S.H., Fesik, S., Zhang, H., 2003. Chk1 mediates S and G2 arrests through Cdc25A degradation in response to DNA-damaging agents, J. Biol. Chem. 278, 21767-21773. doi: 10.1074/jbc.M300229200.

Xue, L., Yu, D., Furusawa, Y., Cao, J., Okayasu, R., Fan, S., 2009. ATM-dependent hyper-radiosensitivity in mammalian cells irradiated by heavy ions, Int. J. Radiat. Oncol. Biol. Phys. 75, 235-243. doi: 10.1016/j.ijrobp.2009.04.088; 10.1016/j.ijrobp.2009.04.088.

Yamada, A., Masutani, C., Iwai, S., Hanaoka, F., 2000. Complementation of defective translesion synthesis and UV light sensitivity in xeroderma pigmentosum variant cells by human and mouse DNA polymerase eta, Nucleic Acids Res. 28, 2473-2480.

Yang, X.H., Shiotani, B., Classon, M., Zou, L., 2008. Chk1 and Claspin potentiate PCNA ubiquitination, Genes Dev. 22, 1147-1152. doi: 10.1101/gad.1632808; 10.1101/gad.1632808.

Yang, X.H., Zou, L., 2009. Dual functions of DNA replication forks in checkpoint signaling and PCNA ubiquitination, Cell. Cycle 8, 191-194.

Yoon, J.H., Prakash, L., Prakash, S., 2009. Highly error-free role of DNA polymerase eta in the replicative bypass of UV-induced pyrimidine dimers in mouse and human cells, Proc. Natl. Acad. Sci. U. S. A. 106, 18219-18224. doi: 10.1073/pnas.0910121106; 10.1073/pnas.0910121106.

Zhang, J., Song, Y.H., Brannigan, B.W., Wahrer, D.C., Schiripo, T.A., Harris, P.L., Haserlat, S.M., Ulkus, L.E., Shannon, K.M., Garber, J.E., Freedman, M.L., Henderson, B.E., Zou, L., Sgroi, D.C., Haber, D.A., Bell, D.W., 2009. Prevalence and functional analysis of sequence variants in the ATR checkpoint mediator Claspin, Mol. Cancer. Res. 7, 1510-1516. doi: 10.1158/1541-7786.MCR-09-0033; 10.1158/1541-7786.MCR-09-0033.

Zhao, H., Piwnica-Worms, H., 2001. ATR-mediated checkpoint pathways regulate phosphorylation and activation of human Chk1, Mol. Cell. Biol. 21, 4129-4139. doi: 10.1128/MCB.21.13.4129-4139.2001.

Ziegler, A., Leffell, D.J., Kunala, S., Sharma, H.W., Gailani, M., Simon, J.A., Halperin, A.J., Baden, H.P., Shapiro, P.E., Bale, A.E., 1993. Mutation hotspots due to sunlight in the p53 gene of nonmelanoma skin cancers, Proc. Natl. Acad. Sci. U. S. A. 90, 4216-4220.

Zou, L., Cortez, D., Elledge, S.J., 2002. Regulation of ATR substrate selection by Rad17-dependent loading of Rad9 complexes onto chromatin, Genes Dev. 16, 198-208. doi: 10.1101/gad.950302.

Zou, L., Elledge, S.J., 2003. Sensing DNA damage through ATRIP recognition of RPA-ssDNA complexes, Science 300, 1542-1548. doi: 10.1126/science.1083430.